

Photodissociation regions in the interstellar medium of galaxies

D. J. Hollenbach*

MS 245-3, NASA Ames Research Center, Moffett Field, California 94035

A. G. G. M. Tielens†

Kapteyn Astronomical Institute, P.O. Box 800, 9700 AV Groningen, The Netherlands

The interstellar medium of galaxies is the reservoir out of which stars are born and into which stars inject newly created elements as they age. The physical properties of the interstellar medium are governed in part by the radiation emitted by these stars. Far-ultraviolet ($6 \text{ eV} < h\nu < 13.6 \text{ eV}$) photons from massive stars dominate the heating and influence the chemistry of the neutral atomic gas and much of the molecular gas in galaxies. Predominantly neutral regions of the interstellar medium in which the heating and chemistry are regulated by far ultraviolet photons are termed Photo-Dissociation Regions (PDRs). These regions are the origin of most of the non-stellar infrared (IR) and the millimeter and submillimeter CO emission from galaxies. The importance of PDRs has become increasingly apparent with advances in IR and submillimeter astronomy. The IR emission from PDRs includes fine structure lines of C, C⁺, and O; rovibrational lines of H₂; rotational lines of CO; broad mid-IR features of polycyclic aromatic hydrocarbons; and a luminous underlying IR continuum from interstellar dust. The transition of H to H₂ and C⁺ to CO occurs within PDRs. Comparison of observations with theoretical models of PDRs enables one to determine the density and temperature structure, the elemental abundances, the level of ionization, and the radiation field. PDR models have been applied to interstellar clouds near massive stars, planetary nebulae, red giant outflows, photoevaporating planetary disks around newly formed stars, diffuse clouds, the neutral intercloud medium, and molecular clouds in the interstellar radiation field—in summary, much of the interstellar medium in galaxies. Theoretical PDR models explain the observed correlations of the [CII] 158 μm with the CO $J=1-0$ emission, the CO $J=1-0$ luminosity with the interstellar molecular mass, and the [CII] 158 μm plus [OI] 63 μm luminosity with the IR continuum luminosity. On a more global scale, PDR models predict the existence of two stable neutral phases of the interstellar medium, elucidate the formation and destruction of star-forming molecular clouds, and suggest radiation-induced feedback mechanisms that may regulate star formation rates and the column density of gas through giant molecular clouds. [S0034-6861(99)01001-6]

CONTENTS

Introduction	174	C. The molecular transition observed in edge-on PDRs	201
II. Physical and Chemical Processes	178	D. The origin of [CI] emission	202
A. The penetration of far-ultraviolet radiation	179	E. CI recombination lines	203
B. Chemistry in PDRs	180	F. The [CII]-CO correlation	204
1. H ₂ formation, destruction, and heating	181	G. OH and CH ₃ OH maser regions	204
2. Non-Maxwellian chemistry	183	H. The galactic center	205
3. PDR chemical networks	184	I. Starburst galactic nuclei	206
a. Oxygen and carbon	184	V. PDRs in Different Radiation Fields	209
b. Nitrogen	185	A. Planetary nebulae	209
c. Sulfur and silicon	185	B. X-ray dissociation regions	209
d. Polycyclic aromatic hydrocarbons (PAHs)		VI. Diffuse, Translucent, and Molecular Clouds in the Interstellar Radiation Field	212
PDR chemistry		A. Diffuse and translucent clouds	212
C. Interstellar PAHs and grain photoelectric heating in PDRs	186	B. Molecular clouds	213
1. Observations of the unidentified infrared emission bands	186	1. HI halos of molecular clouds	213
2. Unidentified infrared emission bands and interstellar PAH molecules	186	2. C ⁺ halos around molecular cores in the Magellanic Clouds and irregulars	214
3. The grain size distribution	187	3. CO line profiles and the H ₂ mass to CO $J = 1-0$ luminosity ratio	214
4. Photoelectric heating	188	VII. The Global Interstellar Medium of Galaxies	214
D. Heating and cooling	188	A. The neutral phases of the interstellar medium	214
III. PDR Models	190	B. The HI/H ₂ transition in galaxies and the formation of molecular clouds	216
A. Steady-state, stationary PDR models	191	C. The destruction of molecular clouds	216
B. Time-dependent and nonstationary PDRs	192	D. The [CII] emission from the galaxy	216
C. PDR models of photoevaporating protoplanetary disks	193	1. Diffuse HI clouds (cold neutral medium)	216
D. PDR models with cool sources	194	2. PDRs on molecular cloud surfaces	218
IV. Observations of PDRs	194	3. Diffuse HII regions and warm ionized medium	218
A. Physical conditions	195	4. Discussion	218
B. The H ₂ spectrum	198		

5. Energy balance of the interstellar gas	219
E. Far-ultraviolet regulation of star formation in galaxies	219
VIII. Conclusions, Summary, and Future Directions	220
Acknowledgments	221
References	222

I. INTRODUCTION

Galaxies are huge collections of stars, planets, unseen “dark matter,” gas, and dust held together by mutual gravitational attraction. The vast bulk of the volume of a galaxy is filled with the interstellar medium (ISM), the gas and dust which exist between the stars. However, often the mass of a galaxy is found in the invisible dark matter and the stars. The Milky Way Galaxy has about 8×10^9 solar masses (M_\odot) of gas and dust, while it has about $10^{11} M_\odot$ of stars. Nevertheless, the main activity of a spiral galaxy is the cyclic process in which stars eject gas and dust into the ISM, while at the same time gas and dust clouds in the ISM gravitationally collapse to form stars. The ISM is the birthplace of the stars, but the stars control the structure, and therefore star formation rate, of the ISM. Several decades ago, the ISM was thought of as a fairly quiescent place, with interstellar clouds wafting along and gradually forming stars. However, after the discovery of a voluminous, hot ($T \sim 10^6$ K) intercloud medium, caused by enormous shock waves from supernovae (exploding stars) propagating through the ISM (Cox and Smith, 1974; Jenkins and Meloy, 1974; York, 1974; Burstein *et al.*, 1977), it was clear the ISM was not as quiescent as previously believed. McKee and Ostriker (1977) formulated a theory of the ISM in which supernova shocks played the dominant role in determining the overall morphology of the medium. McCray and Snow (1979) coined the phrase “the violent ISM.” In the past decade, however, there has been a reemphasis on the quiescent aspects of the ISM, especially in the relatively gentle interaction of the ultraviolet photons from the massive stars in the galaxy with the ISM.¹

In order to understand the effect of ultraviolet photons on the ISM, it is necessary to understand the basic properties of the interstellar dust and gas, as revealed by decades of astrophysical research. Hydrogen gas is the most abundant species (by both number and mass) in the ISM. The interstellar dust abundance relative to hydrogen, as well as the gas-phase abundances of heavier

elements relative to hydrogen, vary somewhat both within a given galaxy and from galaxy to galaxy. Nevertheless, as a general rule, the mass of material in dust particles is of order 0.01 times the mass in hydrogen, regardless of the density of the gas. Dust particles usually range in size from the molecular domain to sizes of order $0.3 \mu\text{m}$ and are composed largely of amorphous carbon or graphite, aromatic hydrocarbons, silicates, ices (especially water ice), silicon carbide, and possibly iron particles, metallic oxides, and sulfides. At the small end of the size regime lie polycyclic aromatic hydrocarbons (PAHs), which are really large, planar molecules rather than “solid” dust particles. In the gas, helium is the next most abundant element after hydrogen, roughly 10% of hydrogen by nucleus number and 40% by mass. Oxygen and carbon follow, with elemental number abundances relative to hydrogen of about 3×10^{-4} and 1.4×10^{-4} in the local ISM of our Milky Way Galaxy. A substantial fraction of elemental oxygen and (to a lesser extent) carbon is generally in the gas phase rather than incorporated in dust. Generally, a large fraction of the refractory elements like silicon, iron, and magnesium, and a significant fraction of carbon is found in dust particles.

The ISM is made up of a number of components, which can be described by their hydrogen gas densities, their temperatures, and their state of ionization. Three of these components fill most of the volume of the ISM: the warm neutral medium (WNM) with hydrogen nucleus density $n \sim 0.3 \text{ cm}^{-3}$ and $T \sim 8000$ K, the warm ionized medium (WIM) with similar n and T but with the hydrogen nearly completely ionized, and the hot ionized medium (HIM, the supernova-shocked intercloud medium), with $n \sim 3 \times 10^{-3} \text{ cm}^{-3}$ and $T \sim 10^6$ K (McKee and Ostriker, 1977; Kulkarni and Heiles, 1987). Four of these components make up three “phases” of the ISM: the HIM hot phase, the combined WIM and WNM warm phase, and a cold phase (CNM, for cold neutral medium) of neutral clouds with $n \sim 30 \text{ cm}^{-3}$ and $T \sim 100$ K. The term “phases” is used to denote components that may exist in thermal pressure equilibrium, with $P/k = nT \sim 3 \times 10^3 \text{ cm}^{-3} \text{ K}$ in the solar vicinity (Jenkins *et al.*, 1983). However, there are also components, small in volume filling factor, with much higher thermal pressures than the average ISM thermal pressure. The ultimate origin for these higher pressures is gravity: clouds achieve critical masses where their self-gravity makes them gravitationally bound. The pressures in their cores then rise in an attempt to produce pressure gradients that will offset gravity. Generally, these dense cloud cores are cold ($T \sim 1-30$ K), opaque to optical or ultraviolet photons, and molecular (H_2). Their hydrogen gas densities range from $\sim 10^3 \text{ cm}^{-3}$ to over 10^7 cm^{-3} . The denser cores are not in equilibrium but are either collapsing to form stars, or are expanding due to the interaction of radiation or winds from embedded or nearby stars. For example, the extreme-ultraviolet ($h\nu > 13.6 \text{ eV}$ —the ionization potential of hydrogen atoms) photons from massive stars near interstellar molecular clouds produce the bulk of the fully ionized

*Electronic address: hollenbach@ism.arc.nasa.gov

[†]Electronic address: tielens@astro.rug.nl

¹Massive stars, some 10 to 100 times as massive as the sun, are much less numerous than solar-type stars in a galaxy like the Milky Way, but they produce the bulk of the ultraviolet photons because they are hotter and roughly 10^4-10^6 times as luminous as the sun. Astrophysicists classify stars by letters; massive stars are O and B stars, O being more massive.

gas (HII regions²) in the galaxy. Some of the extreme-ultraviolet photons escape to distant regions to produce the warm ionized medium, but photons impinging on the cloud photoionize the hydrogen and the resulting energetic photoelectrons collisionally heat the gas in the HII portion of the cloud to 10^4 K. These HII regions have electron densities that range from 1 cm^{-3} to $\gtrsim 10^5 \text{ cm}^{-3}$, and with their high pressures and large thermal velocities they often expand into the ambient ISM, thereby destroying and dispersing the gravitationally bound molecular cloud. In summary, two higher-pressure components of the ISM are HII regions and gravitationally bound molecular clouds.³

Most of the mass of the ISM is in neutral regions, either cold neutral medium or gravitationally bound molecular clouds, and it is in the latter where star formation occurs. The study of photodissociation regions⁴ (PDRs) is the study of the effects of stellar far-ultraviolet ($6 \text{ eV} < h\nu < 13.6 \text{ eV}$) photons on the structure, chemistry, thermal balance, and evolution of the neutral interstellar medium of galaxies. One important aspect of this study is understanding the process of star formation. Far-ultraviolet photons not only illuminate star-forming regions, causing them to glow in infrared emission, diagnostic of the physical conditions, but they may also play an important role in regulating the star formation process.

Historically, observational study of PDRs goes back to the early parts of this century, when optical absorption lines seen in the spectra of stars were shown to originate in interstellar rather than stellar photospheric gas. Much of this absorption occurred in relatively transparent ($A_V \lesssim 2$, see footnote 5) neutral clouds called

²Astrophysicists use “I” to denote neutral atoms, “II” to denote singly ionized species, “III” to denote doubly ionized species, and so forth. Therefore HII refers to H^+ or protons, and CII refers to singly ionized carbon or C^+ .

³Physicists should note that what astrophysicists call “high-pressure” ISM is a better vacuum than achievable in the laboratory! Because of the low densities and the non-blackbody radiation fields, local thermodynamic equilibrium cannot be assumed in calculating the chemical abundances or level populations of the interstellar species.

⁴Photodissociation regions have also been called “photon-dominated regions”; we prefer “photodissociation regions” because it implies the presence of ultraviolet photons, which are not energetic enough to ionize hydrogen and create HII regions, but which can dissociate most molecules. This term remains sufficiently general to include regions that are mostly H_2 or CO but where ultraviolet fluxes still appreciably dissociate other species.

⁵Astrophysicists often measure the thickness or the depth into a cloud by the amount of visual extinction A_V ($\lambda \sim 5550 \text{ \AA}$) of the incident radiation field caused by the dust column to this thickness or depth. $A_V = 1$ corresponds to a reduction by a factor of 2.5 in the incident visual flux and, because of the assumed constant ratio of gas to dust, corresponds to a hydrogen nucleus column density of about $2 \times 10^{21} \text{ cm}^{-2}$.

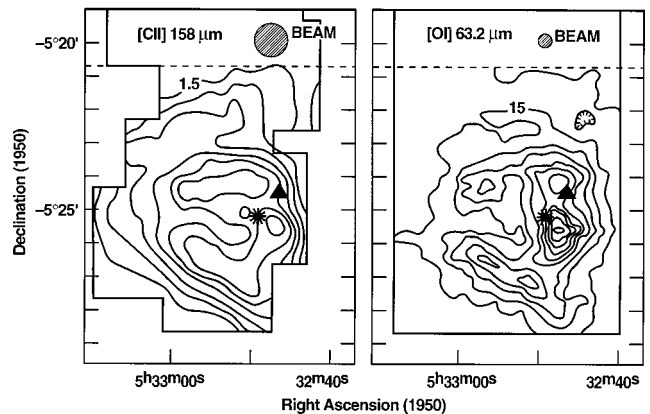


FIG. 1. [CII] $158 \mu\text{m}$ and [OI] $63 \mu\text{m}$ maps of the Orion A molecular cloud behind the Trapezium (adapted from Herrmann *et al.*, 1997). The [CII] contours are in steps of $5 \times 10^{-4} \text{ erg cm}^{-2} \text{ s}^{-1} \text{ sr}^{-1}$ beginning with $1.5 \times 10^{-3} \text{ erg cm}^{-2} \text{ s}^{-1} \text{ sr}^{-1}$. The [OI] are in steps of $10 \times 10^{-3} \text{ erg cm}^{-2} \text{ s}^{-1} \text{ sr}^{-1}$ beginning with $15 \times 10^{-3} \text{ erg cm}^{-2} \text{ s}^{-1} \text{ sr}^{-1}$. A small area of $\approx 1'$ ($\approx 0.15 \text{ pc}$) around IRC 2 has significant [OI] shock emission. The asterisk and triangle indicate the locations of $\theta^1 \text{ C Ori}$ and IRC 2, respectively.

“diffuse clouds,” which often are identical to the cold-neutral-medium phase ($n \sim 30 \text{ cm}^{-3}$ and $T \sim 100 \text{ K}$) of the ISM. Theoretical models of diffuse clouds appeared in the 1970s (e.g., Glassgold and Langer, 1974, 1976; Black and Dalgarno, 1976, 1977), stimulated by observations with the Copernicus space-borne telescope of ultraviolet absorption lines of trace quantities of rotationally excited H_2 and other species (reviewed by Spitzer and Jenkins, 1975). Somewhat later, thicker molecular clouds ($A_V \sim 2-5$), still studied through absorption lines in stellar spectra, were labeled “translucent clouds.”

The study of dense PDRs on the surfaces of opaque ($A_V >> 2$) molecular clouds was stimulated by the observations of the massive star-forming regions Orion A and M17 in the fine-structure lines [CII] $158 \mu\text{m}$ and [OI] $63 \mu\text{m}$ by Melnick, Gull, and Harwit (1979), Storey, Watson, and Townes (1979), and Russell *et al.* (1980, 1981). The early [CI] $609 \mu\text{m}$ observations of extensive columns of atomic carbon in molecular clouds also stimulated the modeling and understanding of dense PDRs (Phillips and Huggins, 1981; Keene *et al.*, 1985). These observations pointed to predominantly neutral, infrared-luminous regions lying outside the HII regions. Molecules in these PDRs are photodissociated and, for elements like carbon with ionization potentials below 13.6 eV, largely photoionized by the far-ultraviolet fluxes generated by nearby O stars. The luminosity in the [CII] and [OI] lines, which dominate the cooling of the atomic gas, is of order 10^{-3} to 10^{-2} of the infrared (IR) luminosity from the dust that absorbed the starlight. Figure 1 presents a more recent map of the [CII] $158 \mu\text{m}$ and [OI] $63 \mu\text{m}$ emission from Orion A (Herrmann *et al.*, 1997), showing the large extent (5' by 5' or

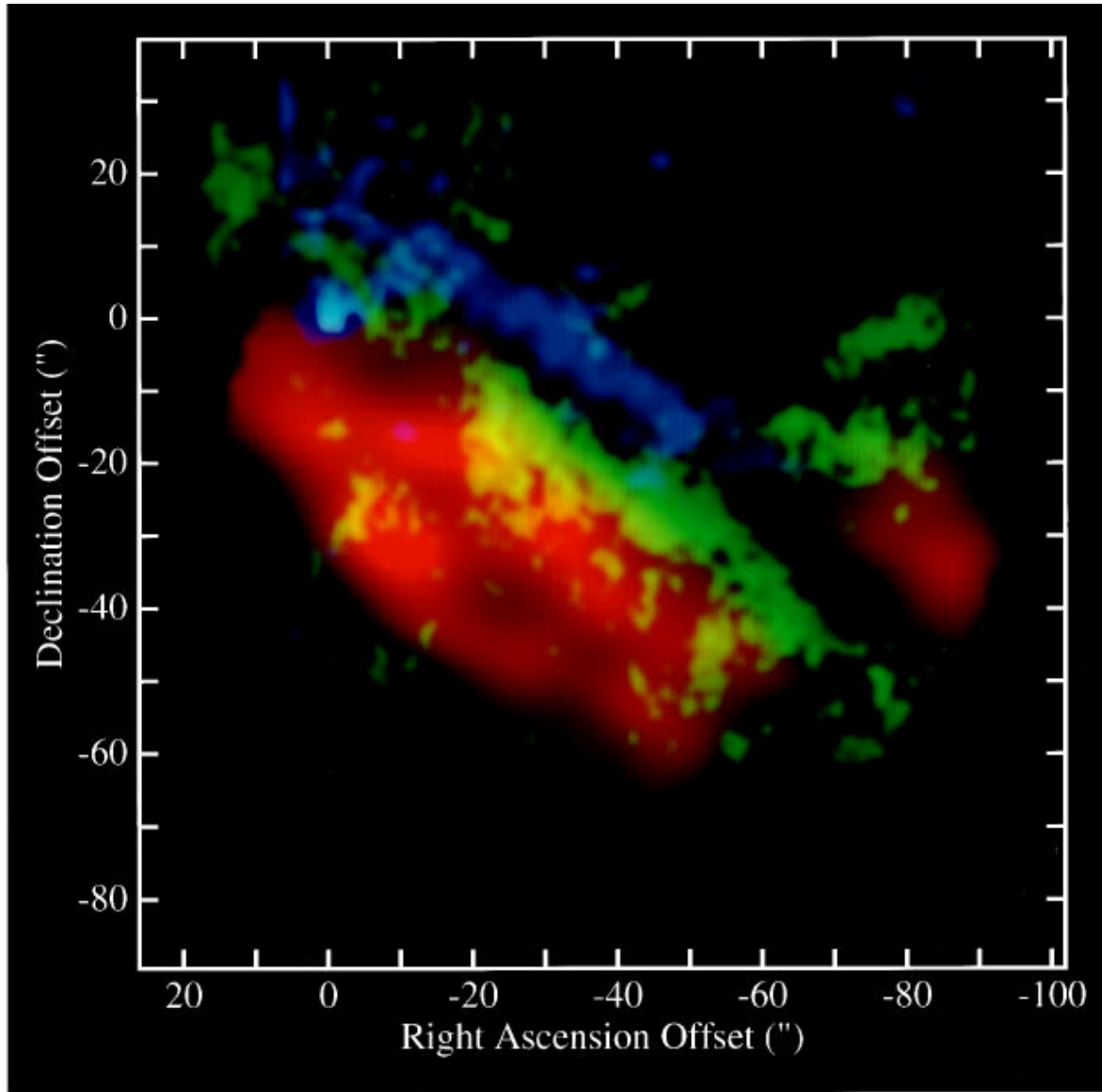


FIG. 2. (Color) The Orion Bar region mapped in the 3.3- μm PAH feature (blue), H_2 1-0 S(1) emission (yellow), and CO $J = 1-0$ emission (red; Tielens *et al.*, 1993). The (0,0) position corresponds to the (unrelated) star θ^2 A Ori. The illuminating source, θ^1 C Ori, and the ionized gas are located to the northwest (upper right). For all three tracers, the emission is concentrated in a bar parallel to but displaced to the southeast from the ionization front. The PDR is seen edge on; a separation of $\approx 10''$ is seen between the PAH emission and the H_2 emission, and between the H_2 emission and the CO emission, as predicted by PDR models (see text).

0.75 pc by 0.75 pc; see footnote 6) and luminosity ($L_{\text{CII}} \sim 80L_\odot$ and $L_{\text{OI}} \sim 600L_\odot$) of the infrared-glowing neutral gas associated with the Trapezium stars. Figure 2 (Tielens *et al.*, 1993) shows a smaller-scale map of the Orion Bar, where the neutral gas outside of the HII region is viewed edge-on. A layered appearance is evident; moving away from the excitation source, the ionization front, HI layer, H_2 emission, and CO emission appear in succession.

⁶Astrophysicists measure distances in parsecs or pc, the distance at which the sun-earth system would subtend 1 arcsecond of angle. 1 pc ≈ 3 light years $\approx 3 \times 10^{18}$ cm.

Despite these historical roots, the study of PDRs is not simply the study of diffuse and translucent clouds and the photodissociated gas that lies just outside of dense, luminous HII regions in the Galaxy; it includes as well the pervasive warm neutral medium, giant molecular clouds, reflection nebulae, the neutral gas around planetary nebulae, photodissociated winds from red giant and asymptotic giant branch stars, and the interstellar medium in the nuclei of starburst galaxies and galaxies with active galactic nuclei. PDRs include all interstellar regions where the gas is predominantly neutral but where far-ultraviolet photons play a significant role in the chemistry and/or the heating. Figure 3 schematically illustrates the structure of an opaque PDR.

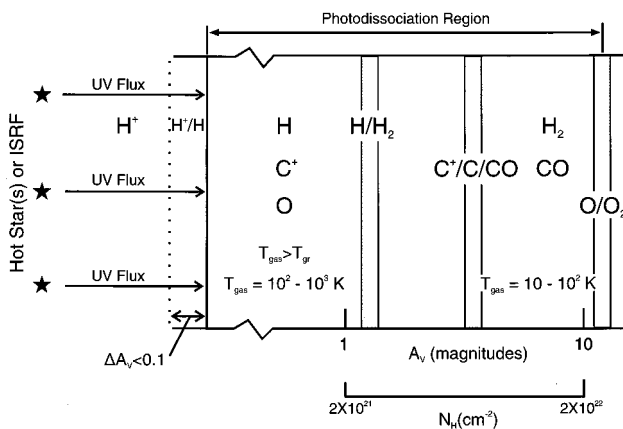


FIG. 3. A schematic diagram of a photodissociation region. The PDR is illuminated from the left and extends from the predominantly atomic surface region to the point where O_2 is not appreciably photodissociated ($A_V=10$). Hence the PDR includes gas whose hydrogen is mainly H_2 and whose carbon is mostly CO. Large columns of warm O, C, C^+ , and CO, and vibrationally excited H_2 are produced in the PDR.

The ultraviolet flux from, for example, the interstellar radiation field (ISRF) or from nearby hot stars is incident on a neutral cloud of hydrogen nucleus density n . The incident far-ultraviolet flux G_0 (in units of an average interstellar flux between $6 \text{ eV} \leq h\nu \leq 13.6 \text{ eV}$ of $1.6 \times 10^{-3} \text{ erg cm}^{-2} \text{ s}^{-1}$; Habing, 1968) can range from the local average ISRF ($G_0 \sim 1.7$; Draine, 1978) to $G_0 \geq 10^6$, appropriate, for example, to gas closer than 0.1 pc from an O star.⁷ Typically, densities n range from $\sim 0.25 \text{ cm}^{-3}$ in the warm neutral medium to $\sim 10\text{--}100 \text{ cm}^{-3}$ in diffuse clouds, to $\sim 10^3\text{--}10^7 \text{ cm}^{-3}$ in the PDRs associated with molecular gas. As illustrated in Fig. 3, PDRs are often overlaid with HII gas and a thin HII/HI interface that absorb the Lyman continuum photons. Although dependent on the ratio G_0/n , the PDR itself is often characterized by a layer of atomic hydrogen which extends to a depth $A_V \sim 1\text{--}2$ (or a hydrogen nucleus column of $N = 2\text{--}4 \times 10^{21} \text{ cm}^{-2}$) from the ionization front (near-infrared emission from PAH molecules absorbing the starlight peaks here), far-ultraviolet-pumped H_2 emission peaking at the HI/ H_2 interface, a layer of C^+ which extends to a depth $A_V \sim 2\text{--}4$, and a layer of atomic oxygen which extends to a

⁷ G_0 is an equivalent one-dimensional flux incident on a PDR; i.e., rates of photoreactions at the surface are equal to the photon flux given by G_0 times the relevant cross sections. For distributed sources and optically thin PDRs, such as diffuse clouds in the interstellar radiation field, G_0 is 4π times the mean intensity. $G_0=1.7$ corresponds to the Draine (1978) ISRF in such a case. For distributed sources and an opaque PDR, the radiation is only incident from 2π steradians at the surface, so that $G_0=0.85$ for the Draine field in this case. However, it should be noted that the attenuation of such a field as a function of A_v into the opaque cloud is not the same as the attenuation of a one-dimensional flux (e.g., from a single point source) incident perpendicular to the surface.

depth $A_V \sim 5\text{--}10$. Atomic carbon largely exists near the C^+/CO interface. Figure 2 observationally shows this morphology in PAH, H_2 , and CO emission. The H, C^+ , and O layers are maintained by the far-ultraviolet photodissociation of molecules and photoionization of C. Diffuse clouds or warm-neutral-medium gas typically have $A_V \lesssim 2$, so they are often nearly entirely atomic.

Traditionally, PDRs have been associated with atomic gas. However, with the above definition, PDRs include material in which the hydrogen is molecular and the carbon mostly in CO, but where far-ultraviolet flux still strongly affects the chemistry of oxygen and carbon not locked in CO (photodissociating OH, O_2 , and H_2O , for example) and the ionization fraction. The transition from C^+ to CO occurs in PDRs, and CO is arguably the most important molecule in astrophysics. Although H_2 is more abundant, CO is more readily observed and has been used extensively as a tracer of molecular gas and star-forming regions. With the exception of the molecular gas in dense, star-forming cores, most molecular gas in the Galaxy is found at $A_V \lesssim 10$ in giant molecular clouds. Therefore, *all of the atomic and at least 90% of the molecular gas in the Galaxy is in PDRs*.

Not only do PDRs include most of the mass of the interstellar medium, but PDRs are the origin of much of the IR radiation from the ISM (the other significant sources are HII regions and dust heated by stars too cool to emit appreciable far-ultraviolet radiation). The incident starlight is absorbed primarily by large carbon molecules (polycyclic aromatic hydrocarbons or PAHs) and grains inside a depth $A_V \sim 1$. Most of the absorbed energy is used to excite the PAHs and heat the grains and is converted to PAH infrared features and far-infrared continuum radiation of the cooling grains. However, typically 0.1–1% of the absorbed far-ultraviolet energy is converted to energetic ($\sim 1 \text{ eV}$) photoelectrons that are ejected from PAHs and grains and that heat the gas (“photoelectric heating”). Although the gas receives $10^2\text{--}10^3$ times less heating energy per unit volume than the dust, the gas attains higher equilibrium temperatures, $T > T_{gr}$, because of its much less efficient cooling (via [CII] 158 μm and [OI] 63 μm) relative to the radiative dust cooling. Much of the [CII], [OI], and [SiII] fine structure, carbon recombination, H_2 rotational and vibrational emission, and CI(9850 \AA) emission in galaxies originates from depths $A_V \lesssim 4$ in PDRs. Most of the [CI] fine structure and the CO rotational emission in galaxies comes from regions somewhat deeper in the photodissociation regions. For example, the 4–1000- μm spectrum of our Milky Way Galaxy (Wright *et al.*, 1991) obtained by the COBE satellite is dominated by PDR emission (see Fig. 4), with the exception of the [NII] and a fraction of the [CII] fine-structure emission, which originates in diffuse HII gas. The [CII] fine-structure transition is often the dominant cooling line from the ISM of a galaxy.

Astronomers use a number of acronyms and units that will be unfamiliar to physicists. We therefore define in Table I the acronyms and units used in this review.

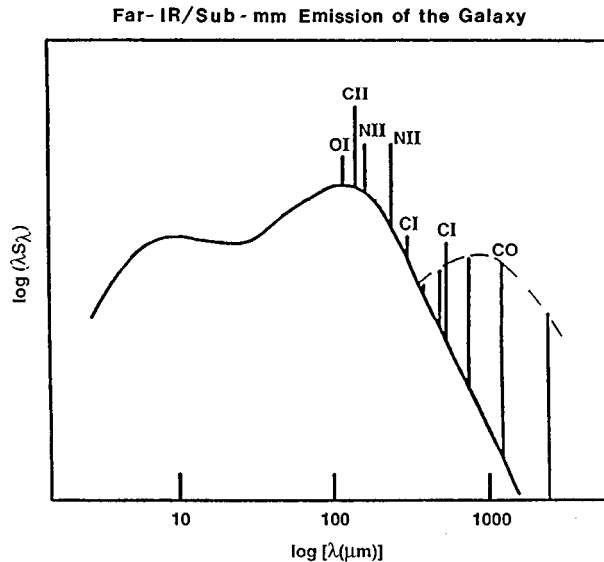


FIG. 4. The Cosmic Background Explorer (COBE) observation of the far-infrared spectrum of our Milky Way Galaxy (Wright *et al.*, 1991; figure from Genzel, 1991). With the exception of the [NII] emission and a controversial portion of the [CII] emission, the bulk of the emission is from PDRs. Note that there is no information from COBE on the line spectrum of the Milky Way at wavelengths less than the [OI] 145 μm line.

We discuss the physical and chemical processes in PDRs in Sec. II, followed by a summary of the theoretical models in Sec. III. The observations of PDRs (Sec. IV) span a wide variety of phenomena, including dense gas around HII regions, reflection nebulae, OH and CH₃OH maser regions, the Galactic Center, and starburst galactic nuclei. PDR models explain the H₂ spectra, the origin of [CI], the correlation of [CII] to CO $J = 1 - 0$, and the correlation of ([CII]+[OI]) to the infrared continuum intensity (Sec. IV). Some PDRs are illuminated by harder radiation fields, such as the neutral gas illuminated by the central stars of planetary nebulae and clouds irradiated by x-ray sources (Sec. V). On the scale of individual clouds illuminated by the interstellar radiation field, PDR models describe diffuse and translucent clouds, the structure of HI or C⁺ halos around molecular clouds, and the scaling of the CO $J = 1 - 0$ luminosity with H₂ mass (Sec. VI). On a global scale, PDR models help explain the origin of the Galactic [CII] emission, the distribution of HI and H₂ in galaxies, the existence and heating of the neutral phases of the ISM, the formation and destruction of molecular clouds, and the regulation of star formation in galaxies (Sec. VII).

Although we have striven to be comprehensive in this review, we do not emphasize here the PDRs associated with mass outflows from giant stars (see the recent review by Glassgold, 1996), or 21-cm HI observations (see Kulkarni and Heiles, 1987). Other PDR reviews include those of Genzel *et al.* (1989), Jaffe and Howe (1989), Hollenbach (1990), Genzel (1991, 1992), Burton (1992), Sternberg (1992, 1998), van Dishoeck (1992), Hollenbach and Tielens (1996, 1997), Sternberg *et al.* (1998), and Walmsley (1998).

TABLE I. Acronyms and astronomical units.

AU	Astronomical Unit, earth-sun distance, $1.5 \times 10^{13} \text{ cm}$
BICE	Balloon-borne Infrared Carbon Explorer
CNM	cold neutral medium, the $T \sim 100 \text{ K}$ phase of the ISM
COBE	Cosmic Background Explorer
CSO	Caltech Submillimeter Observatory
ELD	extended low-density ionized regions of the ISM
EUV	extreme ultraviolet, $h\nu \geq 13.6 \text{ eV}$, capable of ionizing hydrogen
FIR	far infrared
FIRST	Far Infrared and Submillimeter Telescope
FUV	far ultraviolet, $6 \text{ eV} \leq h\nu \leq 13.6 \text{ eV}$
HI	atomic hydrogen
HII	ionized hydrogen
HIM	hot ionized medium, the $T \sim 10^6 \text{ K}$ phase of the ISM
HST	Hubble Space Telescope
IR	infrared
IRAS	Infrared Astronomical Satellite
ISM	interstellar medium
ISO	Infrared Space Observatory
ISRF	interstellar radiation field
JCMT	James Clarke Maxwell Telescope
L_\odot	solar luminosity or $3.9 \times 10^{33} \text{ erg s}^{-1}$
LTE	local thermodynamic equilibrium
M_\odot	solar mass or $2.0 \times 10^{33} \text{ gm}$
NGC	New General Catalogue, a catalogue of optically bright nebulae
PAH	polycyclic aromatic hydrocarbons, large robust organic molecules
pc	parsec, or 3.26 light years, or $3.1 \times 10^{18} \text{ cm}$
PDRs	photodissociation regions, sometimes called "photon-dominated regions"
Proplyds	protoplanetary disks
SOFIA	Stratospheric Observatory for Infrared Astronomy
SWS	Short-wavelength spectrometer on board the ISO
UIR	unidentified infrared emission bands, now identified with PAH origin
UV	ultraviolet
VLBI	very long baseline interferometer
VLT	very large telescope
WIM	warm ionized medium, the $T \sim 10^4 \text{ K}$ ionized phase of the ISM
WNM	warm neutral medium, the $T \sim 10^4 \text{ K}$ neutral phase of the ISM
XDR	x-ray dissociation region

II. PHYSICAL AND CHEMICAL PROCESSES

The many different physical and chemical processes that play a role in the composition and structure of PDRs are all in some way connected to the penetrating far-ultraviolet photons. Radiative transfer in the far-ultraviolet is largely regulated by small dust grains, which dominate the opacity over most of the non-H-ionizing ($h\nu < 13.6 \text{ eV}$) continuum. Some molecules absorb far-ultraviolet radiation in strong lines and dissociate; these molecules can be very important opacity

sources as well. This so-called “self-shielding” can control the abundance gradient through the PDR for a molecule that does the absorbing, and this is particularly important for the abundant H₂ molecule. In general, the penetrating far-ultraviolet photons drive the chemistry through photoionization and photodissociation reactions. The gas also couples thermally to the far-ultraviolet photon flux, but in rather indirect ways. First, heating of the gas can occur through the photoelectric effect on large molecules and small dust grains, whereby the excess kinetic energy of the ejected photoelectron is converted into thermal energy of the gas through collisions. Second, H₂ molecules can be excited through far-ultraviolet photon absorption, and collisional relaxation then leads to heating of the gas. This section discusses some of the more important physical and chemical processes, starting with the dust-dominated radiative transfer of far-ultraviolet photons in the continuum (Sec. II.A). Section II.B.1 discusses various aspects of the H₂ molecule in PDRs, including self-shielding, gas heating, and formation and destruction. PDR chemical networks are more fully discussed in Sec. II.B.2. Heating of the gas through the photoelectric effect is described in Sec. II.C. The various heating and cooling processes are then summarized in Sec. II.D.

A. The penetration of far-ultraviolet radiation

One of the keys to understanding PDR structure lies in understanding the attenuation of the far-ultraviolet continuum flux through the PDR. The penetration of far-ultraviolet radiation is determined by dust absorption and scattering, as well as by the geometry and global structure of interstellar clouds. Various authors have studied the penetration of far-ultraviolet radiation inside homogenous clouds. In particular, Roberge *et al.* (1981, 1991) solved the radiative transfer equation for plane-parallel slabs of various thicknesses using the spherical harmonics method (Flannery *et al.*, 1980) and calculated depth-dependent photodissociation and photoionization rates for a variety of astrophysically relevant molecules. Deep inside semi-infinite slabs, the mean intensity scales with $\exp[-k\xi_\lambda A_V]$, where k is the smallest eigenvalue of the characteristic equation (Flannery *et al.*, 1980), which depends on the scattering properties, ξ_λ is the ratio of the extinction at λ to that at visual wavelength, and A_V is the visual extinction measured from the surface. To first order, k is given by the diffusion approximation,

$$k = \sqrt{3(1-\omega)(1-\omega g)}, \quad (1)$$

with ω the albedo and g the mean cosine of the scattering angle (Flannery *et al.*, 1980). For optically thin ($k\xi_\lambda A_V \lesssim 1$) clouds, a correction factor has to be included for photons penetrating from the other side of the slab. Generally, a biexponential fit to the radiative transfer solution suffices for the depth-dependent photoionization and photodissociation rates (van Dishoeck, 1988; Roberge *et al.*, 1991).

The intensity of the radiation field inside an interstellar cloud depends critically on the adopted absorption and scattering properties of the dust. Generally, theoretical studies rely on either directly measured “average” properties of interstellar dust (see Savage and Mathis, 1979; Mathis, 1990) or on models that fit these “average” properties (e.g., Draine and Lee, 1984). These “average” dust properties refer exclusively to a (biased) sample of lines of sight through diffuse interstellar clouds. Moreover, the dust properties are known to vary from one diffuse cloud to another (Cardelli *et al.*, 1989). Dust in molecular clouds is generally characterized by a high value for R , the ratio of total to selective extinction. If diffuse clouds are a guide, this implies much lower far-ultraviolet extinction per H atom than commonly adopted.

Recently, the far-ultraviolet scattering properties of dust have been measured for the well-studied PDR associated with the reflection nebula NGC 7023. While the data at wavelengths longer than 1600 Å are in good agreement with the dust properties adopted in the widely used molecular dissociation and ionization rates calculated by Roberge *et al.* (1991) and van Dishoeck (1988), at shorter wavelengths there are differences. In particular, rather than remaining constant, the albedo decreases from 0.6 at 1600 Å to 0.4 at 1100 Å (Witt *et al.*, 1992, 1993; Murthy *et al.*, 1993). The scattering phase function is not revised by these new measurements. This decrease in the albedo at shorter wavelengths will lead to higher far-ultraviolet fluxes inside PDRs, and this difference may amount to 50% in $k\xi_\lambda$. For those species which are dissociated or ionized only by photons at the shortest wavelengths (i.e., H₂, CO, CI), this can lead to much enhanced photodissociation and photoionization rates at moderate to high A_V .

In recent years, it has become increasingly clear that interstellar clouds are inhomogeneous on all scales (Falgarene and Phillips, 1996, and references therein). This clumpy nature of interstellar clouds can have a profound influence on the penetration of far-ultraviolet radiation (Stutzki *et al.*, 1988; Boissé, 1990; Spaans, 1996; Hegmann and Kegel, 1996). A schematic illustration of a clumpy molecular cloud is presented in Fig. 5.

The study by Boissé is particularly instructive and establishes simple scaling laws which can be easily adopted for PDR modeling (cf. Tauber and Goldsmith, 1990; Howe *et al.*, 1991; Meixner and Tielens, 1993; Hobson and Scheuer, 1993). Boissé limited himself to isotropic scattering (i.e., $g=0$). His results show that, in most astrophysically relevant cases, the radiative transfer in an inhomogeneous medium can be reduced to that in a homogeneous medium of (lower) effective albedo and extinction coefficient. Consider a two-phase medium consisting of clumps with filling factor p_0 and extinction coefficient κ_0 and an interclump medium with extinction coefficient κ_1 . The effective albedo ω_e and extinction coefficient κ_e of this inhomogeneous medium are a function of p_0 , κ_0 , and κ_1 (Boissé, 1990). Generally, κ_e can be expressed in a simple manner,

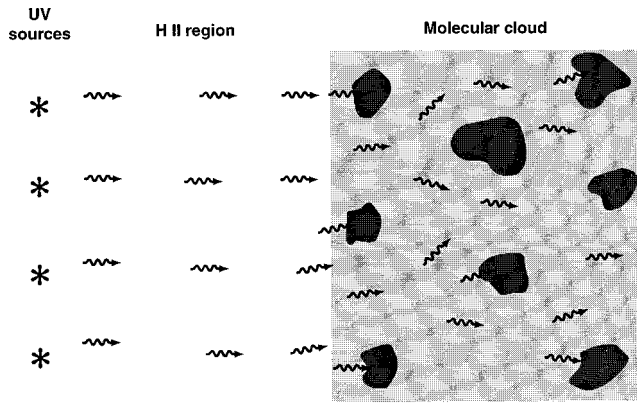


FIG. 5. An illustration of a clumpy photodissociation region (Meixner and Tielens, 1995). The far-ultraviolet photons scatter and penetrate through the interclump material and reach points deeper in the regions than if the material were uniformly spread throughout the region. Photodissociation regions are located on the surfaces of clumps (dark gray) closest to the UV source and throughout the interclump medium (light gray).

$$\kappa_e = \frac{\kappa_o \kappa_1 + \langle \kappa \rangle \ell^{-1}}{\kappa_o + \kappa_1 + \ell^{-1}} \approx \kappa_o \frac{\tau_1 + p_o}{\tau_0 + 1}, \quad (2)$$

where $\langle \kappa \rangle$ is the average opacity [$= p_o \kappa_o + (1 - p_o) \kappa_1$], ℓ is the correlation length (i.e., clump size), and the optical depth scale τ_i is given by $\kappa_i \ell$. Thus, depending on the clump filling factor and the density contrast between clump and interclump gas, the penetration of far-ultraviolet radiation can vary by orders of magnitude (Boissé, 1990). Figure 6 shows an example of the effects of clumps on the intensity of the penetrating far-ultraviolet field. For example, in the limit $\tau_o \gg 1$ and $\tau_1 \gg p_o$ (few clumps), the effective extinction coefficient is equal to κ_1 and the solution is well described by the homogenous solution for the interclump gas. In the opposite limit, $\tau_1 \ll p_o$ (empty interclump medium), κ_e is equal to $p_o \ell^{-1}$ or $p_o \kappa_o$, depending on the ratio of the extinction size scale to the clump size scale. In this limit the clumps control the far-ultraviolet penetration.

Observations show that bright PDRs, such as the Orion Bar or the M17SW core, are in the first limit where the interclump gas controls the far-ultraviolet penetration. For typical parameters of the M17SW core, for example, the effective extinction coefficient, $\kappa_e \approx \kappa_1$, is about 10 pc^{-1} . The same mass distributed homogeneously would have an extinction coefficient of $\approx 420 \text{ pc}^{-1}$ (Stutzki *et al.*, 1988; Meixner and Tielens, 1993). Thus, over the size of this core (2 pc), the far-ultraviolet extinction is 20 in the clumped distribution as compared to 840 for the homogenous distribution. The second limit discussed above seems to be more appropriate for penetration of far-ultraviolet radiation in giant molecular clouds, where the clump to interclump contrast is very large, $\gtrsim 10^3$. With scale sizes of 35 AU, densities of $5 \times 10^4 \text{ cm}^{-3}$, $\tau_o = 0.03$, a volume filling factor of 0.003 for the clumps, and interclump densities of $\approx 50 \text{ cm}^{-3}$ (Falgarone and Phillips, 1996), shadowing of

one clump by another now regulates molecular abundances.

One important characteristic of far-ultraviolet penetration into clumpy clouds is the existence of large fluctuations in the mean intensity at a given depth (Boissé, 1990; Spaans, 1996). These fluctuations are particularly important when individual clumps are optically thick, scattering in the clump or interclump gas is unimportant ($\kappa_1 / \kappa_o \ll 1$), and the cloud is illuminated by a unidirectional field (i.e., a nearby star). This is illustrated in Fig. 7, which shows that, for these conditions, at great depth the variance becomes larger than the average intensity. In this limit, the far-ultraviolet field can fluctuate by $\sim \exp(\tau_o)$ (Monteiro, 1991; Störzer *et al.*, 1997). When any of these restrictions is relaxed, fluctuations become of lesser importance and may be no more than a small factor in realistic situations (Boissé, 1990).

B. Chemistry in PDRs

PDR chemistry has been discussed in detail by Tielens and Hollenbach (1985a, 1985c), Hollenbach *et al.* (1991), Le Bourlot *et al.* (1993), Fuente *et al.* (1993, 1995), Jansen *et al.* (1995a, 1995b), Sternberg and Dalgarno (1995), and Bergin *et al.* (1997). It derives rather directly from the chemistry of those more transparent PDRs, diffuse and translucent clouds (Glassgold and Langer, 1974, 1976; Black and Dalgarno, 1977; Federman *et al.* 1980, 1984, 1994; Danks *et al.*, 1984; van Dishoeck and Black, 1986, 1988, 1989; Viala, 1986; Viala *et al.*, 1988; Federman and Huntress, 1989; van Dishoeck, 1991; Heck *et al.*, 1992; Turner, 1996, and references therein). PDR chemistry differs from standard, interstellar, ion-molecule chemistry⁸ in a number of ways. Obviously, because of the high far-ultraviolet flux, photoreactions are very important, as are reactions with atomic H. The formation and photodissociation of H₂ is central to PDRs, and we begin with a discussion of H₂ chemistry and H₂ far-ultraviolet-pumped heating. Once H₂ has formed on grain surfaces and evaporated into the gas, gas-phase chemistry can produce the other species. Electron recombination and charge-exchange reactions are important for the ionization balance. Photodissociation of CO and photoionization of C keeps carbon in C⁺ relatively deep into the cloud and produces significant columns of C at intermediate depths. The far-ultraviolet

⁸Standard interstellar chemistry is concerned with reactions inside dense molecular cloud cores that are opaque to far-ultraviolet photons. Such cores can still be penetrated by energetic cosmic-ray particles, leading to ionization of the abundant H₂ and He. This ionization can be passed on to other species through charge-transfer reactions until it is finally lost through recombination reactions. The resulting low level of nonequilibrium ionization drives the chemistry in these regions. In contrast to most neutral-neutral reactions, exothermic ion-molecule reactions generally possess no activation barriers, because of the Coulomb energy, and consequently are fast even at the low interstellar temperatures and densities. For a review, see Herbst (1987).

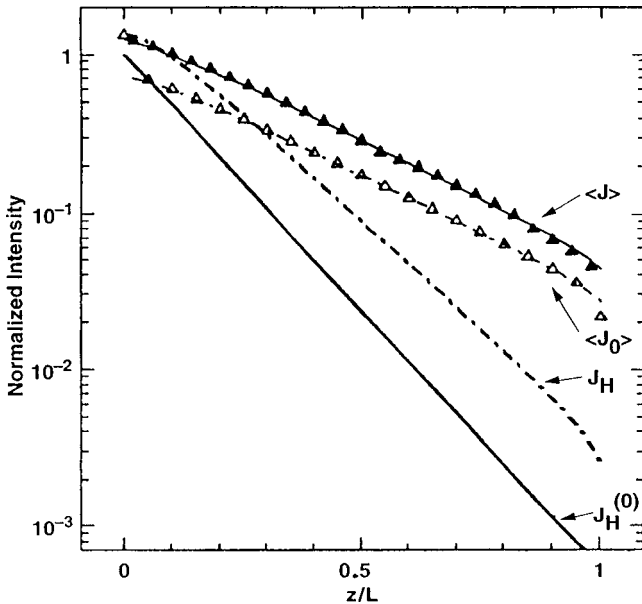


FIG. 6. The average intensity inside a layer (size L) with an average optical depth ($\langle \kappa \rangle L$) of 7.5, a clump filling factor $p_o = 0.1$, and optical depth scales $\tau_o = 2.5$ and $\tau_1 = 0.0556$ (Boissé, 1990). The mass fraction in the clumps is then ≈ 0.8 . The adopted albedo ω is 0.6. The results of numerical calculations are shown as triangles. For these parameters, $\langle J \rangle$ is essentially the average intensity incident upon the surface of a clump at a depth z in the PDR, while $\langle J_o \rangle$ is the average intensity in the clump. The results for a homogenous model, J_H , with the same ω and τ is shown for comparison, while $J_H^{(0)}$ is the average intensity due to incident photons that made it to that depth without scattering. These averaged intensities are normalized to the incident intensity and hence, because of backscattering, they may exceed unity at the surface.

flux keeps atomic O very abundant throughout the PDR, and hence burning reactions are effective. Absorption of a far-ultraviolet photon by H_2 , followed by radiative decay, will generally leave the molecule vibrationally excited. This far-ultraviolet pumping makes vibrationally excited H_2 abundant, and this species can play a decisive role in PDR chemistry. If the gas gets very warm (≥ 500 K) or if the translational motion is non-Maxwellian, the activation barrier of reactions of atoms and radicals with H_2 can be easily overcome, and these types of reactions can dominate.

1. H_2 formation, destruction, and heating

The formation of H_2 in the ISM proceeds on the surfaces of interstellar dust grains (see Hollenbach and Salpeter, 1970, 1971; Hollenbach *et al.*, 1971), and the H_2 formation rate per unit volume, R_f , can be expressed as

$$R_f = \frac{1}{2} S(T, T_{gr}) \eta(T_{gr}) n_{gr} n_H \sigma_{gr} v_H, \quad (3)$$

where $S(T, T_{gr})$ is the sticking probability of an H atom with temperature T colliding with a grain of temperature T_{gr} , $\eta(T_{gr})$ is the probability that a “stuck” H atom will migrate across the grain surface, find another

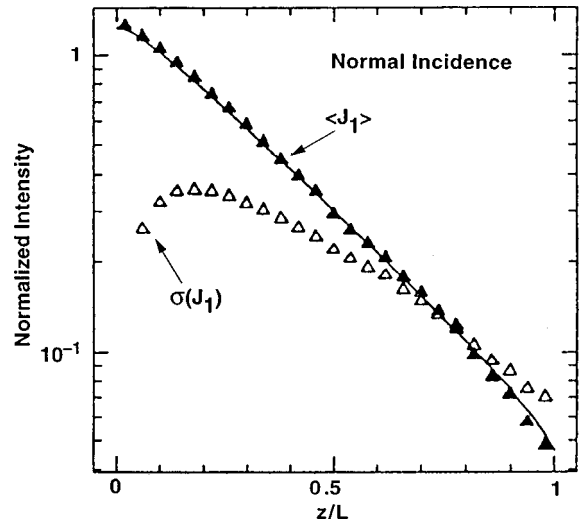


FIG. 7. The average intensity incident upon clumps and its rms fluctuations for the same parameters as for Fig. 6 (Boissé, 1990). The results of numerical calculations are shown as triangles. Normal incidence is assumed. These averaged intensities are normalized to the incident intensity and hence, because of backscattering, they may exceed unity at the surface.

H atom, and form H_2 before evaporating from the grain surface, n_{gr} is the grain number density, n_H is the H atom density, σ_{gr} is an average grain cross section, and $v_H \propto T^{1/2}$ is the thermal speed of the H atoms. Equation (3) represents an integral over the distribution of grain sizes, so that $n_{gr}\sigma_{gr}$ represents an average cross-sectional area per unit volume of space. Typically, $n_{gr}\sigma_{gr} \sim n(10^{-21} \text{ cm}^{-2})$ and $v_H \sim 10^5 T_2^{1/2} \text{ cm s}^{-1}$, where $T_2 = T/100$ K. Equation (3) becomes then $R_f = 5 \times 10^{-17} T_2^{1/2} S(T, T_{gr}) \eta(T_{gr}) n n_H \text{ cm}^{-3} \text{ s}^{-1}$. For sufficiently low temperatures, S and $\eta \sim 1$, but S and η tend to decrease with increasing temperature as atoms bounce from the grain surfaces or evaporate before reacting. Burke and Hollenbach (1983), Hollenbach and McKee (1989), and Buch and Zhang (1991) make theoretical estimates of the T and T_{gr} dependence of S and η . Lin and Vidali (1996) and Pirronello *et al.* (1997a, 1997b) have recently reported new laboratory measurements of S .

Much of the existing literature is, for historical reasons, geared towards H physisorbed on interstellar (ice) surfaces or on surfaces with nearly all the chemical bonds saturated. Graphitic and silicate surfaces, which are currently considered likely interstellar grain surfaces, may have a large fraction of chemisorption sites with binding energies of 1–2 eV. H_2 formation on a purely chemisorbing surface has been touched upon in an astrophysical context by Tielens and Allamandola (1987). Balancing H accretion and H_2 formation by neighboring chemisorbed H atoms, the surface coverage of chemisorbed H, θ_H , is then given by $\theta_H = a/[1 + 4/a]^{0.5} - 1$, where a is the ratio of the accretion rate to the reaction rate (per site); viz., $a = 10^{-23} n_H T^{0.5} S(T) \exp[E_a/kT_{gr}]$. The activation barrier for the reaction of neighboring chemisorbed H atoms,

E_a/k , is approximately 1000 K for both graphite and silicates (Tielens and Allamandola, 1987, and references therein). For typical diffuse ISM conditions ($T_{gr} \approx 10$ K), $a \gg 1$ and θ_H is very close to unity. At low T_{gr} , sticking will still occur initially in the physisorbed sites on “top” of the chemisorbed H layer and the temperature dependence of S and η is described by the theoretical studies mentioned above. However, for high T but low T_{gr} , H_2 formation can proceed by direct reaction between an impinging H atom and the chemisorbed H it hits, rather than by reaction between adsorbed species. This will limit the factor by which the impinging H flux is reduced in Eq. (3); i.e., the factor $S(T, T_{gr})\eta(T_{gr})$ in Eq. (3) is then given by $\exp(-E_a/kT)$. For dense PDRs, however, where $T_{gr} \gtrsim 50$ K, a is much less than 1 and $\theta_H \approx a/2$. Neighboring chemisorbed atoms can react with each other to form H_2 , evaporate from the surface, and leave the surface quite bare. In this case, the sticking coefficient may be much less affected by the gas temperature, since the adsorption potential well depth is now so deep as to trap (chemisorb) the incoming gas atoms. In this limit, all H that sticks will leave through H_2 formation [i.e., $\eta(T_{gr})=1$].

Overall, the theoretical and laboratory results have not been completely developed and their applicability to interstellar dust remains uncertain. Given the uncertainties in interstellar dust properties, the best solution at present may be to derive the rate coefficient semiempirically by comparison of PDR models with observations, which give

$$R_f = \gamma_{H_2} n n_H, \quad (4)$$

with a rate coefficient $\gamma_{H_2} \sim 1-3 \times 10^{-17} \text{ cm}^3 \text{ s}^{-1}$ (Jura, 1975; Andersson and Wannier, 1993).

Photodissociation and self-shielding of H_2 have been studied by Field *et al.* (1966), Stecher and Williams (1967), Hollenbach *et al.* (1971), Jura (1974), Black and Dalgarno (1977), Shull (1978), Federman *et al.* (1979), de Jong *et al.* (1980), van Dishoeck and Black (1986), Abgrall *et al.* (1992), Heck *et al.* (1992), LeBourlot *et al.* (1995), and Lee *et al.* (1996); the field has been reviewed by van Dishoeck (1987) and recently discussed in detail by Draine and Bertoldi (1996). H_2 absorbs far-ultraviolet photons via Lyman and Werner electronic transitions in the 912–1100-Å range. The electronically excited state fluoresces to the vibrational continuum of the ground electronic state about 10–15% of the time (see Fig. 8). The H_2 photodissociation rate then follows from a summation over all lines. When the H_2 column density exceeds 10^{14} cm^{-2} , the far-ultraviolet absorption lines become optically thick and self-shielding becomes important. The photodissociation rate then depends on the H_2 abundance and level population distribution as a function of depth in the cloud. Various approximations, appropriate for chemical modeling, have been described by Jura (1974), Federman *et al.* (1979), van Dishoeck and Black (1986), and Draine and Bertoldi (1996).

An understanding of the HI/ H_2 transition can be gained by using the simplest self-shielding approxima-

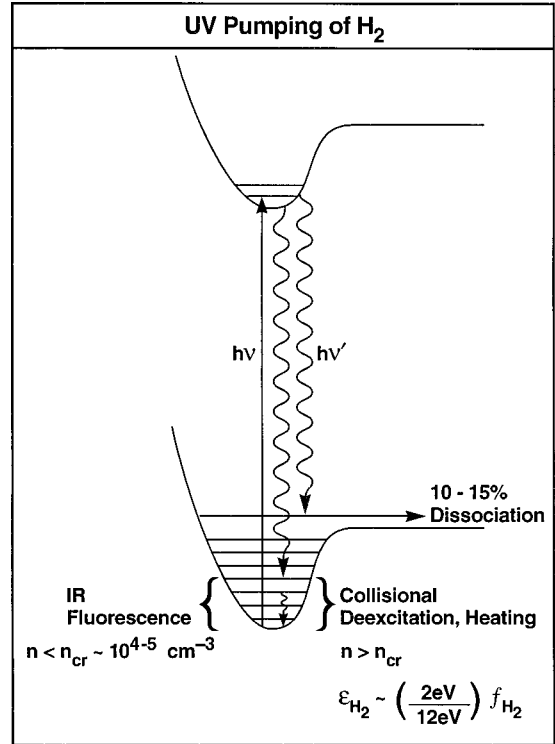


FIG. 8. A schematic of the H_2 far-ultraviolet pumping, dissociation, and heating mechanisms for PDRs. Far ultraviolet fluorescence can leave a H_2 molecule vibrationally excited in the ground electronic state. Collisional deexcitation of this excited molecule can then heat the gas. In about 10–15% of the pumping cases, the cascade goes to the vibrational continuum of the ground electronic state, which leads to photodissociation of the H_2 molecule. A simple expression for the heating efficiencies ϵ is indicated. See text for details.

tion given by Draine and Bertoldi (1996). The photodissociation rate of H_2 per unit volume, R_{diss} , is given as

$$R_{\text{diss}} = f_{\text{shield}}(N_{H_2}) e^{-\tau_{gr,1000}} I_{\text{diss}}(0) n_{H_2}, \quad (5)$$

where n_{H_2} is the H_2 density, $I_{\text{diss}}(0) \approx 4 \times 10^{-11} G_0 \text{ s}^{-1}$ is the unshielded dissociation rate per H_2 , $\tau_{gr,1000}$ is the optical depth of the dust at 1000 Å, N_{H_2} is the H_2 column density into the PDR, and f_{shield} is the self-shielding factor given approximately (accurate to a factor of ~ 1.5) by

$$f_{\text{shield}} = 1, \quad N_{H_2} \leq 10^{14} \text{ cm}^{-2},$$

$$f_{\text{shield}} = \left(\frac{N_{H_2}}{N_0} \right)^{-0.75}, \quad N_0 = 10^{14} \text{ cm}^{-2} \leq N_{H_2} \leq 10^{21} \text{ cm}^{-2}. \quad (6)$$

Equating the H_2 formation rate [Eq. (4)] with the photodissociation rate [Eq. (5)] in the region $N \leq 10^{21} \text{ cm}^{-2}$, so that dust opacity is negligible, we obtain the following steady-state expression for N_{H_2} and the H_2 abundance $x_{H_2} = n_{H_2}/n$ as a function of the column density of hydrogen nuclei, $N = N_{\text{H}} + 2N_{H_2}$, in the PDR,

$$N_{\text{H}_2} = A^4 \left(\frac{N}{N_0} \right)^4 N_0, \quad (7)$$

$$x_{\text{H}_2} = 4A^4 \left(\frac{N}{N_0} \right)^3, \quad (8)$$

where $A = \gamma_{\text{H}_2} n / [4I_{\text{diss}}(0)]$ (note that $A \propto n/G_0$, a ratio which controls the PDR structure). Equations (7) and (8) are approximately correct if $N_0 = 10^{14} \text{ cm}^{-2} \leq N_{\text{H}_2} \leq 10^{21} \text{ cm}^{-2}$ and if $N \leq 10^{21} \text{ cm}^{-2}$. Setting $x_{\text{H}_2} = 1/4$ in Eq. (8), we obtain the hydrogen nucleus column density N_{DF} in the PDR, where the gas is half molecular and half atomic (the HI/H₂ interface or dissociation front):

$$N_{\text{DF}} = 5A^{-4/3}N_0. \quad (9)$$

The dust opacity becomes important when $N_{\text{DF}} \gtrsim 5 \times 10^{20} \text{ cm}^{-2}$, or when

$$G_0/n \gtrsim 4 \times 10^{-2}, \quad (10)$$

assuming $\gamma_{\text{H}_2} = 3 \times 10^{-17} \text{ cm}^3 \text{ s}^{-1}$.

Self-shielding alone dominates H₂ dissociation and hence the location of the HI/H₂ transition when $G_0/n \leq 4 \times 10^{-2} \text{ cm}^3$. This includes diffuse clouds exposed to the interstellar radiation field and dense clumps in PDRs with higher far-ultraviolet fluxes. Because of the self-shielding, the H₂ column and abundance increase rapidly with depth N or, equivalently, distance if the PDR has constant n [see Eqs. (7) and (8), $N_{\text{H}_2} \propto N^4$ and $x_{\text{H}_2} \propto N^3$]. Therefore the HI/H₂ transition zone is very sharp.

Photodissociation regions associated with bright far-ultraviolet sources typically have $G_0/n \sim 1 \text{ cm}^{-3}$. The location of the HI/H₂ transition is then dominated by dust absorption and typically occurs at $A_V \approx 2$. At that point, dust has reduced the H₂ photodissociation rate sufficiently that an appreciable column of H₂ can build up, H₂ self-shielding takes over, and the HI/H₂ transition will be very rapid again. For warm dense PDRs ($n \gtrsim 10^6 \text{ cm}^{-3}$, $G_0 \gtrsim 10^4$), chemical destruction of H₂ through reaction with abundant C⁺ and O can change the location of the HI/H₂ dissociation front from that predicted by Eq. (9) (Bertoldi, 1998).

As discussed above, the line absorption of a far-ultraviolet photon will pump H₂ molecules to a bound excited electronic state, from which they will fluoresce back to the vibrational continuum of the ground electronic state and dissociate (10–15% of the time) or they will fluoresce back to an excited vibrational state in the electronic ground state (85–90% of the time, Fig. 8). Typically, a pump leads to a molecule with $E_{\text{vib}} \sim 2 \text{ eV}$ of vibrational energy. At low densities, the excited (bound) vibrational states can cascade down to the ground vibrational state through the emission of IR photons, giving rise to a characteristic far-red and near-IR rovibrational spectrum (see Sec. IV.B). At high densities, $n \gtrsim 10^{4-5} \text{ cm}^{-3}$ depending on T (Martin and Mandy, 1995; Martin *et al.*, 1996), collisions with atomic H can also be an important deexcitation mechanism, leading to heating of the gas and thermalization of the rovibrational states. The heating efficiency of this process is then ap-

proximately $\epsilon_{\text{H}_2} \approx (E_{\text{vib}}/h\nu)f_{\text{H}_2} \approx 0.17f_{\text{H}_2}$. The fraction of the far-ultraviolet photon flux pumping H₂ ($13.6 \geq h\nu \geq 11 \text{ eV}$), f_{H_2} , depends on the location of the HI/H₂ transition zone (Draine and Bertoldi, 1996). Thus, when $G_0/n \leq 4 \times 10^{-2} \text{ cm}^3$, H₂ self-shielding is important, the H₂ transition is near the surface, and most of the photons that can pump H₂ are absorbed by H₂ rather than dust. Under these conditions, $n > n_{cr}$ and $G_0/n \leq 4 \times 10^{-2} \text{ cm}^3$, $f_{\text{H}_2} \approx 0.25$, and this process provides an efficient coupling to the far-ultraviolet photon flux of the star. Figure 8 schematically summarizes H₂ heating. Sternberg and Dalgarno (1989) and Burton, Hollenbach, and Tielens (1990) provide a detailed description of how H₂ heating depends on G_0 and n .

2. Non-Maxwellian chemistry

Neutral-neutral reactions are often endothermic and/or possess appreciable activation barriers, since bonds have to be broken or rearranged. In PDRs, reactions of molecular hydrogen with C⁺, O, N, S⁺, and Si⁺ are particularly important in initiating the chemistry. Far-ultraviolet pumping of H₂ can lead to a vibrational excitation temperature that is considerably higher than the gas temperature. Reactions with vibrational hot H₂ (H₂^{*}) have been discussed in an astrophysical context by Wagner and Graff (1987). Nonequilibrium excitation conditions can give rise to reaction rates that are considerably enhanced over the thermal ones (Gardiner, 1977; Dalgarno, 1985). The reaction of atomic O with H₂ is a case in point. In the ground state, this reaction is endothermic by 1000 K and has an activation barrier of ≈ 4500 K. In contrast, the reaction of O(³P) with H₂^(v=1) is exothermic by ≈ 5000 K and the reaction rate is measured to be enhanced over the ground-state rate by a factor of 3000 at 300 K (Light, 1978). Quantum chemical studies show an even larger enhancement for H₂ in higher vibrational states (Schinke and Lester, 1979; Schatz *et al.*, 1981; Lee *et al.*, 1982). Rotational excitation can play a similar role in promoting this reaction (Schinke and Lester, 1979; Herbst and Knudson, 1981; Wagner and Graff, 1987), but that is of little importance in PDRs.

Other reactions can likewise be affected by vibrational excitation. Studies of the OH+H₂^{*} and C⁺+H₂^{*} reactions show a large enhancement with vibrational excitation of H₂ (Light, 1978; Schinke and Lester, 1979; Schatz and Elgersma, 1980; Schatz, 1981; Schatz *et al.*, 1981; Lee *et al.*, 1982; Jones *et al.*, 1986). However, state-to-state chemistry is very selective and, for example, vibrational excitation of OH does not enhance the reaction rate of OH+H₂. Since the vibrational excitation energy of far-ultraviolet pumped H₂ ($\approx 2.5 \text{ eV}$) is so much larger than the typical activation barriers of reactions of interest ($\approx 0.5-1.0 \text{ eV}$), most studies of the chemistry in PDRs generally assume that reactions with H₂^{*} occur at the collision rate. Nevertheless, it is not always correct to assume that the activation barrier will be reduced by the vibrational excitation energy of the coreactants.

Translational energy can also be effective in promoting chemical reactions. In particular, the presence of turbulence can lead to non-Maxwellian velocity fields and hence non-Maxwellian reaction rates. This effect has been evaluated in detail by Spaans *et al.* (1999) for the reaction $\text{C}^+ + \text{H}_2$, which is endothermic by 0.4 eV. Using a detailed model for the cascade of interstellar turbulence to the small size scales relevant for chemical reactions and adopting measured reaction cross sections as a function of translational energy, they report reaction rates of $10^{-14} - 10^{-13} \text{ cm}^3 \text{s}^{-1}$ for the turbulent conditions ($\Delta v = 1 - 2 \text{ km/s}$) appropriate for PDRs. Because of their larger activation barriers, the reactions $\text{O} + \text{H}_2$ and $\text{N} + \text{H}_2$ are much less affected. Because of the absence of reaction cross sections, Spaans and Jansen (in preparation; see Spaans, 1995) have evaluated in a simplified way the effects of turbulence on sulfur chemistry. These reaction rates can only be considered indicative until the specific dependence of cross sections on translational and vibrational excitation are known. Finally, Falgarone *et al.* (1995) examined the enhancement of OH, H_2O , CH^+ , and HCO^+ in turbulent PDRs.

3. PDR chemical networks

a. Oxygen and carbon

The most important reactions in the chemistry of carbon and oxygen compounds are schematically shown in Fig. 9. Figure 9 is adapted from Sternberg and Dalgarno (1995), who provide a detailed discussion of PDR chemistry. The emphasis here is on small species and, for example, reactions of carbon hydrides with C^+ to form species with two or more carbon atoms have been ignored. The PDR surface layer consists largely of neutral or cationic atoms created by photodissociation and ionization reactions. Atomic O is in rapid equilibrium with O^+ through charge exchange with protons produced by cosmic-ray ionization of H. In regions with low far-ultraviolet fields (i.e., the general diffuse ISM), the chemistry of oxygen-bearing compounds is then initiated by reactions of O^+ with H_2 (van Dishoeck, 1998). Subsequent reactions with H_2 will lead to H_2O^+ and H_3O^+ . These species dissociatively recombine to OH and H_2O (Fig. 9). However, in (warm) regions with high far-ultraviolet fields, oxygen-bearing radicals (i.e., OH) are built up through reactions of O with H_2^* and H_2 . Most of the OH produced is photodissociated again but a small fraction reacts with C^+ to form CO^+ which charge exchanges with H to form CO. Some CO^+ is also formed through the reaction of CH^+ with O ("burning"). The CO photodissociates again.

The C^+/C balance is generally dominated by photoionization and radiative recombination reactions. A small fraction of the C^+ reacts with H and H_2^* to form CH^+ . Likewise, a small fraction of the neutral C flows to CH through reaction with H_2^* . Through reactions with H, CH^+ , and CH reform C^+ and C, respectively. Photo-reactions are important for C, OH, and CO but, because of their high reactivity, not for the small hydrocarbon radicals and cations. With increasing depth in this so-

called "radical" zone (but recall that, except for H_2 , it is largely atomic), the chemistry involving small radicals, such as the CH_n^+ family and OH, becomes more important. In cool, low-density PDRs, reactions with far-ultraviolet-pumped, vibrationally excited H_2^* are important, while in warm, high-density PDRs, reactions with thermal H_2 molecules dominate. In the latter case, reactions of C^+ with H_2 followed by dissociative electron recombination of CH^+ to C can be an important recombination route for C^+ . This same reaction can be an important destruction mechanism for warm H_2 . As the depth increases, CO formation by burning of small neutral radicals (i.e., CH, CH_2) becomes more important than the OH-driven channel. The CO^+ , produced through the reaction of C^+ with OH, now reacts with H_2 to form HCO^+ , which dissociatively recombines to CO. This is the start of the $\text{C}^+/\text{C}/\text{CO}$ transition zone. Neutralization of C^+ through charge transfer with atomic S becomes a dominant source of C. Eventually, PDR chemistry gives way to standard dark-cloud, ion-molecule chemistry (Prasad and Huntress, 1980; Herbst and Leung, 1989). Formation of OH and H_2O is now initiated through the reaction of H_3^+ with O. Reactions of atomic O with OH then form O_2 .

The transition from C^+ to CO occurs in PDRs, and CO is used to trace molecular gas in the Galaxy (see Sec. VI.B.3). As discussed above, the formation of CO is via several gas-phase chemical routes, and the formation rate tends to be relatively small because the reactants tend to have low abundances. Therefore even a fairly attenuated far-ultraviolet field can appreciably photodissociate CO and produce C and C^+ deep into the cloud. Photodissociation of CO has been studied in detail by Bally and Langer (1982), Glassgold *et al.* (1985), van Dishoeck and Black (1988), Viala *et al.* (1988), and Lee *et al.* (1996). High-resolution laboratory studies show that CO photodissociation occurs through discrete absorption into predissociating bound states, implying that CO is also affected by self-shielding (Eidelsberg *et al.*, 1992). Further complications arise because of line coincidences with H and H_2 . CO shielding functions have been tabulated by van Dishoeck and Black (1988) and by Lee *et al.* (1996). For low ratios of G_0/n , the effects of CO self-shielding can lead to isotopic fractionation effects at the borders of clouds, where the rarer CO isotopes are preferentially photodissociated (Bally and Langer, 1982; Chu and Watson, 1983; Glassgold *et al.*, 1985; van Dishoeck and Black, 1988; Viala *et al.*, 1988; Grede *et al.*, 1994; Minchin *et al.*, 1995; Warin *et al.*, 1996; Keene, Schilke, *et al.* 1998). However, the location of the $\text{C}^+/\text{C}/\text{CO}$ transition in bright PDRs is largely governed by dust extinction. Because of the much lower abundance of CO relative to H_2 , the CO rarely builds up sufficient column to self-shield in the $A_V \leq 1$ layer, and the $\text{C}^+/\text{C}/\text{CO}$ transition is much less sharp than for H/ H_2 . Like H_2 , CO abundances can be appreciable near the surfaces of dense clumps. However, that is not a result of self-shielding but rather reflects the high H_2 abun-

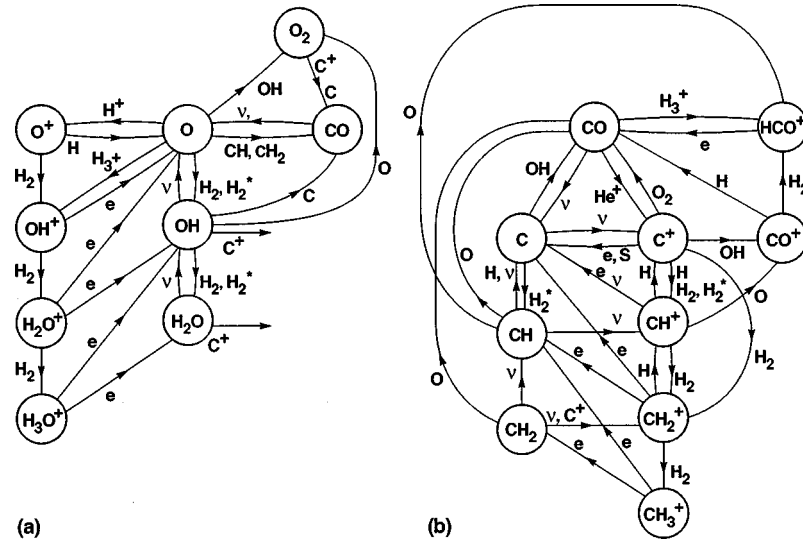


FIG. 9. The most important reactions involved in the PDR chemistry of oxygen-bearing (left) and carbon-bearing (right) compounds (adapted from Sternberg and Dalgarno, 1995).

dance near the surfaces of such clumps which leads to an enhanced CO formation rate.

b. Nitrogen

Nitrogen chemistry in PDRs [Fig. 10(a)] has been discussed by Jansen *et al.* (1995a, 1995b), Sternberg and Dalgarno (1995), Fuente *et al.* (1996), and Young Owl *et al.* (1999) and by Pineau des Forets *et al.* (1990) for dark clouds. At the surface, much of the nitrogen is kept in atomic form by the strong far-ultraviolet flux. N chemistry is then initiated by the reaction of atomic N with vibrationally excited H_2 (H_2^*) to form NH. Reaction with abundant C^+ and with H_2 then leads to the molecular ion H_2CN^+ , which dissociatively recombines to HCN, HNC, and CN. The latter two form HCN through reactions with H and H_2 . Far-ultraviolet photons drive the system back to N and C^+ . Deep in the PDR, N_2 is, of course, the dominant N-bearing species. Atomic N is liberated through reactions of N_2 with He^+ (produced by cosmic-ray ionization). Reaction of N with HCO (formed through charge exchange between HCO $^+$ and neutral metals and PAHs) then leads to HCN formation. Proton transfer, dissociative electron recombination, and reaction with H shuffle the HCN and HNC species. Ammonia is never a very abundant molecule in the PDR surface layers, because the reactions of atomic N with H_2 have a high activation barrier. Deep inside, NH $_3$ is formed through a sequence of reactions starting with $OH + N \rightarrow NO + H$ (see Pineau des Forets *et al.*, 1990). NO reacts with C^+ or He^+ to form N $^+$. The latter can rapidly react with H_2 to form the hydride ions, NH $_n^+$, and protonated ammonia dissociatively recombines to NH $_3$ and NH $_2$. NH $_2$ burns with atomic O to NH + OH. NH also burns with atomic O to OH + N. In contrast, the reaction of NH $_3$ with O has a 3000 K Arrhenius factor. However, proton transfer of NH $_3$ with HCO $^+$ and H $_3O^+$ leads back to NH $_4^+$, which half of the

time channels back to NH $_2$, and this limits the abundance of NH $_3$ inside dense clouds.

c. Sulfur and silicon

Sulfur chemistry in PDRs [See Fig. 10(b)] has been discussed by Jansen *et al.* (1995a, 1995b) and Sternberg and Dalgarno (1995), and in dark cores by Prasad and Huntress (1982), Millar and Herbst (1990), and Charnley (1997). Because of its low ionization potential (10.4 eV), atomic sulfur is largely ionized at the surface and recombines somewhat deeper in the PDR than C $^+$ (ionization potential 11.3 eV). Neutral atomic sulfur is the dominant sulfur species for much of the remainder of the PDR (until $A_V \approx 8$ for $G_0/n \approx 1$). Most of the PDR studies published therefore considered only these two S species (see Tielens and Hollenbach, 1985a). Around an A_V of 4 (for $G_0/n \approx 1$), charge-exchange reactions of neutral sulfur with C $^+$ are an important source of neutral carbon (Tielens and Hollenbach, 1985c). As for nitrogen chemistry, the difficulty in initiating sulfur chemistry rests in the endothermicity of reactions of H $_2$ with the dominant (sulfur) reservoir, S and S $^+$. In a warm gas at the surface, S $^+$ can react with vibrationally excited H $_2^*$ to form SH $^+$. The reaction of the latter with H $_2$ is also endothermic, but reaction with H $_2^*$ leads to H $_2S^+$. Because of these endothermicities, slow radiative association reactions are actually very competitive; viz., S $^+ + H_2 \rightarrow H_2S^+ + h\nu$. However, overall, these chemical pathways are very inefficient, and the abundance of sulfur hydrides is calculated to be small (<10 $^{-8}$).

Deep in the PDR ($A_V \geq 8$), SO and SO $_2$ are predicted to be abundant (Sternberg and Dalgarno, 1995). These species are formed through neutral-neutral reactions with OH, S + OH \rightarrow SO + H, and SO + OH \rightarrow SO $_2$ + H, as well as through S + O $_2 \rightarrow$ SO + O. Both SO and SO $_2$ are destroyed through reactions with He $^+$. Some OCS (at the 10 $^{-8}$ level) is formed through the radiative associa-

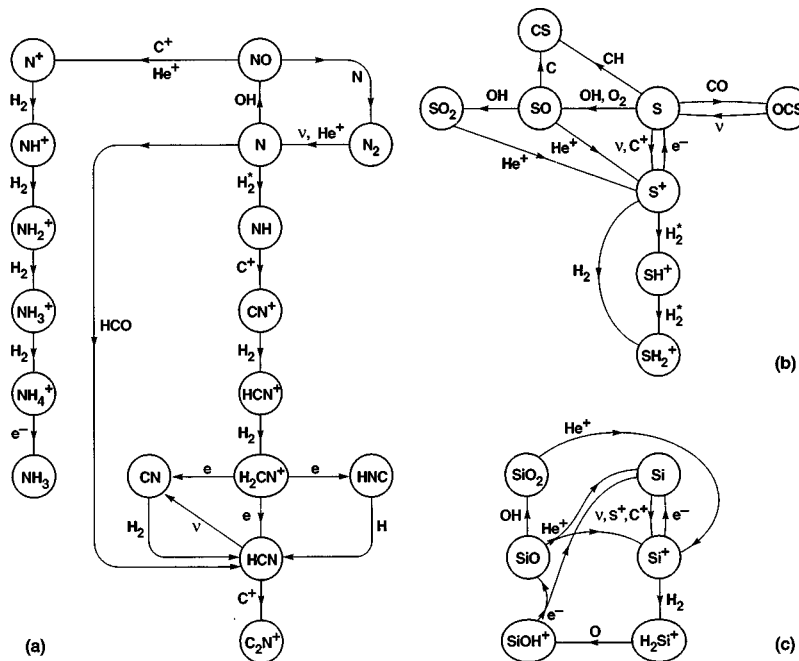


FIG. 10. The most important reactions involved in the PDR chemistry of (a) nitrogen, (b) sulfur, and (c) silicon compounds (adapted from Sternberg and Dalgarno, 1995).

tion reaction of S with CO. The product of the reaction of SO+C is somewhat controversial (Leen and Graff, 1988; Millar and Herbst, 1990). Rather than CS+O, the dominant product may be CO+S. If the reaction SO+C forms CS, then CS is abundant ($\approx 10^{-5}$) around $A_V \approx 8$. Near the surface CS is formed through reactions of S⁺ and S with small carbon hydrides, but it is then much less abundant ($\approx 10^{-10}$).

It should be emphasized that, in general, interstellar sulfur chemistry is not well understood. Observed abundances of SO and SO₂ in dark clouds are in the range $1-5 \times 10^{-9}$ and can only be explained by models if the elemental sulfur abundance is depleted by a factor of 100 compared to solar. This missing sulfur is not in the form of a refractory dust component, nor is it present in the form of sulfur-bearing ices (Palumbo *et al.*, 1997). In PDRs and translucent clouds, H₂S is observed to be more abundant than current models predict. The origin of this discrepancy is unclear.

Silicon chemistry in PDRs [see Fig. 10(c)] has been discussed by Sternberg and Dalgarno (1995). With an ionization potential of 8.2 eV, silicon is predominantly ionized through the PDR to a depth of $A_V \approx 6$ (for $G_o/n \approx 1$). Radiative recombination leads to neutral atomic silicon. Deeper in the cloud, however, SiO becomes the dominant Si-bearing species. This is initiated via the radiative association reaction between Si^+ and H_2 , leading to SiH_2^+ . The latter can react with O to form SiOH^+ , which dissociatively recombines to SiO (and to Si). Reaction of SiO with OH then produces a fair amount of SiO_2 . Both SiO and SiO_2 are destroyed through reactions with He^+ .

d. Polycyclic aromatic hydrocarbons and PDR chemistry

The presence of an abundant population of large molecules (see Sec. II.C) can have a profound effect on the

chemical composition of molecular clouds. As originally discussed by Lepp and Dalgarno (1988), charge-transfer reactions of neutral PAHs with cationic species provide an efficient recombination channel. Particularly for atomic cations, which otherwise recombine only rather slowly radiatively, this can be of great importance. The effects on the chemistry of PDRs have been discussed by Lepp *et al.* (1988) and Bakes and Tielens (1998). The charge balance of PAHs in PDRs has been discussed extensively by Bakes and Tielens (1994) in connection with their study of the photoelectric effect (see Sec. II.C.4). These studies show that, throughout most PDRs, there is an appreciable (≈ 0.5) fraction of neutral PAH species. As expected, charge transfer of atomic cations such as C^+ , S^+ , and Si^+ can lead to an appreciably increased (by a factor of 2) column density of neutral atoms through the PDR (Bakes and Tielens, 1998). PAHs can also provide a surface on which gas-phase species can react. Indeed, PAHs and very small grains dominate the surface area of the interstellar grain size distribution, creating a different surface chemistry from that of classical-sized grains (Tielens, 1993b). In particular, when negatively charged PAHs are involved, an anion-molecule chemistry can be initiated. Also, the reaction heat liberated can lead to evaporation of the product into the gas phase (Allen and Robinson, 1975). The chemical effects on the composition of PDRs has not yet been considered.

C. Interstellar PAHs and grain photoelectric heating in PDRs

1. Observations of the unidentified infrared emission bands

The near- and mid-IR spectra observed towards HII regions are dominated by emission features at 3.3, 6.2,

7.7, 8.6, and 11.3 μm , collectively known as the unidentified infrared bands (UIR; Cohen *et al.*, 1986, 1989; Bregman *et al.*, 1989; Roelfsema *et al.*, 1996; Verstraete *et al.*, 1996). These emission features originate in the PDRs adjacent to the ionized gas, as is evident from the Orion Bar study shown in Fig. 2 (Tielens *et al.*, 1993). The UIR bands are a general characteristic of interstellar material illuminated by far-ultraviolet photons. They also dominate the IR spectra of reflection nebulae (e.g., NGC 2023 and NGC 7023; Sellgren *et al.*, 1985), nuclei of starburst galaxies (e.g., M82; Willner *et al.*, 1977; Genzel *et al.*, 1998), the infrared cirrus discovered by IRAS (Matilla *et al.*, 1996), and, in fact, the general diffuse ISM of the Milky Way as well as other galaxies (Helou *et al.*, 1996; Onaka *et al.*, 1996). The carrier of the UIR bands has to be carbonaceous in nature, since these bands are also prominent in C-rich planetary nebulae which have only locally synthesized dust around them (e.g., NGC 7027; Cohen *et al.*, 1985; Graham *et al.*, 1993).

Figure 11 shows spectra obtained with the Short-Wavelength Spectrometer (SWS) on board the Infrared Space Observatory (ISO) of a number of HII regions, illustrating the incredible richness of the UIR spectrum (Roelfsema *et al.*, 1996). Besides the five main features, an additional ≈ 15 weaker ones, not always the same ones, can be recognized in each spectrum. Here we point out the presence of a feature at 6.0 μm , the splitting up of the 7.7 μm feature into components at 7.6 and 7.8 μm , and the 11.0 μm band. Some of these details were already known from ground-based or airborne data (Bregman, 1989; Roche *et al.*, 1991).

An important characteristic of the UIR spectra is their detailed variation from source to source. First, not all the weaker features are present in all sources and, when perused in detail, each spectrum is unique, implying that the carriers of the UIR bands are sensitive to the local physical conditions (Geballe, 1997). Obvious examples are the relative strengths of the 7.6 and 7.8 μm components which make up the 7.7 μm feature, the features in the 3.3–3.6 μm range, and the 11 to 15 μm region with the 11.0, 11.3, 12.7, and underlying plateau emission (Fig. 11; Bregman, 1989; Jourdain de Muizon *et al.*, 1990; Roche *et al.*, 1991). The best studied example, the ratio of the 3.4/3.3 μm features, varies systematically with distance into the Orion Bar PDR, pointing to photochemically driven variations tied to the penetration of the far-ultraviolet flux from the exciting star θ^1 C Ori into the PDR (Geballe *et al.*, 1989; Joblin *et al.*, 1996). Second, in a few specific sources, major differences exist. For example, in a few regions, the 8.6 μm band dwarfs the normally much stronger 7.7 μm band (Roelfsema *et al.*, 1996; Verstraete *et al.*, 1996). Apparently, in these very specific sources, additional species are present that are either rapidly destroyed or not formed in other sources. These variations point towards a material or family of related species whose composition is readily modified by the local physical conditions and yet is not easily destroyed.

2. Unidentified infrared emission bands and interstellar PAH molecules

The UIR bands are characteristic of aromatic hydrocarbon materials (Duley and Williams, 1981; Léger and Puget, 1984; Allamandola *et al.*, 1985). The 3.3, 8.6 and 11.3 μm bands are due to the stretching and in-plane and out-of-plane bending modes of the aromatic C–H bond. The 6.2 and 7.7 μm bands are due to C–C stretching modes. While the assignment of the UIR bands to vibrations of aromatic structures is generally agreed upon, the identification with PAH *molecules* rather than carbonaceous solids is still doubted in some circles. There are spectroscopic arguments against a solid carrier for the UIR bands (e.g., Tielens, 1998). However, the key argument relies on an analysis of the energetics involved (Sellgren, 1984). The UIR bands are still very bright far from the illuminating star, where dust grains in radiative equilibrium would be too cool to emit in the near and mid infrared. For example, in the Orion Bar the 3.3 μm feature peaks in the PDR that is $\approx 2'$ from θ^1 Ori C (Fig. 2), where the dust temperature, derived from the far-infrared continuum, is only 75 K (Werner *et al.*, 1976). Studies with ISO and with the Japanese satellite IRTS have reinforced this argument. Even the IR spectrum of the entire diffuse ISM in the Milky Way and other galaxies shows strong bands, dominating the near and mid-infrared spectrum (Mattila *et al.*, 1996; Onaka *et al.*, 1996). Dust heated by the interstellar radiation field reaches radiative temperatures of $\approx 15(a/3000 \text{\AA})^{0.2}$ K. In contrast, the observed emission temperature of the UIR bands is ≈ 650 K. As a result, it is now generally accepted that the emission is due to small species which, because of their limited heat capacity, are heated to high temperatures through the absorption of a single far-ultraviolet photon, i.e., $T \approx 1500(E_{\text{FUV}}/N_c)^{0.5}$ K, where E_{FUV} is the photon energy in eV and N_c the number of carbon atoms. The observed emission temperature then corresponds to species with ≈ 50 carbon atoms for a typical photon energy of 10 eV. The combination of this size and the aromatic hydrocarbon structure therefore pinpoints PAH molecules.

It has sometimes been suggested that aromatic molecular moieties within a carbonaceous solid could be thermally isolated from the rest of the solid structure and emit as isolated molecules (Duley and Williams, 1988). Direct transfer of vibrational excitation from the fundamental modes of these moieties ($\approx 1500 \text{ cm}^{-1}$) to the phonons modes ($\approx 50 \text{ cm}^{-1}$) is improbable because many phonons (≈ 30) have to be excited at the same time. However, energy transfer within solids occurs step-wise (Tielens, 1993b) where the excitation of one vibrational mode is transferred to another mode slightly lower in energy, with the simultaneous excitation of a low-energy phonon. In this way the excitation energy cascades down the vibrational ladder until everything is transferred to the phonon modes in ≈ 30 steps. Extensive experimental and theoretical studies on energy transfer in mothballs (Dlott, 1989)—a solid consisting of the two-ringed PAH naphthalene, bonded by weak van

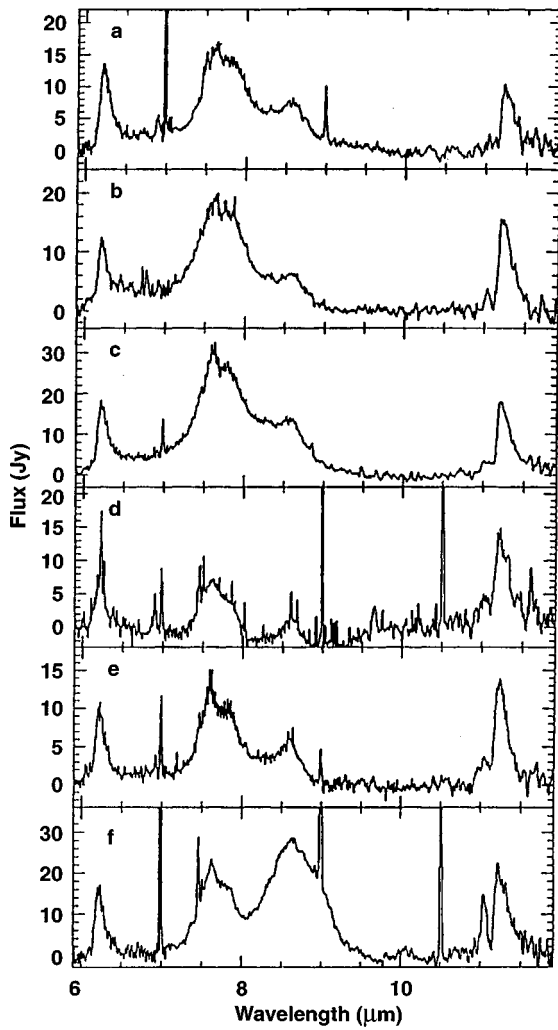


FIG. 11. The unidentified infrared bands in the (continuum subtracted) ISO short-wavelength spectrometer spectra of a sample of compact HII regions and associated PDRs (Roelfsema *et al.*, 1996). The bands primarily arise from the PDRs. The sources are IRAS: (a) 18116–1646; (b) 18162–2048; (c) 19442+2427; (d) 21190+5140; (e) 22308+5812; and (f) 18434–0242.

der Waals interactions, and an extreme example of the solid structures envisioned in these “UIR by solids” proposals—show that the energy cascade from the vibrations to the long-wavelength phonons takes about 10^{-9} s. This energy transfer is fast because there are so many accepting modes close in frequency—recall the richness of the aromatic spectrum. In contrast, the IR emission time scale is 0.1 s. Hence only about 10^{-8} of the total vibrational excitation energy would be emitted in the near- and mid-IR fundamental vibrational modes in a solid; the remainder would give rise to a far-IR phonon continuum. In contrast, the observed ratio of the UIR bands to the far-IR continuum is 5% in astronomical sources. The conclusion is inescapable: The UIR bands are carried by small (≈ 50 C atoms) PAH molecules.

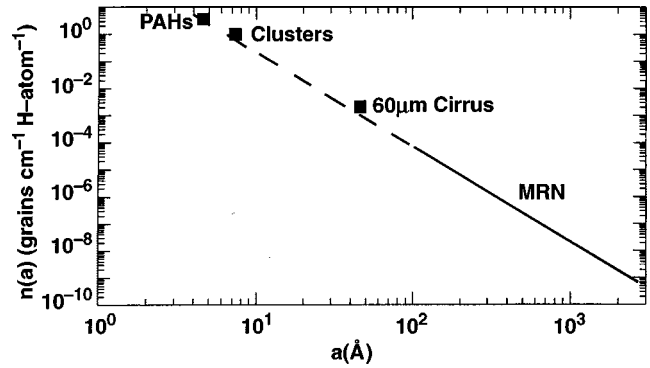


FIG. 12. The derived interstellar grain size distribution. The squares indicate abundances of the carriers of the unidentified infrared bands (PAHs), the underlying plateaus (clusters), and the 25 and 60 μm cirrus emissions. The MRN (Mathis, Rumpl, and Nordsieck, 1977) grain size distribution derived from observations of extinction of starlight is also indicated.

3. The grain size distribution

The abundance of PAHs can be derived rather directly from the observations. The UIR bands are observed to contain about 5% of the total IR flux from PDRs. Hence PAHs absorb about 5% of the incident far-ultraviolet flux; the remainder is absorbed by larger dust grains and reradiated as far-infrared continuum. Adopting standard dust properties ($A_{FUV}/A_v = 1.8$; $N_H/A_v = 1.9 \times 10^{21} \text{ cm}^{-2} \text{ mag}^{-1}$) and a typical far-ultraviolet absorption cross section of 10^{-17} cm^{-2} per C atom, we find about 1% of the elemental C has to be locked up in PAHs. With a typical PAH size of 50 C atoms, the abundance of PAHs relative to hydrogen is about 10^{-7} (Allamandola *et al.*, 1985).

Measured IR spectra also show broad emission plateaus underlying the UIR bands (Bregman *et al.*, 1989; Cohen *et al.*, 1989). The strength of these plateaus relative to the UIR bands varies with position in the Orion Bar and hence these plateaus are carried by an independent “dust” component. Spectroscopically, an aromatic carrier is again called for, but the size is somewhat larger than for the UIR band carriers (≈ 400 C atoms; Bregman *et al.*, 1989). These species are often called clusters, indicating that they might consist of several PAHs stuck together in a three-dimensional structure (Tielens, 1990a, 1990b). The abundance of these clusters can be derived in a manner analogous to that for PAH abundances (see Fig. 12). The 25 and 60 μm cirrus reveals the presence of even larger (up to 10^5 C atoms) species, which fluctuate in temperature (Draine and Anderson, 1985). The resulting grain size distribution is summarized in Fig. 12. It seems that the interstellar grain size distribution extends all the way from the molecular-sized PAHs up to “macroscopic” carbon dust particles (Draine and Anderson, 1985; Tielens, 1990b).

4. Photoelectric heating

Photoelectric heating is dominated by the smallest grains present in the ISM (Watson, 1972; Jura, 1976).

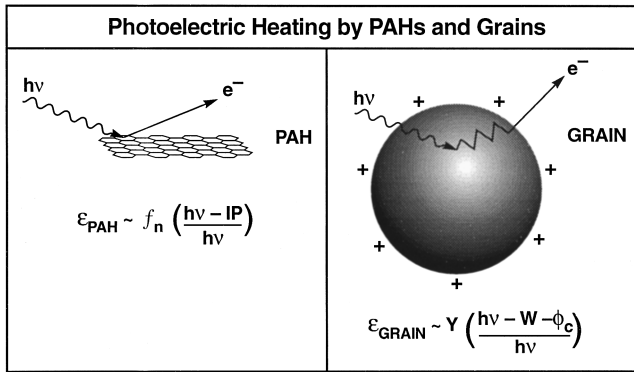


FIG. 13. A schematic of the photoelectric heating mechanism. A far-ultraviolet photon absorbed by a dust grain creates a photoelectron which diffuses through the grain until it loses all its excess energy due to collisions with the matrix or finds the surface and escapes. For PAHs, the diffusion plays no role. A simple expression for the heating efficiency ϵ is indicated. See text for details.

Therefore PAHs and very small grains play an important role in the heating of interstellar gas (d'Hendecourt and Léger, 1987; Lepp and Dalgarno, 1988; Verstraete *et al.*, 1990; Bakes and Tielens, 1994).

Figure 13 schematically shows the physics associated with the photoelectric effect on interstellar grains and PAHs. Far-ultraviolet photons absorbed by a grain will create energetic (several eV) electrons. These electrons may diffuse in the grain, reach the surface, overcome the work function W of the grain and any Coulomb potential ϕ_c if the grain is positively charged, and be injected into the gas phase with excess kinetic energy. The efficiency ϵ_{grain} of the photoelectric effect on a grain, or the ratio of gas heating rate to the grain far-ultraviolet absorption rate, is then given by the yield Y , which measures the probability that the electron escapes, times the fraction of the photon energy carried away as kinetic energy by the electron; viz.,

$$\epsilon_{\text{grain}} \approx Y \left(\frac{h\nu - W - \phi_c}{h\nu} \right). \quad (11)$$

The yield is a complex function of the grain size a , the collision length scale for low-energy electrons in solids ℓ_e ($\approx 10 \text{ \AA}$), the far-ultraviolet absorption length scale inside a grain, ℓ_a ($\approx 100 \text{ \AA}$), and the photon energy $h\nu$ (Watson, 1972; Draine, 1978; Bakes and Tielens, 1994). For large grains and photon energies well above threshold, the photons are absorbed $\sim 100 \text{ \AA}$ inside the grain and the photoelectrons rarely escape ($Y/\ell_e/\ell_a \approx 0.1$). With a typical far-ultraviolet photon energy of 10 eV and a work function of 5 eV, the maximum efficiency is only 0.05. Generally, because of positive charging, the efficiency will be much less. A simple, semiempirical model was developed by de Jong (1977) for the charging of interstellar grains and its effect on the photoelectric efficiency. The parameters in this model were then fit to the heating rates of interstellar gas inferred from Copernicus observations (Pottasch *et al.*, 1979). Draine (1978) derived a similar grain photoelectric heating model,

based on laboratory studies and theoretical considerations. The de Jong model formed the basis for the early models of dense PDRs (see Tielens and Hollenbach, 1985a).

In recent years, these models have been extended to include very small grains and PAH molecules. While some of the photon energy may remain behind as electronic excitation energy (~ 0.5), the yield is much higher for planar PAH molecules than for classical-sized grains. The limiting factor is now that the ionization potential IP of a charged PAH can be larger than 13.6 eV. Far-ultraviolet photons absorbed by such a PAH cation do not lead to the creation of a photoelectron or, therefore, to any gas heating. The ionization potential is given by $IP = W + \phi_c = W + (Z + 0.5)e^2/C = W + (Z + 0.5)\pi e^2/2a$, where W is the work function of bulk graphite, ϕ_c is the Coulomb potential, Z is the PAH charge, a is the PAH "radius," and C is the capacitance of the PAH. For compact PAHs, C is $2a/\pi$. In the limit of large grains, the ionization potential goes to the bulk work function, but for small sizes and positive charge, IP can exceed 13.6 eV. For example, the second ionization potential of pyrene, $C_{16}H_{10}$, is 16.6 eV, well above the hydrogen ionization limit (Leach, 1987). The photoelectric heating efficiency ϵ_{PAH} for small PAHs is then reduced by the fraction f_n of PAHs that can still be ionized by far-ultraviolet photons, viz.,

$$\epsilon_{PAH} \approx \frac{1}{2} f_n \left(\frac{h\nu - IP}{h\nu} \right). \quad (12)$$

Thus, with a typical photon energy of 10 eV and an ionization potential of 7 eV, the maximum efficiency is 0.15.

Bakes and Tielens (1994) have calculated the photoelectric heating by a grain size distribution that extends into the molecular PAH domain. A typical result of this calculation is shown in Fig. 14, which shows that about half the gas heating is due to grains with sizes less than 15 \AA ($N_c \approx 1500$ C atoms). The other half originates in grains with sizes between 15 and 100 \AA ($1500 < N_c < 5 \times 10^5$ C atoms). Grains larger than 100 \AA contribute negligibly to the photoelectric heating of the interstellar gas.

The photoelectric heating efficiency ϵ depends on the charge of a grain. A higher charge implies a higher Coulomb barrier (i.e., higher ionization potential) that has to be overcome. Thus a smaller fraction of the electrons "dislodged" in the grain will escape. Moreover, those that do escape will carry away less kinetic energy (de Jong, 1977). For PAHs, the charge determines whether further ionizations can still occur. Hence the photoelectric heating efficiency will depend on the ratio γ of the photoionization rate over the recombination rate of electrons with neutral grains/PAHs. When $\gamma (\propto G_0/n_e)$ is small, grains/PAHs are predominantly neutral and the photoelectric heating has the highest efficiency. When γ increases, the grains/PAHs will charge up and the photoelectric efficiency will drop. Extensive theoretical calculations on the heating by an MRN (Mathis, Rumpl, and Nordsieck, 1977) grain size distribution of PAHs and small grains, including the effects of charge, have

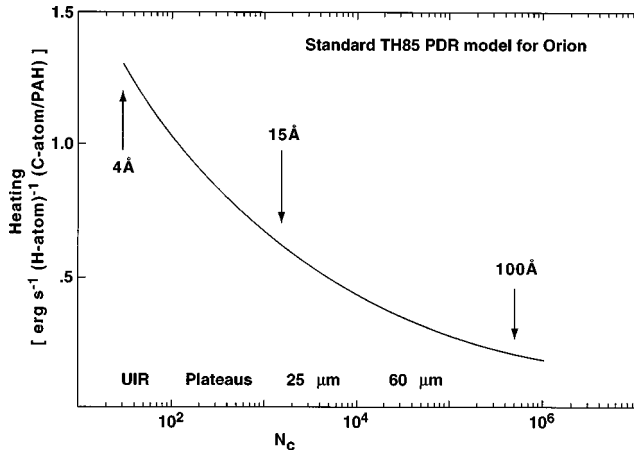


FIG. 14. The contribution to the photoelectric heating of interstellar gas by grains of different sizes (Bakes and Tielens, 1994). The results of these calculations are presented in such a way that equal areas under the curve correspond to equal contributions to the heating. Species with ≈ 50 C atoms are the carriers of the IR emission features at 3.3, 6.2, 7.7, and 11.3 μm . The plateaus underneath these features and the 12 μm cirrus are carried by somewhat larger species (≈ 200 C atoms). The 25 and 60 μm cirrus correspond to species with 5×10^4 and 5×10^5 C atoms, respectively.

been performed by Bakes and Tielens (1994) and the resulting efficiencies ϵ (ratio of gas heating to far-ultraviolet absorption rate of grains and PAHs) have been fitted to a simple analytical formula,

$$\epsilon = \frac{4.87 \times 10^{-2}}{1 + 4 \times 10^{-3} \gamma_o^{0.73}} + \frac{3.65 \times 10^{-2} (T/10^4)^{0.7}}{1 + 2 \times 10^{-4} \gamma_o}, \quad (13)$$

with $\gamma_o = G_0 T^{1/2} / n_e$. For neutral grains ($\gamma_o \ll 10^3 \text{ K}^{1/2} \text{ cm}^3$), a maximum efficiency of $\sim 5\%$ is reached.

D. Heating and cooling

Two main mechanisms couple the gas to the far-ultraviolet photon energy of stars: the photoelectric effect on PAHs and small dust grains and far-ultraviolet pumping of H₂ molecules followed by collisional deexcitation. These heating mechanisms have been treated in Secs. II.B.1 and II.C.4. Other heating mechanisms—gas collisions with warm grains, cosmic-ray ionization and excitation, ionization of C, pumping of gas particles to excited states by the far-infrared radiation field of the warm dust followed by collisional deexcitation—play only a limited role in the heating or become important at great depth in the PDR (Tielens and Hollenbach, 1985a).

The gas in PDRs is cooled by far-infrared fine-structure lines, such as [CII] 158 μm , [OI] 63, 146 μm , [SiIII] 35 μm , [CI] 609, 370 μm , and by molecular rotational lines, particularly of CO and H₂. The dominant coolants in the PDR surface ($A_V \lesssim 1$), where most of the far-ultraviolet flux is absorbed, are generally the [CII] and [OI] fine-structure lines. Figure 15 shows their energy-level diagrams. For high densities and G_0 , the

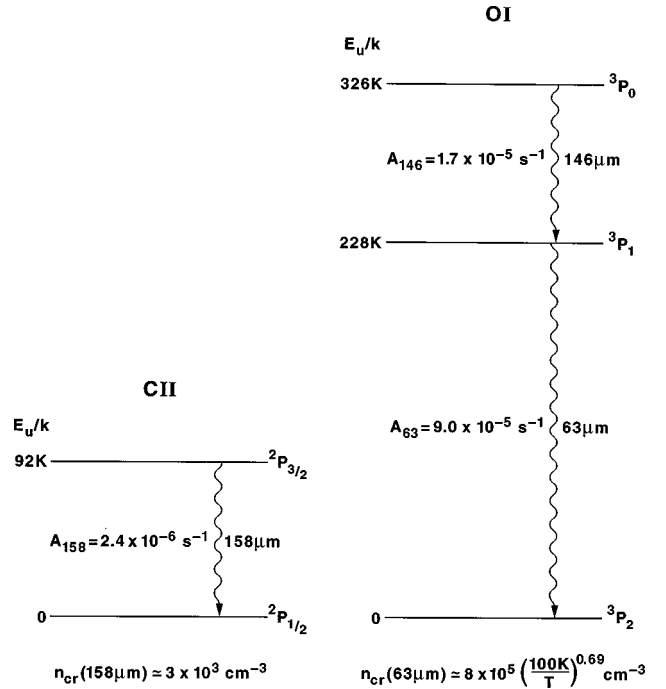


FIG. 15. The energy-level diagrams for the fine-structure levels of [OI] and [CII]. The Einstein A values and the critical densities ($n > n_{cr}$ means local thermal equilibrium) for collisions with neutral hydrogen are also shown.

gas at the surface of the PDR attains temperatures $\gtrsim 5000 \text{ K}$, and significant cooling in [FeII](1.26, 1.64 μm), [OI] 6300 \AA , and [SII] 6730 \AA results (Burton, Hollenbach, and Tielens, 1990).⁹ At high gas density, cooling by collisions with the cooler dust grains may be significant (Burke and Hollenbach, 1983). The local, radiative cooling rate of a species is also affected by radiative transfer and, hence, depends on the global distribution of the level populations throughout the PDR. In PDR studies, generally, the escape probability (Sobolev approximation) formalism is used to calculate the local cooling rate. Comparison with full-scale radiative transfer codes, which solve the radiative transfer and level populations self-consistently throughout the cloud, show good agreement with the Sobolev approximation for the level populations as well as the total intensity of the cooling line, provided the optical depth to the surface is calculated from the actual column density in the relevant states rather than approximated from the local level populations (Wolfire *et al.*, 1993). As a result, in semi-infinite slabs the PDR temperature structure can be calculated from the outside to the inside without the

⁹Convenient fitting formulae for the collisional excitation rates have been published by Tielens and Hollenbach (1985a), Hollenbach and McKee (1989), and Spaans *et al.* (1994) for the atomic fine structure and forbidden lines, by Hollenbach and McKee (1979), McKee *et al.* (1982), Draine and Roberge (1984), and Schinke *et al.* (1985) for rotational transitions of CO, and by Martin and Mandy (1995) and Martin *et al.* (1996) for rovibrational transitions of H₂.

need for global iterations. However, for clumpy and turbulent clouds, line transfer can be very complicated when photons escape through 4π steradians (Köster *et al.*, 1994; Störzer *et al.*, 1996) and when line transfer occurs between clumps or between clumps and an inter-clump medium (Hegmann and Kegel, 1996; Spaans, 1996).

III. PDR MODELS

A. Steady-state, stationary PDR models

Considerable effort has been expended over the past two decades in constructing PDR models with the assumption of thermal and chemical balance and ignoring any flow through the PDR. Basically, this is equivalent to assuming that the time scale for H_2 formation on grains, $\tau_{H_2} \sim (10^9 \text{ cm}^{-3}/n)$ years, which dominates the chemical time scales, is short compared to the dynamical time scales or the time scales for significant change in the far-ultraviolet flux. Equilibrium PDR models of the transition of H to H_2 and C^+ to CO, including dust attenuation and self-shielding of the far-ultraviolet flux, have a long history.¹⁰ Models focusing on the H_2 spectrum are discussed in Sec. IV.B and on diffuse, translucent, and molecular clouds in the interstellar radiation field ($G_0 \sim 1$) in Sec. VI. However, intense far-ultraviolet fields ($G_0 \gg 1$) and high A_V often characterize dense PDRs. Tielens and Hollenbach (1985a), Sternberg and Dalgarno (1989), Hollenbach *et al.* (1991), Abgrall *et al.* (1992), Le Bourlot *et al.* (1993, 1995), Diaz-Miller *et al.* (1998), and Luhman *et al.* (1997) model the thermal balance and chemistry in one-dimensional, homogeneous PDRs subjected to a range of elevated far-ultraviolet fluxes.

Generally, these models consider a plane-parallel, semi-infinite slab illuminated from one side by an intense far-ultraviolet field. Figure 16 shows a typical case with $G_0/n > 4 \times 10^{-2} \text{ cm}^3$, so that H_2 does not self-shield until dust attenuation of the far-ultraviolet flux is significant. The penetrating far-ultraviolet photons create an atomic surface layer. At a depth corresponding to $A_V \approx 2$, the transition from atomic H to molecular H_2 occurs. Because of rapid photodestruction, vibrationally excited molecular hydrogen, H_2^* , does not peak until $A_V \approx 2$. Because of dust attenuation, the carbon balance shifts from C^+ to C and CO at $A_V \approx 4$. The second peak in the neutral-carbon abundance results from charge exchange between C^+ and S. Except for the O locked up in CO, essentially all the oxygen is in atomic form until

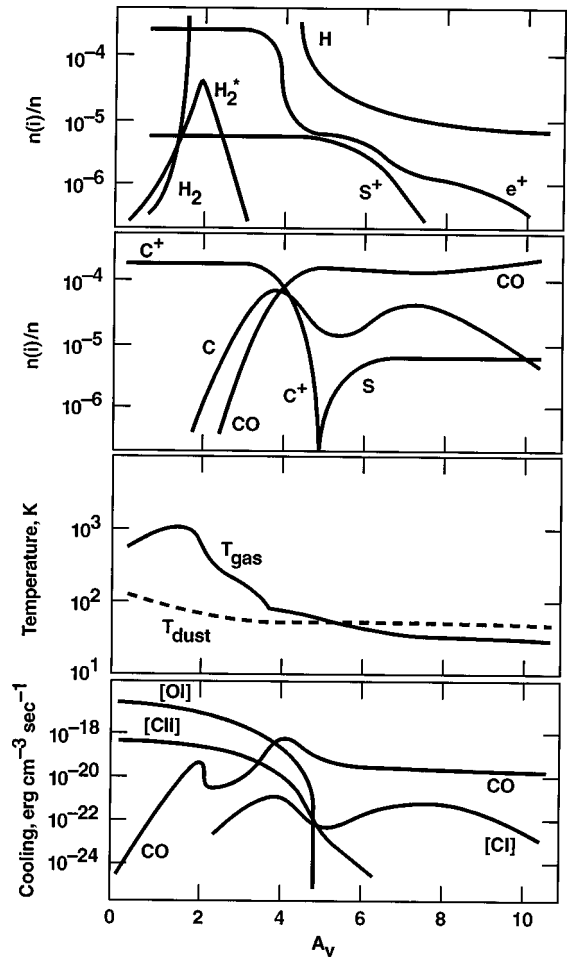


FIG. 16. Calculated structure of the PDR in Orion ($n = 2.3 \times 10^5 \text{ cm}^{-3}$, $G_0 = 10^5$) as a function of visual extinction A_V , in the PDR (Tielens and Hollenbach, 1985b). The illuminating source is to the left. Top two panels: Abundances relative to total hydrogen. Third panel: Gas and dust temperatures. Bottom panel: Cooling in the various gas lines.

very deep in the cloud $A_V \sim 8$. Because of their low ionization potential, trace species such as S can remain ionized through a substantial portion of the photodissociation region.

Besides the chemical composition, the far-ultraviolet photons also control the energy balance of the gas through the photoelectric effect (see Sec. II.C). Typically, about 0.1–1% of the far-ultraviolet energy is converted into gas heating this way. The rest is emitted as far-infrared dust continuum radiation. The gas in the surface layer is then much warmer ($\approx 500 \text{ K}$) than the dust ($30\text{--}75 \text{ K}$). Somewhat deeper into the PDR ($A_V > 4$), penetrating red and near-IR photons keep the dust warm, and gas-grain collisions couple the gas to slightly below the dust temperature. In PDRs, the gas cools through the far-infrared fine-structure lines of mainly [OI] 63 μm and [CII] 158 μm at the surface and the rotational lines of CO deeper into the PDR. Figure 16 quantitatively shows this chemical and thermal structure for conditions appropriate for the Orion PDR behind the Trapezium stars.

¹⁰Transition models include those of Hollenbach *et al.*, 1971; Jura, 1974; Glassgold and Langer, 1975; Langer, 1976; Black and Dalgarno, 1977; Clavel *et al.*, 1978; Federman *et al.*, 1979; de Jong *et al.*, 1980; van Dishoeck and Black, 1986, 1988; Viala, 1986; Viala *et al.*, 1988; Sternberg, 1988; Abgrall *et al.*, 1992; Heck *et al.*, 1992, 1993; Andersson and Wannier, 1993; Köster *et al.*, 1994; Jansen *et al.*, 1995a, 1995b; Draine and Bertoldi, 1996; Störzer *et al.*, 1996; Warin *et al.*, 1996.

Recently, models have been constructed of clumpy PDRs, many of them focused on the C⁺/C/CO transition and the origin of [CI], H₂ 2-μm, and CO rotational emission.¹¹ In addition, specialized models have been constructed to explain CI fine structure, near-red, and radio recombination lines, as well as various aspects of molecular chemistry. We discuss these in separate sections of this paper.

B. Time-dependent and nonstationary PDRs

There are two basic phenomena that can cause significant time-dependent effects on the chemical abundances and temperatures in a PDR. The first is a change of G_0 or n in a smaller time scale than τ_{H_2} , the time scale for H₂ formation or destruction. For example, an O or B star suddenly “turns on” in a cloud, clumps moving in PDRs produce rapid shadowing effects, or a photodissociation shell quickly expands around the central star of a planetary nebula. The second, viewed in the frame of the ionization front, is the flow of the neutral gas through the PDR (hence “nonstationary PDR”) in a time short compared to τ_{H_2} . In this case, the chemical and thermal structure can achieve a steady state, but the resulting structure differs from the structure of a stationary PDR because of the rapid advection of molecular material from the shielded regions into the surface zones. In both cases H₂ is the most likely species to go out of equilibrium, because of its relatively slow formation rate on grain surfaces and its slow destruction rate by (self-shielded) photodissociation. The H₂, in turn, affects the temperature structure and the chemical abundances of the other species. Assuming that the H₂ formation rate is dominated by grain surface catalysis [Eq. (4)] and its destruction rate is dominated by far-ultraviolet photodissociation [Eq. (5)], we find that the time-dependent rate equation for H₂ is

$$\frac{\partial n_{H_2}}{\partial t} = \gamma_{H_2} n n_H - f_{\text{shield}} e^{-\tau_{gr,1000}} I_{\text{diss}}(0) n_{H_2} - \frac{\partial(n_{H_2} v)}{\partial z}. \quad (14)$$

If the left-hand side of Eq. (14) is zero, then the H₂ has achieved steady state. The last term on the right-hand side represents the advection term due to material flowing at speed v through the PDR. If this term is also negligible, then the PDR is both steady state and stationary, a condition commonly called “equilibrium” in the literature.

Hill and Hollenbach (1978), London (1978), and Roger and Dewdney (1992) consider the time-dependent evolution of the ionization front and H₂ dissociation front when O or B stars suddenly turn on in a

neutral cloud. Goldshmidt and Sternberg (1995) look in detail at the enhancement of H₂ fluorescent emission when a low-density ($n \leq 10^4 \text{ cm}^{-3}$) molecular cloud is suddenly illuminated with intense far-ultraviolet radiation; Hollenbach and Natta (1995) examine the collisionally modified H₂ spectra when $n > 10^4 \text{ cm}^{-3}$. Störzer *et al.* (1997) study the temporary enhancement of C⁰ abundance and [CI] emission caused by C⁺ recombination when the far-ultraviolet flux is suddenly shadowed by moving, opaque clumps. Monteiro (1991) finds a similar enhancement for rotating clumps in PDRs. Gerola and Glassgold (1978), Tarafdar *et al.* (1985), Prasad *et al.* (1991), Heck *et al.* (1992), Lee *et al.* (1996), Nelson and Langer (1997), and Shematovich *et al.* (1997) examine the time-dependent evolution of diffuse atomic clouds into molecular clouds and the collapse toward star formation. Lee *et al.* (1996) also study the time-dependent chemistry of an inhomogeneous molecular cloud suddenly exposed to far-ultraviolet radiation. Bergin *et al.* (1997) produce both steady-state and time-dependent PDR chemical models of giant molecular cloud cores.

The first PDR modeling to incorporate fast flows or advection were chemical models that used rapid turbulent eddies or diffusion to mix molecular gas from opaque molecular cores with surface photodissociated gas (Phillips and Huggins, 1981; Boland and de Jong, 1982; Williams and Hartquist, 1984, 1991; Chièze and Pineau des Forêts, 1989, 1990; Chièze *et al.*, 1991; Xie *et al.*, 1996). Recently, Bertoldi and Draine (1996) have discussed in detail the time-dependent effect on the PDR structure of the advance of the ionization front and dissociation front through a cloud. In this case the “flow” velocity is equivalent to the speed v_{PDR} of the ionization front advancing into the PDR. Figure 17 schematically diagrams such a nonstationary PDR. The advected flow is relatively fast when the photoevaporating HII gas is free to flow to lower-pressure regions, as in the case of neutral clumps photoevaporating well inside an HII region; in these cases the flow speed in the HII gas near the ionization front is of order the sound speed c_{HII} . Assuming approximate thermal pressure equilibrium between the photoevaporating HII gas and the neutral PDR gas on the other side of the ionization front, and assuming a typical PDR temperature of $\sim 1000 \text{ K}$, one obtains the PDR density $n_{\text{PDR}} \approx 20n_{\text{HII}}$. Assuming that the free-flowing HII gas evaporates from the ionization front at $c_{\text{HII}} \sim 10 \text{ km s}^{-1}$, the flow speed $v_{\text{PDR}} \sim (n_{\text{HII}}/n_{\text{PDR}})c_{\text{HII}}$ through the PDR is about 0.5 km s^{-1} . The flow time through the PDR is $\tau_{\text{PDR}} \approx (N_{\text{PDR}}/n_{\text{PDR}})/v_{\text{PDR}}$. Equating τ_{PDR} to τ_{H_2} , we obtain a critical flow speed of $\sim 0.7 \text{ km s}^{-1}$, above which the H₂ abundance may be significantly higher than its “stationary” (no-flow) value.

The fact that for free-flowing gas the estimated v_{PDR} is so close to the estimated critical speed indicates that nonstationary PDRs may be important. Bertoldi and Draine (1996) show how v_{PDR} can be related to the extreme-ultraviolet flux reaching the ionization front, since these photons create the new ionizations which

¹¹Clumpy PDR models include those of Burton, Hollenbach, and Tielens, 1990b; Tauber and Goldsmith, 1990; Gierens *et al.*, 1992; Meixner and Tielens, 1993; Wolfire *et al.*, 1993; Köster *et al.*, 1994; Hegmann and Kegel, 1996; Spaans, 1996; Störzer *et al.*, 1996; Spaans and van Dishoeck, 1997.

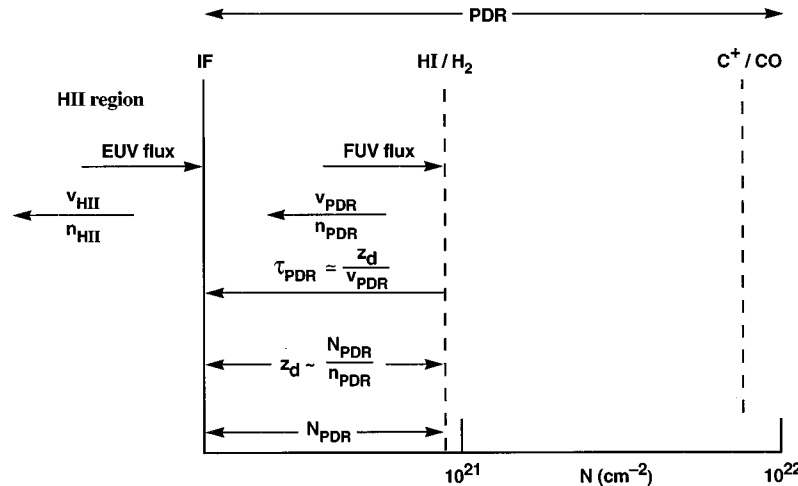


FIG. 17. Schematic of a nonstationary PDR (Störzer and Hollenbach, 1998). The Lyman continuum flux eats into the neutral gas; in the frame of the ionization front IF, the neutral gas flows through the IF at v_{PDR} and then accelerates to $v_{HII} \sim c_{HII}$ in the HII region. HI/H₂ marks the position of the dissociation front if the flow is slow, where N is the hydrogen column from the ionization front. If the flow is sufficiently fast ($\geq 0.7 \text{ km s}^{-1}$, see text), then the H₂ photodissociation time is long compared to the travel time t_f across the region between HI/H₂ and the ionization front, and the H₂ survives to the ionization front. In this case, the chemistry of the PDR is far from the steady-state values for stationary PDRs because of the rapid advection of H₂.

push the front into the PDR. The extreme-ultraviolet flux depends on the dust attenuation in the ionized gas and the morphology (e.g., size of clump and distance from star) of the region. This morphology determines the geometrical dilution of the flux and the extreme-ultraviolet attenuation by recombined atomic hydrogen in the predominantly ionized evaporative flow. Bertoldi and Draine argue that for a broad range of conditions, including the famous photodissociation region in Orion (Figs. 1 and 2), time-dependent effects may be of some importance.

Much larger effects can be expected when the H₂ survives all the way to the ionization front as it flows from the opaque regions, leading to the merging of the dissociation front with the ionization front. In this case the critical question, for relatively high far-ultraviolet fluxes, is whether the self-shielded H₂ at a column $N \sim 10^{21} \text{ cm}^{-2}$ (or $\tau_{FUV} \sim 1$, where it emerges from dust shielding) has a dissociation time scale long compared to the flow time τ_{PDR} across this destructive region. This comparison results in the condition

$$v_{PDR} \geq 3(G_0/n) \text{ km s}^{-1} \quad (15)$$

for H₂ to survive to the ionization front, where n is in cm^{-3} . Bertoldi and Draine (1996) quantitatively determine when the ionization and dissociation fronts merge. Qualitatively, the merger tends to occur for hotter stars (with a high ratio of extreme-ultraviolet to far-ultraviolet photons), illuminating clumps or clouds with a geometry such that relatively little attenuation of the extreme-ultraviolet flux occurs by recombining hydrogen in the evaporating flow or HII region (e.g., a small, freely evaporating clump near the hot star). Apparently, the condition is not met in the Orion Bar (Fig. 2), since the observed layered structure clearly shows the H₂ off-

set from the ionization front; in fact, Tielens *et al.* (1993a, 1993b) find good agreement with steady-state, stationary PDR models.

The consequences of rapid advection through PDRs have not yet been fully determined. Bertoldi and Draine (1996) suggest that H₃⁺ may be produced in a merged ionization/dissociation front and that enhanced H₂ infrared emission and reduced HI columns will result. Considerable effort is currently directed at numerically modeling these nonstationary PDRs. Störzer and Hollenbach (1998) confirm Eq. (15) for cases with moderately high $G_0 \leq 10^4 - 10^5$ and $n \leq 10^5 - 10^6$. However, for higher n and G_0 , H₂ is destroyed by C⁺ and O in the warm PDR before reaching the ionization front, even when Eq. (15) is satisfied. Although H₂ may survive to the ionization front when v_{PDR} satisfies Eq. (15), the C⁺ and O often remain abundant in the region $A_v \leq 2$ because of the much shorter photodissociation time scale for CO. In addition, the PDR temperature remains high ($\sim 1000 \text{ K}$) so that the [CII] 158-μm and [OI] 63-μm intensities are relatively unchanged from the stationary case. Therefore it is still possible to estimate the physical conditions in nonstationary PDRs by comparing the intensities of these lines and the infrared continuum with stationary PDR models. However, as predicted by Bertoldi and Draine (1996), the H₂ infrared line intensities are enhanced. Störzer and Hollenbach find enhancement factors of at most 2–3.

C. PDR models of photoevaporating protoplanetary disks

Nonstationary PDR models may find interesting application in the photoevaporating protoplanetary disks found in the Orion nebula (Churchwell *et al.*, 1987; O'Dell *et al.*, 1993). These objects, called “proplyds” by

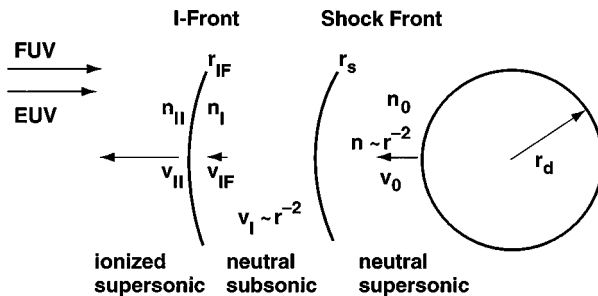


FIG. 18. Schematic diagram showing three distinct regions through which far-ultraviolet-dominated flows pass (Johnstone *et al.*, 1998). In the case of proplyds, r_d is the disk radius and neutral material is launched at v_0 (1–2 times the sonic speed) from the disk, passes through an isothermal shock at r_s , moves subsonically at v_I through a shell between the shock front and the ionization front, flows into the D-type ionization front at $v_{IF} \sim 0.5 \text{ km s}^{-1}$, and is ionized and accelerated to v_{II} (1–2 times the HII sonic speed) in the 10^4 K HII gas to the left of the ionization front.

O'Dell for PROtoPLanetary DiskS, are generally seen in radio free-free images (Churchwell *et al.*, 1987; Garay *et al.*, 1987; Felli *et al.*, 1993) or optical and near-infrared images (Laques and Vidal, 1979; O'Dell *et al.*, 1993; McCaughrean and Stauffer, 1994; O'Dell and Wen, 1994; Stauffer *et al.*, 1994; McCullough *et al.*, 1995; O'Dell and Wong, 1996; Bally *et al.*, 1998) of their bright ionization fronts, their central low-mass star ($M \sim 0.3 M_\odot$; Hillenbrand, 1997), or their silhouetted disks. The ionization fronts are often about 100 AU from the central star and are cometary in shape, with their tails pointing away from the ultraviolet-luminous, massive star θ^1 Ori C. The disks, when seen in silhouette, are also of order 100 AU in size, although there is sometimes a significant separation between disk and ionization front. Over 50 ionization fronts have been observed within roughly 0.1 pc of θ^1 Ori C, and in 14 of them a central disk is seen either in silhouette using the background [OIII] emission of the Orion HII region or in [OI] 6300 Å emission (see, for example, Bally *et al.*, 1998).

Churchwell *et al.* (1987) were the first to suggest that these objects were photoevaporating disks around low-mass stars externally illuminated by θ^1 Ori C. Johnstone *et al.* (1998) modeled the region between the disk and the ionization front as a photodissociation region and showed that in a number of cases it is the pressurized PDR gas which initiates the photoevaporation, setting up a supersonic neutral PDR wind. Figure 18 schematically diagrams these PDR-dominated flows. The supersonic PDR wind shocks and then moves subsonically through the stationary (D-type) ionization front. The models and observations determine mass loss rates $\sim 10^{-7} M_\odot \text{ yr}^{-1}$ for 41 observed objects. Assuming that the surface density in the disk decreases outwards, the disk photoevaporates from outside in, and the disk shrinks in size with time. If the surface density Σ in the disk follows a power law, $\Sigma \propto r^{-\alpha}$ with $0 \leq \alpha \leq 2$, most of the mass of the disk is contained in its outer regions, and the current mass of the disk is given by $\sim \dot{M} t_{\text{evap}}$, where

\dot{M} is the current mass loss rate and t_{evap} is the evaporation time scale ($\sim 10^5$ years).

Johnstone *et al.* derive disk masses ($\sim 0.01 M_\odot$), disk sizes when not directly observed ($\sim 3 \times 10^{14} \text{ cm}$), and disk lifetimes ($\sim 10^{5-6} \text{ yr}$), and constrain α (~ 1.5) by applying their PDR models to proplyds in Orion. The photoevaporation lifetimes are shorter than the giant planet formation time scales inferred for the solar nebula, indicating that giant outer planets may only form around the fraction of low-mass stars born in more isolated, and less hostile, environments than the cluster of stars around θ^1 Ori C.

D. PDR models with cool sources

Most PDR models (and observations) have concentrated on bright PDRs created by O stars on nearby molecular gas. However, the Infrared Space Observatory (ISO) has allowed studies of much fainter PDRs associated with reflection nebulae illuminated by F–B stars. Protoplanetary nebulae are another class of objects in which relatively cool stars illuminate nearby, dense, molecular material. The color temperature of the radiation field can have an important influence on the composition and structure of PDRs (Rodger and Dewdney, 1992; Spaans *et al.*, 1994; Diaz-Miller *et al.*, 1998). First, the reduction in the far-ultraviolet field reduces the efficiency of the photoelectric effect on PAHs and small dust grains. This is particularly true for the smallest PAHs, whose absorption is limited to far-ultraviolet wavelengths. Theoretical models show that this can reduce the photoelectric efficiency by an order of magnitude for the coolest stars ($T_{\text{eff}} = 6000 \text{ K}$; Spaans *et al.*, 1994). The reduced far-ultraviolet flux also leads to much reduced photodissociation and photoionization rates. Species with the highest thresholds are, of course, the most affected (i.e., H₂ and CO; Rodger and Dewdney 1992; Spaans *et al.*, 1994). As a result, the H₂ and CO transitions shift towards the surfaces of PDRs in cooler radiation fields. The dominant cooling lines are [OI] and [CII] for the hotter radiation fields but rotational CO emission becomes progressively more important for cooler radiation fields. The [CII]/CO and [OI]/CO ratios are good diagnostics for the color temperature of the radiation field (Spaans *et al.*, 1994).

IV. OBSERVATIONS OF PDRS

Photodissociation regions are bright in the far-infrared dust continuum, in the PAH emission features, the far-infrared fine-structure lines of [OI] and [CII], and the rotational lines of CO. Besides these dominant cooling processes, PDRs are also the source of (fluorescent or collisionally excited) rovibrational transitions of H₂ in the far-red and near-infrared, the atomic fine-structure lines of [CI] 609 and 370 μm and [SiII] 35 μm, and the recombination lines of CI in the radio (e.g., C91α) and the far red (e.g., 9850 and 8727 Å). They are also observed in rotational transitions of trace molecules

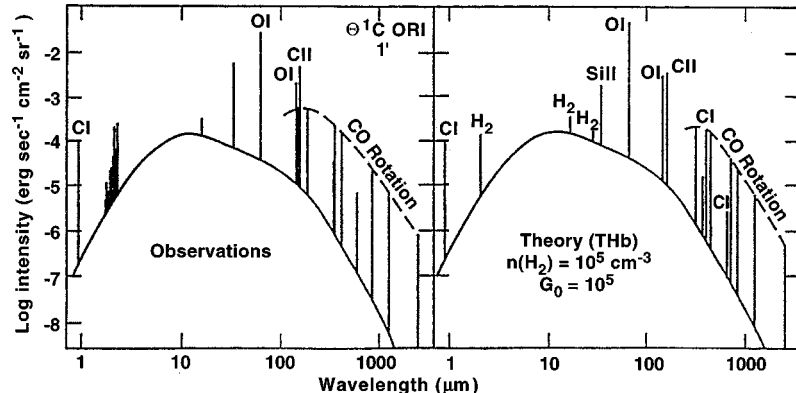


FIG. 19. A comparison between observed and model PDR spectra. The Orion spectra and model are taken from Tielens and Hollenbach (1985b), Hollenbach (1990), and Hollenbach and Tielens (1996). Emission from the HII region has been excluded. A good fit is obtained for $n \sim 10^5 \text{ cm}^{-3}$ and $G_0 \sim 10^5$.

like CO^+ , CN , and C_2H . Photodissociation regions associated with the diffuse interstellar medium can also be well studied through optical and far-ultraviolet absorption lines against bright background sources.

A. Physical conditions

These observations can be compared to PDR models to determine the physical conditions in the emitting gas. The far-infrared fine-structure lines are particularly useful in that respect, since the critical densities of the [CII] and [OI] lines ($3 \times 10^3 - 3 \times 10^5 \text{ cm}^{-3}$) and excitation energies (100–300 K) span the n, T range present in many PDRs (see Fig. 15). The [CII] 158- μm line, which is (marginally) optically thin, can be used to determine the total mass of emitting gas. These analyses do require assumed C and O elemental abundances (or abundance ratios) that are somewhat uncertain (Mathis, 1997; Cardelli *et al.*, 1996). Often, the physical conditions (e.g., densities) are also constrained by the ratio of the total cooling rate (i.e., the [OI]+[CII] intensity) to the far-infrared dust continuum. This ratio is equal to the photoelectric heating efficiency, which depends on the local density through the charging of the grains (see Sec. II.C.4). Of course, this analysis requires a good understanding of the photoelectric heating process itself and hence is also uncertain. Figure 19 shows a comparison of the observed infrared spectrum (1 μm –1000 μm) from a 1' beam centered on the Trapezium stars of Orion with the theoretical PDR model of Tielens and Hollenbach (1985b). Derived physical conditions include the density ($\sim 10^5 \text{ cm}^{-3}$), the incident far-ultraviolet flux ($G_0 \sim 10^5$), and either a relatively high gas-phase carbon abundance $\geq 2-3 \times 10^{-4}$ or a relatively low far-ultraviolet extinction by the dust in this dense cloud.

Boreiko and Betz (1996a, 1996b) have derived temperatures, column densities, and a $^{12}\text{C}/^{13}\text{C}$ isotopic ratio (~ 58) in M42 by observing the [OI] 63- μm and both isotopic [CII] 158- μm lines with very-high-velocity resolution (see Fig. 20). The derived temperatures ($\sim 200 \text{ K}$) are somewhat lower and columns ($\sim 10^{22} \text{ cm}^{-2}$) somewhat higher than homogeneous PDR

models. The [OI] FWHM linewidth of 6.8 km s^{-1} is slightly broadened by optical depth effects, but the relatively narrow linewidths of both [CII] and [OI] are consistent with a (turbulent) PDR origin. The temperature

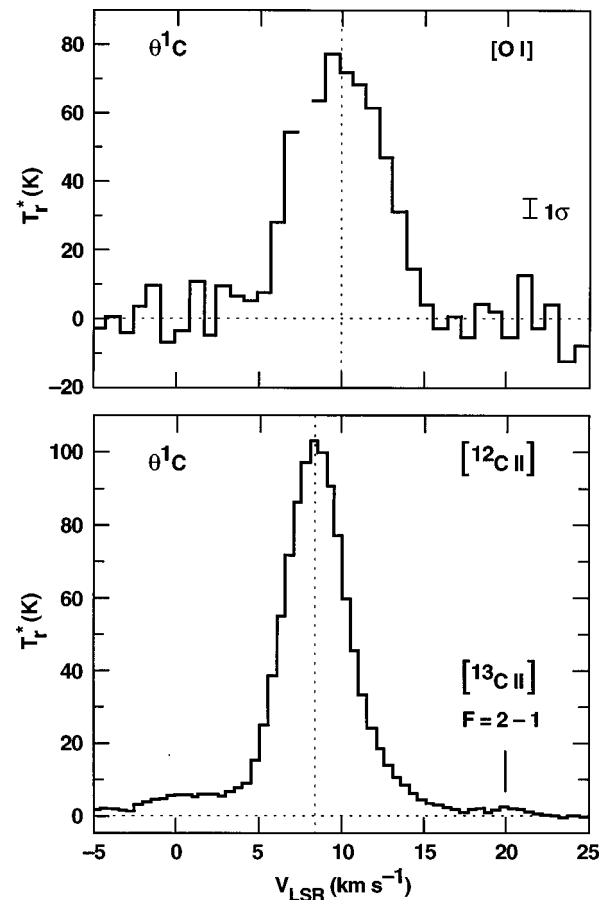


FIG. 20. The [OI] 63- μm and [CII] 158- μm fine-structure lines observed towards $\theta^1 \text{ C Ori}$ (Boreiko and Betz, 1996a, 1996b). The light vertical line is at $v_{\text{LSR}} = 9.8 \text{ km s}^{-1}$. The gap in the [OI] spectrum near $v_{\text{LSR}} = 8 \text{ km s}^{-1}$ shows the region where telluric OI absorption exceeds 50%. The location of the $F = 2-1$ fine-structure component of the $[^{13}\text{CII}]$ line is indicated. The lines are relatively narrow and consistent with a turbulent PDR origin.

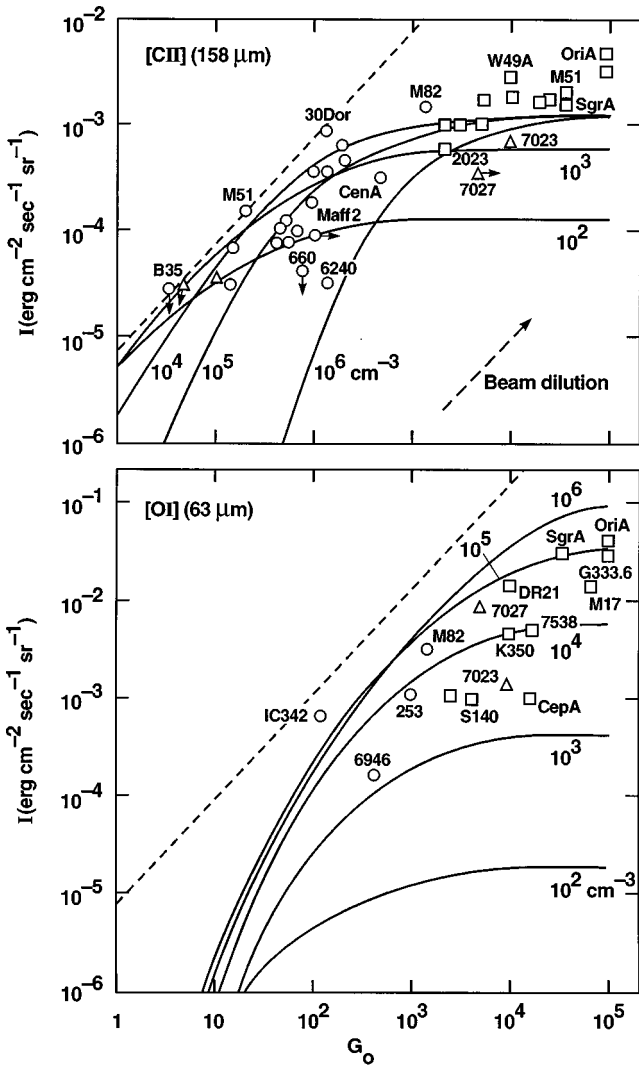


FIG. 21. Comparison of observations and models of the [CII] 158- μm and the [OI] 63- μm line are shown as a function of G_0 (Hollenbach *et al.*, 1991). Squares are PDRs associated with HII regions, triangles are PDRs associated with dark clouds, reflections nebulae, and planetary nebulae, and circles are PDRs associated with the inner 45–60'' of galaxies. Some well-known individual regions have been identified by their catalog numbers. The effects of beam dilution are indicated by the dashed arrow. The different models are labeled by their densities. The dashed line indicates an efficiency of 3% in the conversion of far-ultraviolet photon energy into gas cooling—the maximum expected for the photoelectric effect. See text for details.

and column density of the warm molecular component of PDRs can be determined directly from the lowest, pure rotational lines of H_2 , which have very low critical densities. To date, that has only been done for the Orion Bar (Parmar *et al.*, 1991, Burton, Hollenbach, and Tielens, 1992) and S140 (Timmermann, Bertoldi, *et al.*, 1996). The intensity distribution of the rotational CO levels also provides density and temperature information, although often for a cooler molecular component deeper in the PDR ($A_V > 4$) (Harris *et al.*, 1985; Jaffe *et al.*, 1990; Stutzki *et al.*, 1990; Graf *et al.*, 1993; Howe

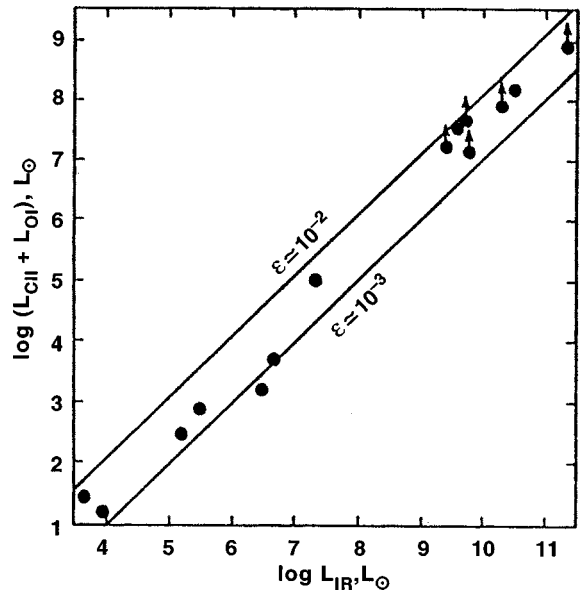


FIG. 22. The luminosity in the [CII] and [OI] fine-structure lines are plotted against the bolometric infrared continuum luminosity L_{IR} from dust for a selection of PDRs associated with reflection nebulae, HII regions, and starburst galaxies (from Hollenbach, 1990). The dominant PDR coolants [CII] and [OI] are typically $\epsilon \sim 10^{-2} - 10^{-3}$ as luminous as the dust, consistent with grain photoelectric heating of the gas.

et al., 1993; Boreiko and Betz, 1997; Lis *et al.*, 1997). Generally, the $J=7-6$ or $6-5$ transition is quite strong in dense PDRs around HII regions, implying densities of $\sim 10^5 \text{ cm}^{-3}$ and temperatures of $\sim 150 \text{ K}$. The presence of CO $J=14-13$ emission in some sources indicates even higher densities and temperatures (10^7 cm^{-3} , 500 K).

In Fig. 21, observations of the [CII] 158 μm and [OI] 63 μm lines are plotted as a function of the intensity of the incident far-ultraviolet field, G_0 ($= \frac{1}{2} I_{\text{IR}} / 1.3 \times 10^{-4} \text{ erg cm}^{-2} \text{ s}^{-1} \text{ sr}^{-1}$, where I_{IR} is the observed infrared intensity, the denominator is the normalization factor for the interstellar far-ultraviolet radiation field, and the factor 2 approximately accounts for visible photons absorbed by the dust and reradiated in the infrared). Examining these observations, we conclude that the [CII] line dominates the cooling for $G_0 \leq 10^3$. The [OI] line dominates at higher G_0 . Typically, the total cooling line intensity is in the range $10^{-2} - 10^{-3}$ of the total far-infrared continuum intensity. Figure 22 shows that this rough correlation extends over a large range in G_0 and an even larger range in IR luminosity ($10^4 - 10^{11} L_\odot$, Hollenbach, 1990). Clearly, the gas is fairly well coupled to the incident far-ultraviolet photon energy, the PDRs are the source of much of the IR luminosity, [CII] and [OI] dominate the gas cooling, and the observed efficiency is in good agreement with theoretical models of the photoelectric effect working on PAHs and small dust grains (see Sec. II.C).

Also shown in Figure 21 are PDR model calculations for different densities (Hollenbach *et al.*, 1991). In the models, the [CII] intensity scales with the incident far-ultraviolet flux (or far-infrared intensity) at low G_0 where [CII] is the dominant cooling line. The [CII] in-

TABLE II. Line intensities^a and physical conditions in PDRs.

Object	NGC 2023	Orion Bar	NGC 7027	Sgr A	M 82
[OI] 63 μm	4. (-3)	4. (-2)	1. (-1)	2. (-2)	1. (-2)
[OI] 145 μm	2. (-4)	2. (-3)	5. (-3)	7. (-4)	5. (-4)
[CII] 158 μm	7. (-4)	6. (-3)	1. (-2)	2. (-3)	2. (-3)
[SiII] 35 μm	2. (-4)	9. (-3)	—	2. (-2)	4. (-3)
H ₂ 1-0 S(1)	5. (-5)	2. (-4)	8. (-4)	9. (-4)	5. (-5)
CO $J=7-6$	5. (-5)	2. (-4)	— ^b	1.5 (-3)	5. (-5)
CO $J=14-13$	—	3. (-4)	— ^b	3. (-4)	—
FIR ^c	8. (-1)	5. (0)	4. (1)	5. (1)	6. (0)
PAHs ^d	9. (-2)	1.5 (-1)	1.8 (0)	—	1.4 (-1)
G_0	1.5 (4)	4. (4)	6. (5)	1. (5)	1. (4)
Interclump conditions					
n [cm ⁻³]	7.5 (2)	5. (4)	1. (5) ^e	1. (5)	1. (4)
T [K] ^f	250	500	1000 ^e	500	400
M_a/M_m	0.2	0.6	0.3	0.04	0.1
Clump conditions					
n [cm ⁻³]	1. (5)	1. (7)	1. (7) ^e	1. (7)	—
T [K] ^f	750 ^g	(2000)	(2000) ^e	(2000)	—
f_v	0.1	0.005	0.05	0.06	4. (-4)
References ^h	1,2,3,4	5, 6, 7	8, 9, 10	10, 11, 12	11, 13, 14

^aIntensities in units of erg cm⁻² s⁻¹ sr⁻¹.^bBright CO $J=17-16$ has been observed by Justtanont *et al.* (1997).^cTotal far-IR dust continuum intensity.^dIntensity in the PAH emission features.^eInterclump and clump refer to halo and torus, respectively (Justtanont *et al.*, 1997).^fTemperatures derived from observations. Theoretically, temperatures are expected to be sensitive to the depth in the PDR (cf. Fig. 16).^gC91 α indicates 100–200 K (Wyrowski, Walmsley, *et al.*, 1997).^hReferences: (1) Steiman-Cameron *et al.* (1997); (2) Wyrowski, Walmsley, *et al.* (1997); (3) Sellgren *et al.* (1985); (4) Jaffe *et al.* (1990); (5) Tielens *et al.* (1993); (6) Tauber *et al.* (1994); (7) Stutzki *et al.* (1990); (8) Cohen *et al.* (1986); (9) Justtanont *et al.* (1997); (10) Burton, Hollenbach, and Tielens (1990); (11) Wolfire *et al.* (1990); (12) Harris *et al.* (1985); (13) Willner *et al.* (1977); (14) Genzel (1992).

tensity levels off at high G_0 when the temperature exceeds ~ 100 K. At that point, the [OI] 63- μm line becomes a more efficient coolant and its intensity scales with G_0 (for high n , where the effects of grain charging on the photoelectric heating are minimal). The models are in good agreement with the observations for densities in the range 10^3 – 10^5 cm⁻³. We note that, as expected, the PDRs in reflection nebulae such as NGC 7023 and bright rim clouds such as S140 are characterized by somewhat lower densities (3×10^3 cm⁻³) and incident far-ultraviolet fields than those surrounding HII regions, such as M42 in Orion (10^5 cm⁻³). In general, the data imply that $G_0/n \sim 1$ cm⁻³ for these sources, so that stationary PDR models are adequate (see Sec. III.B).

We summarize in Table II the physical conditions in the dense PDRs associated with a number of template objects as derived from observations. They are derived from the listed intensities in the manner described above. Typical densities and temperatures are $n \sim 10^3$ – 10^5 cm⁻³ and $T \sim 200$ – 1000 K. The atomic mass in the C⁺ zone, M_a , is a significant fraction of the molecular

cloud (core) mass, M_m (see also Tielens, 1994).

In general, observations reveal pronounced clumping of the emitting gas. First, the [OI], [CII] and [CI] emission is extended on $\geq 5'$ scale as illustrated in Fig. 1 for Orion. In fact, Stacey *et al.* (1993) and Shibai *et al.* (1993) trace the [CII] extent even further than Fig. 1, and the PDR H₂ emission has likewise been observed on scales of tens of arc minutes by Burton and Puxley (1990), Luhman *et al.* (1994), and Usuda *et al.* (1996). All this gas is photoionized, photodissociated, and (photo)heated by θ¹ Ori C. Similar results have been obtained for Orion B, M17, S140, NGC 2023, and many other sources.¹² This emission scale size is much larger than that expected for a homogeneous region at the density indicated by the line ratios. Figure 23 shows the observations of NGC 1977 compared with models of a ho-

¹²These include Stutzki *et al.*, 1988; Matsuhara *et al.*, 1989; Howe *et al.*, 1991; White and Padman, 1991; Stacey *et al.*, 1993; Jaffe *et al.*, 1994; Plume *et al.*, 1994; Luhmann and Jaffe, 1996; Herrmann *et al.*, 1997; Spaans and van Dishoeck, 1997.

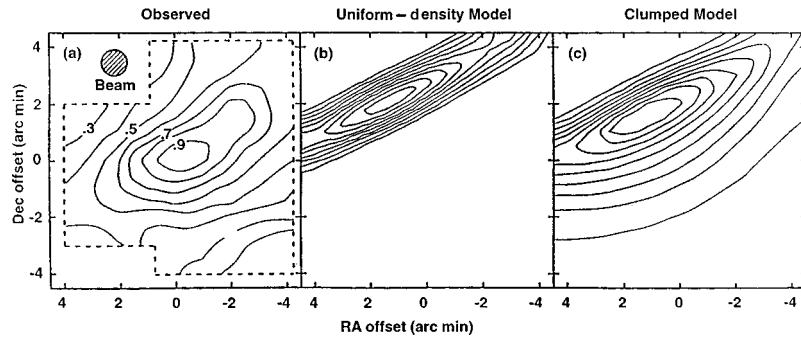


FIG. 23. Models of the [CII] 158- μm distribution in NGC 1977 compared with the observed [CII] distribution (Howe *et al.*, 1991). The uniform-density model ($n = 3 \times 10^4 \text{ cm}^{-3}$) has a far-ultraviolet attenuation length of 0.01 pc, while the clumped gas model corresponds to a far-ultraviolet attenuation scale length of 0.4 pc. The clumped model allows more far-ultraviolet penetration and fits the observed [CII] distribution much better than the uniform-density model. For scale $2' = 0.3 \text{ pc}$.

mogeneous cloud and a clumpy cloud (Howe *et al.*, 1991). Clearly, the gas is organized in filamentary and clumpy structures that allow the penetration of FUV photons to very large distances from the illuminating stars. On a parsec scale, the Orion molecular cloud consists of a highly nonuniform complex of filaments and clumps (Bally *et al.*, 1987). Second, maps in many molecular species (i.e., ^{13}CO , C^{18}O , CS, NH_3 , HCO^+ , HCN, H_2 , and PAHs) show direct evidence for clumping¹³ in PDRs with a surface filling factor of ≈ 0.1 . Third, most PDRs show bright molecular lines [e.g., CO J=14–13, H_2 1–0 and 2–1 S(1)] with high critical densities and high excitation temperatures which attest to the presence of high-density, warm molecular gas. The physical conditions of these clumps are not well constrained and likely span a range of values. Thermal H_2 2–1 S(1)/1–0 S(1) ratios require densities $n \gtrsim 10^5 \text{ cm}^{-3}$ and $T \sim 1000 \text{ K}$. Likewise, CII recombination line studies indicate clumpy, high-density ($\sim 10^5$ – 10^6 cm^{-3}) regions over a large area of the PDRs in Orion and NGC 2023 (Natta *et al.*, 1994; Wyrowski, Schilke, *et al.*, 1997; Wyrowski, Walmsley, *et al.*, 1997). Somewhat higher densities, $n \gtrsim 10^6$ – 10^7 cm^{-3} are required to produce bright CO J=14–13, 17–16 or 23–22 emission. Table II lists estimates for clump physical conditions in several PDRs. We note that homogeneous PDR models fall typically short of observed mid-J (e.g., 6–5 or 7–6) CO intensities, especially from the ^{13}CO isotope (Graf *et al.*, 1993; Lis *et al.*, 1997). Clump models may resolve this discrepancy (Köster *et al.*, 1994), or it may be that models underestimate the gas temperatures in the C^+/CO transition regions where these lines originate. Tauber *et al.* (1994) discuss various explanations of this discrepancy.

The inferred thermal pressures for these clumps (10^9 – $10^{10} \text{ K cm}^{-3}$) are well in excess of that sustainable by the interclump medium (or the HII region pressure). These clumps may therefore be confined by self-gravity and either are on their way to forming stars or already contain an embedded protostar (Meixner *et al.*, 1992). Hence they may be the PDR counterparts of the small partially ionized (Bok) globules (PIGs) and stellar “proplyds” observed in the HII region (see Sec. III.C). These objects seem to be widespread in molecular clouds.

B. The H_2 spectrum

As we shall discuss in Sec. IV.I, the H_2 emission from most galaxies originates in PDRs, and not in interstellar shock waves. Even in our own Milky Way Galaxy, the total H_2 luminosity from individual molecular clouds such as Orion A originates mainly in PDRs, even though strong shocks are present (Luhman *et al.*, 1994; Luhman and Jaffe, 1996). Far-ultraviolet absorption in the Lyman Werner bands excites molecular hydrogen electronically. In 85–90% of these far-ultraviolet “pumps,” electronic (far-ultraviolet) fluorescence (Sternberg, 1989) leaves the molecule in a vibrationally excited state of the ground electronic state (Sec. II.B, Fig. 8). Molecules in these levels decay through electric quadrupole transitions in the far-red and near-infrared. The intensities of these lines thus depend on the detailed distributions of the level populations through the cloud, distributions which themselves depend on the (far-ultraviolet) line radiative transfer (see Sec. II.B) as well as the density and temperature of collision partners. Level populations and IR emission spectra have been calculated for a variety of model clouds.¹⁴ Pure rotational spectra of H_2 have been calculated by Burton,

¹³See, for example, Gatley *et al.*, 1987; Güsten and Fiebig, 1988; Massi *et al.*, 1988; Stutzki *et al.*, 1988; Stutzki and Güsten, 1990; Tauber and Goldsmith, 1990; Chrysostomou *et al.*, 1992, 1993; Minchin *et al.*, 1993; Hobson *et al.*, 1994; Tauber *et al.*, 1994; Hogerheijde *et al.*, 1995; Kramer *et al.*, 1996; Lemaire *et al.*, 1996; Young Owl *et al.*, 1999.

¹⁴See Black and Dalgarno, 1976; Black and van Dishoeck, 1987; Sternberg, 1988, 1990 for the HD isotope; Sternberg and Dalgarno, 1989; Abgrall *et al.*, 1992; Draine and Bertoldi, 1996; and Neufeld and Spaans, 1996.

Hollenbach, and Tielens (1992), Spaans *et al.* (1994), and Timmermann, Bertoldi, *et al.* (1996).

One uncertainty in the calculated spectra resides in the details of the H₂ formation process on grain surfaces. It has been suggested that the newly formed H₂ is vibrationally or rotationally excited when it is injected into the gas phase (e.g., Hollenbach and Salpeter, 1970; 1971; Hunter and Watson, 1978; Wagenblast 1992; Duley and Williams, 1993). However, H₂ might resonantly transfer much of the excess chemical energy to nearby functional groups on the surface before it evaporates, leaving the molecule in $v=1$ or 2 (Tielens and Allamandola, 1987). For the overall energetics of H₂ excitation, the H₂ formation process is of little importance ($\leq 10\%$) compared to the far-ultraviolet fluorescence process when the H₂ chemistry is in equilibrium, since there are about nine far-ultraviolet pumps with resulting fluorescence for every H₂ formation. Nevertheless, if H₂ is preferentially formed in only a few states, this may affect the intensities of the lines from those levels and the subsequent cascade (Wagenblast, 1992; Le Bourlot *et al.*, 1995).

Another uncertainty is associated with the *ortho* to *para* ratio of H₂. Four processes can affect the *ortho* to *para* ratio in PDRs (Burton, Hollenbach, and Tielens, 1992): (1) In warm gas, the conversion can be effected by the reaction H+H₂, which has an activation barrier of 3200 K; (2) in cool gas, reactions of H₂ with H⁺ (and to a lesser extent H₃⁺) can still convert *ortho* to *para* and back (Dalgarno *et al.*, 1973); (3) on grain surfaces, a nuclear spin conversion of H₂ may occur due to the interaction with the nuclear spin of a neighboring species or the unpaired electron of a paramagnetic impurity or lattice defect (Tielens and Allamandola, 1987); (4) formation of H₂ on grain surfaces is expected to lead to an *ortho-para* ratio of 3. But if the newly formed H₂ resides long enough on the grain, process (3) might be more important, even for newly formed H₂. In high-density, high far-ultraviolet flux PDR models, appropriate for the Orion Bar, reactions with atomic hydrogen in the gas dominate the *ortho-to-para* ratio and a value of 3 is expected in the fluorescence zone (Burton, Hollenbach, and Tielens, 1992). If effective, gas-grain collisions would drive the *ortho-to-para* ratio to a value appropriate for the grain temperature deeper in. But only the 0–0 S(0) and S(1) line intensities would be affected by this process. In lower-density, lower far-ultraviolet PDR models (i.e., $T < 300$ K), the first process is of little consequence and the *ortho-para* ratio is set by the formation process. Adopting an intrinsic ratio of 3 for the formation process would result in a predicted ratio of 2.5 in the fluorescing gas of a typical reflection nebula (Burton, Hollenbach, and Tielens, 1992). The second process is never very important over the lifetime of an H₂ molecule in the fluorescence zone (but dominates for dark cloud cores). Recently, Draine and Bertoldi (1996) have shown that for high-density warm PDRs ($n \geq 10^6$ cm⁻³, $G_0 \geq 10^5$), the *ortho-to-para* ratio in the $v=1$ level can exceed 3. Under these conditions, the $v=1$ level is thermalized. Moreover, the column densities in the $v=1$

ortho levels of the $v=1$ (but not the *para* levels) become large enough that self-shielding reduces the far-ultraviolet pumping out of these levels. As a result there is preferential destruction of *para* H₂ as compared to *ortho* H₂ and an *ortho-to-para* ratio larger than 3 results. This effect is only operative when a large fraction of the far-ultraviolet photons are absorbed by vibrationally excited H₂.

At low n ($\leq 10^4$ cm⁻³), collisional deexcitation is unimportant and the infrared spectrum is due to “pure” fluorescence and can be calculated directly from the transition probabilities of the levels involved, taking the radiative transfer into account. For $G_0/n < 10^{-2}$ cm³, H₂ self-shielding dominates the opacity in the 912–1100-Å range, the gas is fully molecular in the fluorescence zone, and the line intensity scales directly with the intensity of the incident far-ultraviolet radiation field and is independent of the density. For $G_0/n \geq 0.1$ cm³, dust opacity is more important, hydrogen is largely atomic in the fluorescence zone, and the line intensities become largely independent of G_0 and are proportional to the density. At high densities, collisional processes are important, modifying the emitted spectrum to a thermal spectrum in the lowest levels (i.e., $v=1-0$ and 2–1; Sternberg, 1986; Hollenbach, 1988; Sternberg and Dalgarno, 1989; Burton, Hollenbach, and Tielens, 1990; Draine and Bertoldi, 1996; Luhman, Jaffe, *et al.*, 1997; Luhman, Luhman, *et al.*, 1997). A relatively large population of high vibrational levels, though reduced by collisions, is maintained by far-ultraviolet pumping.

Far-red and near-infrared H₂ fluorescence spectra have been observed in a variety of classical PDRs such as those associated with NGC 2023, S140, NGC 7023, the Orion Bar, Orion A and B, and ρ Oph.¹⁵ Figure 24 compares the distribution of the H₂ $v=6-4$ Q(1) line towards the Orion region to that of the H₂ $v=1-0$ S(1) and the [CII] 158-μm line (Luhman *et al.*, 1994). The [CII] emission traces PDR gas heated by the illuminating star θ^1 Ori C. The peak H₂ $v=1-0$ S(1) emission, on the other hand, is due to warm gas shocked by the strong wind originating from the embedded protostar IRC 2. Because of its high excitation, the H₂ $v=6-4$ Q(1) emission arises in far-ultraviolet pumped PDR gas. However, the relatively low, measured intensity implies that the upper levels of H₂ are collisionally deexcited and hence the gas is rather dense ($\geq 10^5$ cm⁻³). Figure 25 compares the observed IR spectrum 16'' north of the illuminating star in NGC 2023 (Gatley *et al.*, 1987) with model calculations for the pure-fluorescence case, illustrating the good fit possible (Black and van Dishoeck, 1987). The fit mainly depends on the adopted value for G_0 and the detailed geometry of this emission ridge. It is not sensitive to the density for $n \leq 10^4$ cm⁻³. H₂

¹⁵See, for example, Hayashi *et al.*, 1985; Gatley *et al.*, 1987; Hasegawa *et al.*, 1987; Hippelien and Münch, 1989; Tanaka *et al.*, 1989; Burton, Geballe, *et al.*, 1990; Burton, Bulmer, *et al.*, 1992; Luhmann and Jaffe, 1996; Martini *et al.*, 1997; Marconi *et al.*, 1998.

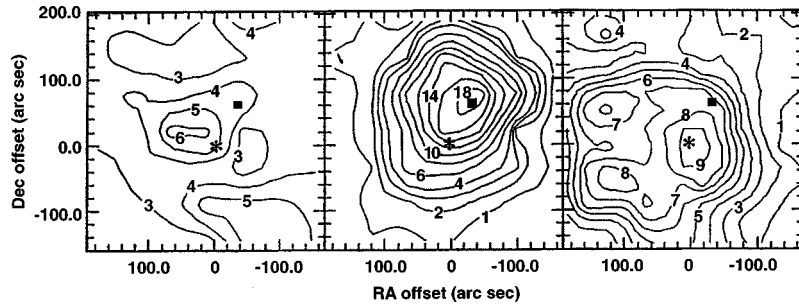


FIG. 24. H_2 and $[\text{CII}]$ emission in the Orion PDR. Left: $v=6-4 Q(1)$ map of the Orion extended PDR. The peak contour level is $6.4 \times 10^{-6} \text{ erg cm}^{-2} \text{ s}^{-1} \text{ sr}^{-1}$ in a $65''$ beam. The $0,0$ position is at $\theta^1 \text{ Ori C}$ (asterisk); the BN-KL outflow is the square. Center: $\text{H}_2 1-0 S(1)$ map of the PDR. Contour units are $3.53 \times 10^{-5} \text{ erg cm}^{-2} \text{ s}^{-1} \text{ sr}^{-1}$ in a $150''$ beam. Both from Jaffe *et al.* (1994). Right: $[\text{CII}]$ 158- μm map of Stacey *et al.* (1993, $55''$ beam). Contour units are $3.9 \times 10^{-4} \text{ erg cm}^{-2} \text{ s}^{-1} \text{ sr}^{-1}$. For scale $60'' = 0.15 \text{ pc}$.

spectra have also been obtained for the bright H_2 ridge, $78''$ south of the star (Gatley *et al.*, 1987; Burton, Bulmer, *et al.*, 1992). This region has a more thermal $1-0S(1)/2-1S(1)$ ratio, and the observed spectrum is consistent with emission by higher-density gas (10^5 cm^{-3} ; Burton, Hollenbach, and Tielens, 1990; Draine and Bertoldi, 1996). Figure 26 shows the best-fit model H_2 column densities in the v,J state compared with the observations assuming $n=10^5 \text{ cm}^{-3}$, $G_0=8500$, and a viewing angle of $\cos \theta=0.2$ (from Draine and Bertoldi, 1996). The observed high density for this region is in good agreement with studies of the dominant PDR cooling lines and molecular line observations (Fuente *et al.*, 1995; Jansen *et al.*, 1995a; Steiman-Cameron *et al.*, 1997; Wyrowski, Walmsley, *et al.*, 1997).

Recent ISO observations reveal pure rotational emission in the S140 photodissociation region (Timmermann, Bertoldi, *et al.*, 1996; we discuss ISO observations of pure rotational H_2 emission in galaxies in Sec. IV.I). Figure 27 summarizes the column densities derived for the different levels from the observed SWS ISO lines and available ground-based data. The pure rotational lines ($J < 7$), because of their small Einstein A values, are

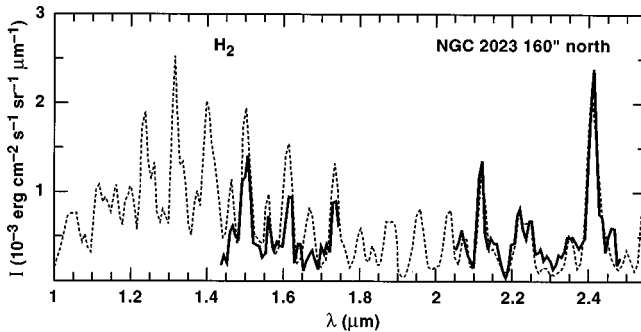


FIG. 25. Comparison of observed and calculated H_2 emission spectra, adapted from Black and van Dishoeck (1987). Solid curve: spectrum observed $160''$ north of the illuminating star in the reflection nebula NGC 2023 (Gatley *et al.*, 1987). Light curve: Calculated emission spectrum for $G_0=200$ and a density of 10^4 cm^{-3} convolved to a resolution of $\lambda/\Delta\lambda=100$ (Black and van Dishoeck, 1987). See text for details.

good indicators of the gas temperature and densities. The observations indicate emission from gas at 500 K with a column density of $1.6 \times 10^{20} \text{ cm}^{-2}$. Higher pure rotational levels start to deviate due to the contribution by far-ultraviolet pumping. Populations of the vibrational levels are displaced towards the right due to UV-pumped fluorescence, but the lower J levels in these vibrationally excited states still indicate temperatures of 500 K. The model (open symbols) was calculated for a density of 10^4 cm^{-3} , an incident far-ultraviolet field of

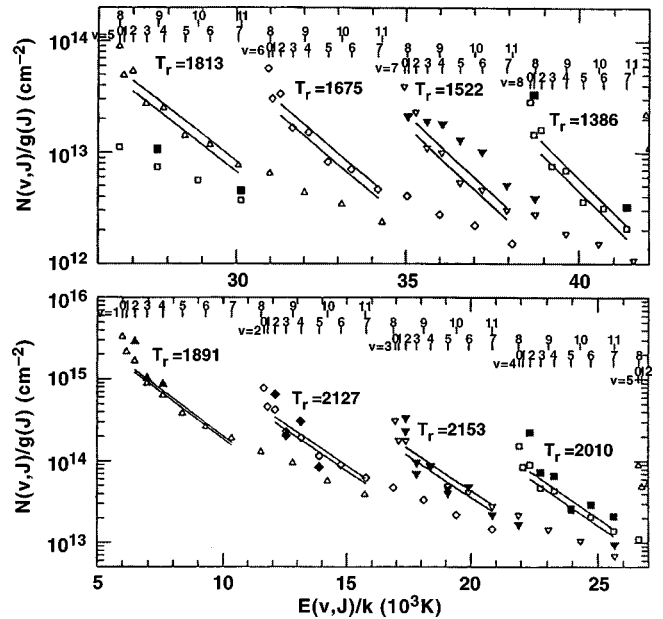


FIG. 26. Column densities $N(v,J)$ of H_2 in the v,J state divided by the level degeneracy $g(J)$ for the NGC 2023 emission ridge (from Draine and Bertoldi, 1996). Filled symbols are derived from observations of Hasegawa *et al.*, (1987) and Burton, Bulmer, *et al.* (1992), corrected for extinction, beam dilution, and calibration errors. Open symbols are for a plane-parallel slab model with $G_0=8500$, $n=10^5 \text{ cm}^{-3}$, and $T=900 \text{ K}$, viewed at an angle with $\cos \theta=0.2$. Solid lines are least-squares fits to the $J=2-7$ populations in each vibrational level. For each vibrational level, the best-fit value of the rotational temperature T_r is indicated.

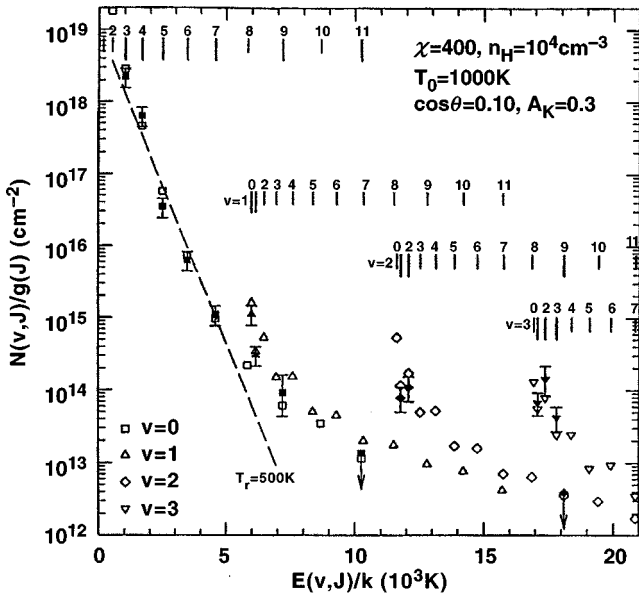


FIG. 27. Observed (filled symbols) and model (open symbols) H_2 column densities divided by the statistical weight of the level as a function of the excitation energy in the PDR of S140 (Timmermann, Bertoldi, *et al.*, 1996).

400, and an assumed temperature distribution that starts at 1000 K but drops smoothly to about 20 K at an A_V of 1. It should be emphasized that PDR models have difficulty explaining the high gas temperature observed towards this source, given the low incident far-ultraviolet field and moderate density (see Wolfire *et al.*, 1990).

C. The molecular transition observed in edge-on PDRs

The edge-on geometry of the Orion Bar PDR lends itself particularly well to detailed studies of the spatial structure of PDRs (see Tielens *et al.*, 1993; Hogerheijde *et al.*, 1995; van der Werf *et al.*, 1996; Fig. 2). Clearly, the H/H_2 transition, as outlined by the peak emission from vibrationally excited H_2 , occurs at about $10''$ into the cloud from the ionization front (i.e., the location of the Bar in [OI] 6300 and [SII] 6731 Å). The CO 1-0 and [CI] 609-μm lines peak rather abruptly at a distance of $20''$ from the ionization front. These observations agree very well with predictions of the global characteristics of stationary PDR models (Tielens *et al.*, 1993; Jansen *et al.*, 1995a; van der Werf *et al.*, 1996). In such models, the location of the H/H_2 transition region and thus the peak in H_2^* emission is displaced inwards from the ionization front by $A_V \approx 2$ and the $\text{C}^+/\text{C}/\text{CO}$ transition occurs another $\Delta A_V \approx 2$ deeper into the cloud (Fig. 16). Using standard dust parameters, the observed spatial scale then translates into a density of $5 \times 10^4 \text{ cm}^{-3}$ (Tielens *et al.*, 1993). Calculated line emission for the fine-structure lines of [OI] 63 and 146 μm, [CII] 158 μm, [SII] 35 μm, [CI] 609 μm, and CO 1-0 agree well with the observed intensities for this density and $G_0 = 5 \times 10^4$, which is appropriate for θ^1 Ori C at the projected distance of the Orion Bar (Table II). The presence of

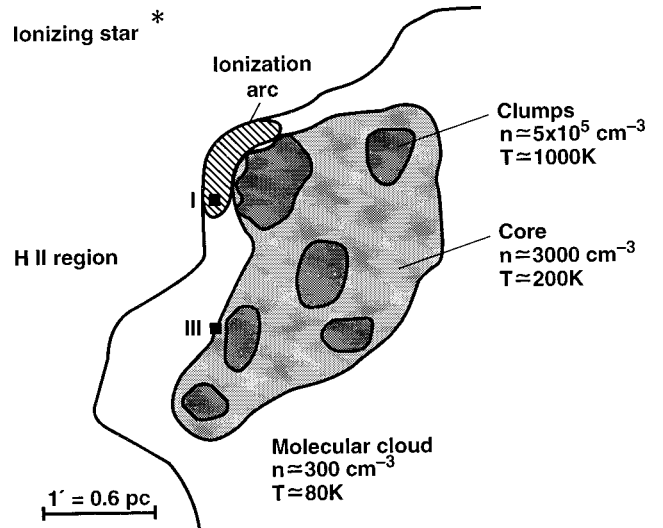


FIG. 28. A schematic of the M17SW PDR region showing a three-component clumpy core and halo model (Meixner *et al.*, 1992). Dense clumps are embedded in an interclump medium in the core, which is surrounded by a more diffuse halo. The [OI], [SII], and high-level CO originate in the high-density clumps. The [CII], [CI], and low-level CO arise in lower-density interclump gas. The low-density halo reproduces the observed extended [CII] and [CI] emission. Approximate densities and temperatures of each component are indicated.

denser clumps (10^7 cm^{-3}) is indicated by bright emission in CO 7-6 and 14-13 (Stacey *et al.*, 1993) and by the presence of other high-density tracers such as CS, H_2CO , and HCO^+ (Tauber *et al.*, 1994; Hogerheijde *et al.*, 1995; van der Werf *et al.*, 1996). However, Marconi *et al.* (1998) present H_2 2 μm observations and Simon *et al.* (1997) present CN and CS observations which suggest a homogeneous PDR in the Bar.

M17SW is another region where the edge-on geometry allows a detailed study of the structure of PDRs (Stutzki *et al.*, 1988; Meixner *et al.*, 1992). As in the Orion Bar region, cross scans show a clear separation between the ionized (free-free), atomic ([OI], [CII], [SII]), and molecular (CO 2-1) gas. M17 is four times farther away than Orion and the scale size is somewhat larger ($40''$ rather than $20''$); both these factors indicate a much lower average gas density ($3 \times 10^3 \text{ cm}^{-3}$) in the interclump regions of this molecular cloud core. The observed high intensity of the [OI], and [SII] lines thus implies that they originate mainly from the surfaces of the dense ($n \lesssim 10^7 \text{ cm}^{-3}$) clumps evident in the molecular observations (Stutzki *et al.*, 1988; Meixner *et al.*, 1992). The [CII] and [CI] lines in contrast originate from the lower-density interclump gas in the M17SW core. Figure 28 shows a schematic diagram of the derived morphology of M17SW from the PDR models and observations of Meixner *et al.* Besides the M17SW photodissociation region, the [CII] and [CI] emission is extended over a size scale of $\approx 10 \text{ pc}$ (Keene *et al.*, 1985; Stutzki *et al.*, 1988; Matsuhara *et al.*, 1989). This emission may well be associated with clumps illuminated at large distances by far-ultraviolet radiation penetrating

into the much-lower-density ($\approx 300 \text{ cm}^{-3}$), 23-km s $^{-1}$ CO cloud, which extends from the northeast, well over the HII region and the M17SW core (Lada, 1976). Alternatively, there may be local B stars exciting this very extended emission (Stutzki *et al.*, 1988; Hansen *et al.*, 1997).

Edge-on PDRs form an excellent laboratory in which to study in detail the interaction of far-ultraviolet photons with gas and dust. One might hope that future studies of, for example, the dominant gas cooling lines and their correlation with the PAH and dust IR emission will allow a semiempirical evaluation of the cooling and, hence, photoelectric heating process and its dependence on physical conditions. Present and future generations of (sub)millimeter arrays also allow a detailed analysis of the effects of far-ultraviolet photons on the molecular composition of interstellar gas. The first studies of this kind have already been undertaken for IC 63 (Jansen *et al.*, 1995b, 1996), the Orion Bar (Tauber *et al.*, 1994, 1995; Hogerheijde *et al.*, 1995; Fuente *et al.*, 1996; van der Werf *et al.*, 1996; Simon *et al.*, 1997; Young Owl *et al.*, 1999) and NGC 2023 (Fuente *et al.*, 1995). Finally, limb brightening due to the edge-on geometry also allows the detection of trace species that are otherwise difficult to detect, for example, CO $^+$ (Latter *et al.*, 1993; Jansen *et al.*, 1995a; Störzer *et al.*, 1995; Fuente and Martin-Pintado, 1997).

D. The origin of [CI] emission

In retrospect, observations of the [CI] 609 μm line formed one of the earliest indications that PDRs are a ubiquitous component of molecular clouds (Phillips and Huggins, 1981). Atomic carbon has long been recognized to be an abundant species near the surfaces of molecular clouds (Langer, 1976; de Jong *et al.*, 1980). However, the early observations of the lowest-lying transition of CI showed more intense emission than expected on the basis of the predicted CI column density. While this discrepancy led to a flurry of papers proposing a variety of schemes to increase the abundance of atomic C inside dense clouds, the first detailed PDR models (Tielens and Hollenbach, 1985a, 1985b, 1985c) calculated about a ten times higher CI column density than the earlier models, partly due to improved chemical schemes (e.g., the inclusion of charge exchange between C $^+$ and S and the far-ultraviolet opacity of atomic carbon) and partly because of an adopted higher gas-phase carbon abundance. PDR theory (Tielens and Hollenbach, 1985a, 1985c; van Dishoeck and Black, 1988; Hollenbach *et al.*, 1991; Bakes and Tielens, 1998) is now in reasonable agreement with the observed line intensities (Phillips and Huggins, 1981; Keene *et al.*, 1985; Genzel *et al.*, 1988; Ingalls *et al.*, 1997). Current models explore the effects of the clumpy structure of molecular clouds (Hegmann and Kegel, 1996; Spaans and van Dishoeck, 1997), the time-dependent effects associated with C $^+$ recombination in cooling PDRs suddenly shadowed from far-ultraviolet flux by moving foreground clumps (Störzer *et al.*, 1997), the dependence of CI on ionization

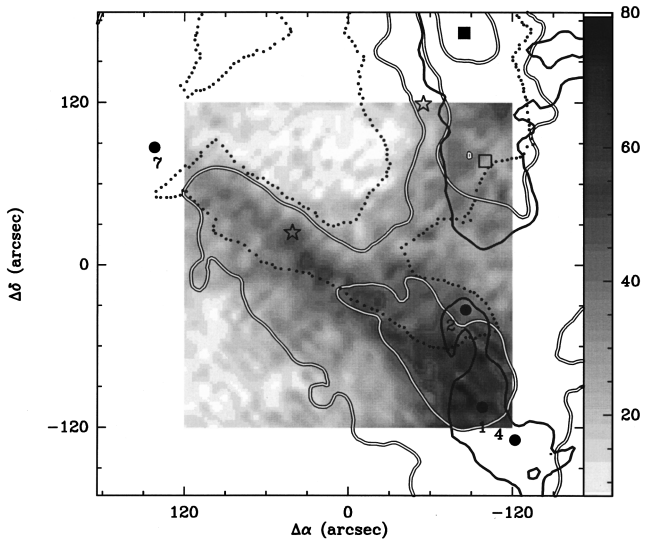


FIG. 29. The [CI] 610- μm emission in the Orion Bar region compared to other tracers (Tauber *et al.*, 1995); integrated [CI] emission (3–13 km/s; gray scale); integrated ^{13}CO $J=2-1$ intensity (double contours); HC_3N $J=12-11$ emission (solid black line); PAH 3.3- μm emission (dotted line). Central position is $(\alpha, \delta)_{1950} = (5^{\circ}32'52.7", -5^{\circ}27'U15UU)$. The two stars are θ^2 Ori A (left) and θ^1 Ori C (right). The protostar IRC2 is indicated by a filled square. The open square is the Orion South source. The dots indicate condensations in the HC_3N emission.

(Flower *et al.*, 1994), and the effects of PAHs on the ionization balance (Bakes and Tielens, 1998).

Higher-spatial-resolution studies with the James Clarke Maxwell Telescope (JCMT) and the Caltech Submillimeter Observatory (CSO) clearly confirm the association of the [CI] emission with the PDR. In particular, in the Orion Bar, the [CI] 609 and 370 μm emission forms a barlike structure at a similar distance from the ionization front to the CO 1–0, in good agreement with theory (White and Padman, 1991; Tauber *et al.*, 1995; White and Sandell, 1995). This is illustrated in Fig. 29. A similar spatial structure is seen in S140, although an embedded source contributes to the [CI] deeper into the cloud as well (Minchin *et al.*, 1993). Similar to the extremely extended [CII] 158 μm emission, the [CI] emission in M17SW is thought to originate from the surfaces of clumps illuminated either by deeply penetrating far-ultraviolet photons or by local B stars (Stutzki *et al.*, 1988; Meixner and Tielens, 1993; Plume *et al.*, 1994). [CI] often correlates with ^{13}CO 2–1 in spatial extent and line profile (Keene, Lis, *et al.*, 1997), indicating that emission of both species is dominated by clump PDR surfaces (Phillips and Huggins, 1981; Meixner and Tielens, 1993; Plume *et al.*, 1994; Spaans and van Dishoeck, 1997). [CI] studies of translucent clouds (Stark and van Dishoeck, 1994; Stark *et al.*, 1996) and opaque molecular clouds (Minchin and White, 1995; Minchin *et al.*, 1995) also indicate that the $N(\text{C})/N(\text{CO})$ ratio varies with A_V and G_0 , as expected in PDR models. The recent observation of the ^{13}CI $^3\text{P}_2 \rightarrow ^3\text{P}_1$ transition in the Orion Bar indicates a high column of ^{13}C there, which suggests

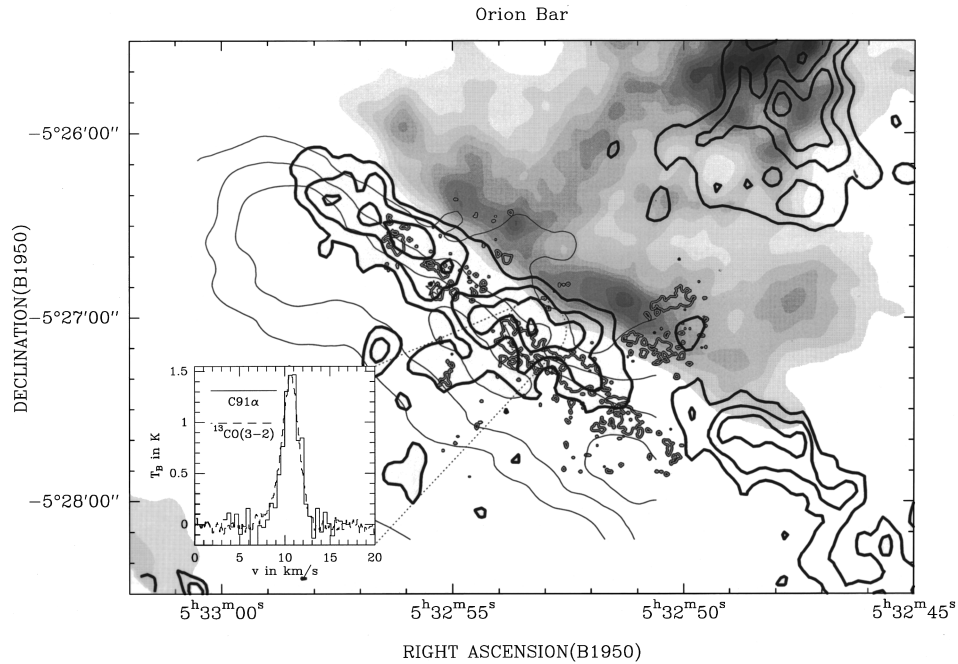


FIG. 30. VLA 3.5-cm continuum [gray-scale, compared to C91 α (VLA) integrated intensity (heavy full contours: 30, 50, 70, 90% of peak intensity 5.5 K km s $^{-1}$) and ^{13}CO (3–2) integrated intensity from Lis *et al.* (1997, light contours; only the region around the Bar was mapped). The black and white contours are H_2 [1–0 S(1)] image of van der Werf *et al.* (1996). The insert in the lower left shows a comparison of C91 α (smoothed to 20'') and ^{13}CO (peak 29 K) spectra towards the indicated position in the Bar.

little chemical fractionation of ^{13}C into ^{13}CO , possibly due to isotope-selective photodissociation of ^{13}CO in the PDR (Keene, Schilke, *et al.*, 1998).

E. CI recombination lines

Emission in CI recombination lines has been studied theoretically by Escalante *et al.* (1991) and by Natta *et al.* (1994). Observations of CI recombination lines date back two decades (Balick *et al.*, 1974; Knapp *et al.*, 1976a, 1976b; Pankonin *et al.*, 1977; Jaffe and Pankonin, 1978; Pankonin and Walmsley, 1978) but only in recent years have their importance for the study of PDRs been fully realized (Natta *et al.*, 1994; Wyrowski, Schilke, *et al.*, 1997; Wyrowski, Walmsley, *et al.*, 1997). Observations show that the CI radio recombination lines also form in PDRs (Fig. 30), but they have a different dependence on the density and temperature than the far-infrared fine-structure lines (e.g., [CII]). This has been exploited by Natta *et al.* (1994) to derive the physical conditions in the emitting gas. The results of these calculations are shown in Fig. 31. The results show that the C91 α line (8.6 GHz) originates in dense (10^6 cm^{-3}), warm (500–1000 K) gas. Even at large distances, the observed high intensity of this line implies high densities (10^5 cm^{-3}).

Photodissociation regions are also bright in the far-red lines of CI at 9850, 9823, and 8727 Å (Hipplein and Münch, 1978, 1989; Münch and Hipplein, 1982; Burton, Hollenbach, and Tielens, 1990). These have been attrib-

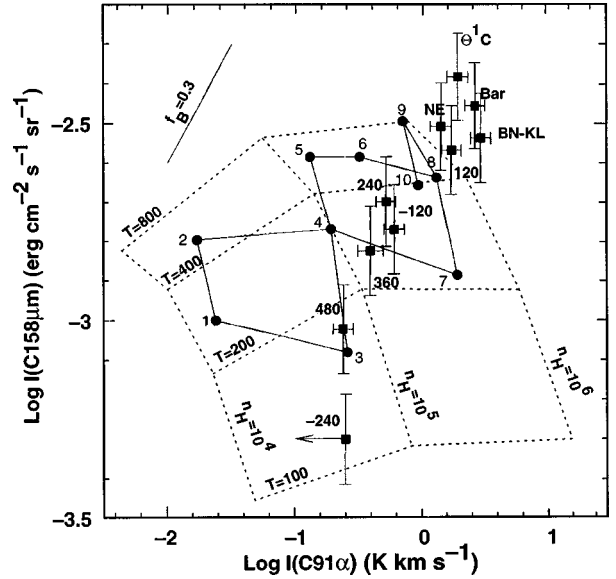


FIG. 31. Plot of the observed [CII] 158- μm intensities vs the C91 α integrated intensities (filled squares with error bars). They are labeled with their names or their offsets from θ^1 Ori C. The light dashed contours show the results for homogenous density and temperature models. The dots give the results of full-fledged PDR models, numbered from 1 to 10. Model density increases towards the right from 10^4 to 10^6 cm^{-3} . Model incident far-ultraviolet fluxes increase towards the top from 10^3 to 10^6 Habing fields. (Model 10 is actually for a G_0 of 10^7 .) The effects of beam dilution by a factor of 0.3 are indicated by the line labeled $f_B=0.3$. From Natta *et al.* (1994).

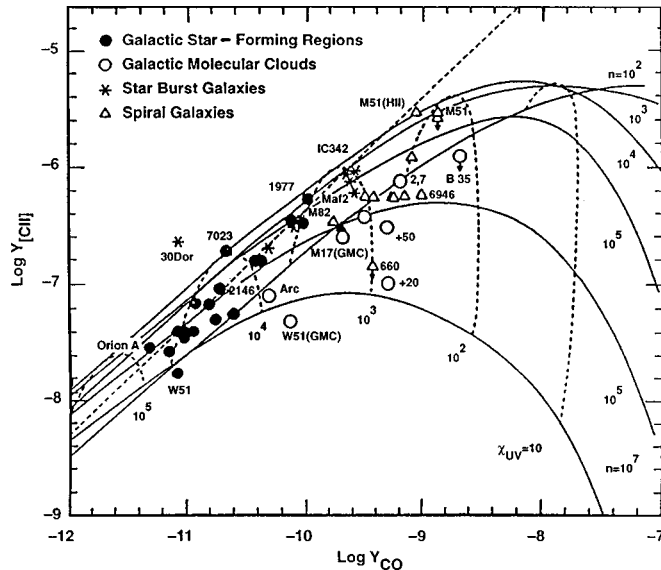


FIG. 32. The ratio Y of the integrated line intensities in [CII] and $^{12}\text{CO } J=1-0$ (in $\text{erg s}^{-1} \text{cm}^{-2} \text{sr}^{-1}$) to the FIR continuum intensity (in units of $2.0 \times 10^{-4} \text{ erg s}^{-1} \text{cm}^{-2} \text{sr}^{-1}$) plotted for a number of observed sources. PDR models as a function of n and χ_{UV} ($=G_0/1.7$) are superimposed (see also Wolfire *et al.*, 1989). The dashed line indicates the [CII]/ $^{12}\text{CO}(1-0)$ line flux ratio (6300) observed for starburst galaxies and galactic OB star formation regions. From Stacey *et al.* (1991).

uted to carbon recombination emission by Cesarsky (1982). Theoretical calculations of the expected intensities have been done by Escalante *et al.* (1991) and Natta *et al.* (1994). These far-red recombination lines depend on $T^{-0.6}$ while the radio recombination lines depend on $T^{-1.5}$. Hence the ratio of the far-red lines to the radio lines is sensitive to high-density ($>10^5 \text{ cm}^{-3}$) clumps, which become very warm ($T>1000 \text{ K}$) when illuminated by a strong far-ultraviolet field ($G_0>10^5$; Natta *et al.*, 1994).

F. The [CII]-CO correlation

Crawford *et al.* (1985) and Stacey *et al.* (1991) show a linear correlation in the observed integrated intensities of [CII] 158- μm and $^{12}\text{CO } J=1-0$ from bright dense galactic PDRs and PDRs in starburst galactic nuclei (see Fig. 32). Wolfire *et al.* (1989) and Stacey *et al.* (1991) explain this correlation with high-field far-ultraviolet opaque PDR models (also shown in Fig. 32) in which the [CII] 158- μm emission arises from the warm, $A_V \lesssim 1-2$, outer regions and the $^{12}\text{CO } J=1-0$ originates from the cooler gas somewhat deeper ($A_V \sim 3-4$) into the cloud. In PDR models with high densities, $n \gtrsim 3 \times 10^3 \text{ cm}^{-3}$, and high incident far-ultraviolet fluxes, $G_0 \gtrsim 3 \times 10^3$, I_{CII} and I_{CO} are relatively constant. The [CII] intensity is constant because at high G_0 the temperature of the gas exceeds the excitation energy, $\Delta E/k = 92 \text{ K}$, of the [CII] 158- μm transition. With $n > n_{cr}$ or local thermodynamic equilibrium, the [CII] 158- μm intensity is not density sensitive, but rather only sensitive to the column density of C^+ . At high G_0 , the column of C^+ is

roughly constant, varying only logarithmically with G_0 because of dust attenuation. Therefore, I_{CII} is roughly constant at high n and G_0 . The CO $J=1-0$ intensity is constant because it is an optically thick transition which, at high densities or local thermodynamic equilibrium (LTE), is mainly sensitive to the temperature of the emitting gas. The $^{12}\text{CO } J=1-0$ transition originates from a deeper, cooler region where the gas temperature varies very slowly with changes in G_0 . In large part, the observed linear correlation in [CII] and $^{12}\text{CO } J=1-0$ arises because the [CII] and CO originate from the same clouds, their *emergent* intensities and intensity ratio are constant, and the effects of beam filling factors or beam dilution produce a linear correlation in the observed intensities. In addition to the beam dilution effect, [CII] 158 μm and CO $J=1-0$ have similar critical densities so that the linear correlation is maintained at low densities and high G_0 , as both emergent intensities drop because of nonequilibrium effects. However, in low far-ultraviolet fields, the [CII]/CO ratio is low because the PDR cools and self-shields, which affects [CII] much more than CO. On the other hand, high [CII]/CO ratios are found in diffuse clouds (pure [CII]) or in HI halos of molecular clouds (Jaffe *et al.*, 1994). High ratios may also result from geometry effects (Köster *et al.*, 1994) or clouds with small molecular cores and large C^+ halos such as in the Magellanic Clouds (see Sec. VI.B). These trends are observed in Fig. 32.

G. OH and CH_3OH maser regions

Many ultracompact HII regions show associated OH and CH_3OH maser emission outside the ionized gas (Moran *et al.*, 1968; Reid *et al.*, 1980; Menten *et al.*, 1988, 1992). The earliest model located the OH maser emission in the dense compressed shell created by the expanding HII region. The shock wave separating the shell from the ambient cloud warms the ambient gas and facilitates the conversion of atomic O into H_2O , which then photodissociates into OH by penetrating far-ultraviolet photons. The dense gas and favorable viewing geometry brings about maser action (Elitzur and de Jong, 1980). However, the observed kinematics of the maser spots does not corroborate the shock origin of the H_2O . Subsequently, it was suggested that the OH maser actually originated in the dense and warm PDR surrounding these HII regions (Hartquist and Sternberg, 1991). Since then, observations have shown that many OH and CH_3OH masers are coincident (see Fig. 33; Menten *et al.*, 1992) and theoretical considerations indicate that methanol is not readily formed and should not have high equilibrium abundance in photodissociated gas. In a slight twist on these models, these masers are currently thought to reflect the evaporation of icy grain mantles in the photodissociation region (Hartquist *et al.*, 1995). Interstellar ices are known to contain appreciable amounts of H_2O and CH_3OH (Tielens, 1989; Tielens and Whittet, 1997). For an intense far-ultraviolet field, the penetrating photons can heat the dust to above 90 K, evaporating the ices and simultaneously dissociating the

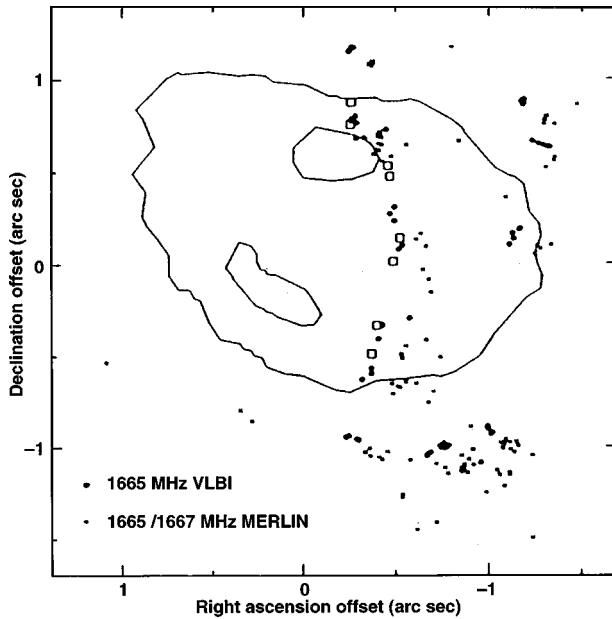


FIG. 33. Comparison of the positions of the $9_2 \rightarrow 10_1 A^+$ methanol masers (open squares) with OH masers in W3(OH). The background contours are the 10% and 70% contours of the radio continuum map of Guilloteau *et al.*, (1983), showing the extent of the HII region. The masers appear to be in a torus that wraps around the HII region, and may arise in PDRs where methanol and water ice is evaporated from grains and photodissociated to form OH. For scale $1'' \approx 0.01$ pc. From Menten *et al.* (1988).

H_2O into OH. Substantial abundances of methanol and hydroxyl can therefore coexist (Hartquist *et al.*, 1995). In this view, these maser regions are merely far-ultraviolet illuminated hot core regions.

H. The galactic center

The center of the Galaxy has been recently reviewed by Genzel, Hollenbach, and Townes (1994) and Morris and Serabyn (1996). We discuss here only some major contributions to our understanding of this region made by PDR observations and modeling. Figure 34 (Genzel *et al.*, 1994) shows a schematic diagram of the Galactic Center region, useful in visualizing the following discussion. About $10^8 M_\odot$, or 10% of the entire interstellar gas mass of the Galaxy resides in the central few hundred parsecs. Pak *et al.* (1996) observe the H_2 1–0 $S(1)$ luminosity of the central 400 pc to be about $8 \times 10^3 L_\odot$. The $v=2-1$ and $3-2$ transitions suggest the H_2 is far-ultraviolet-excited in PDRs. The ratio of 1–0 $S(1)$ luminosity to far-infrared continuum luminosity is about 10^{-5} , which is similar to the ratio in starburst and ultraluminous infrared bright galaxies. The observed strong correlation suggests a PDR origin for H_2 emission in all these sources. This conclusion seems quite reasonable, but it needs to be reconciled with the conclusion of Nakagawa *et al.* (1995) that the observed low ratio of [CII]

PHENOMENA IN THE GALACTIC CENTER

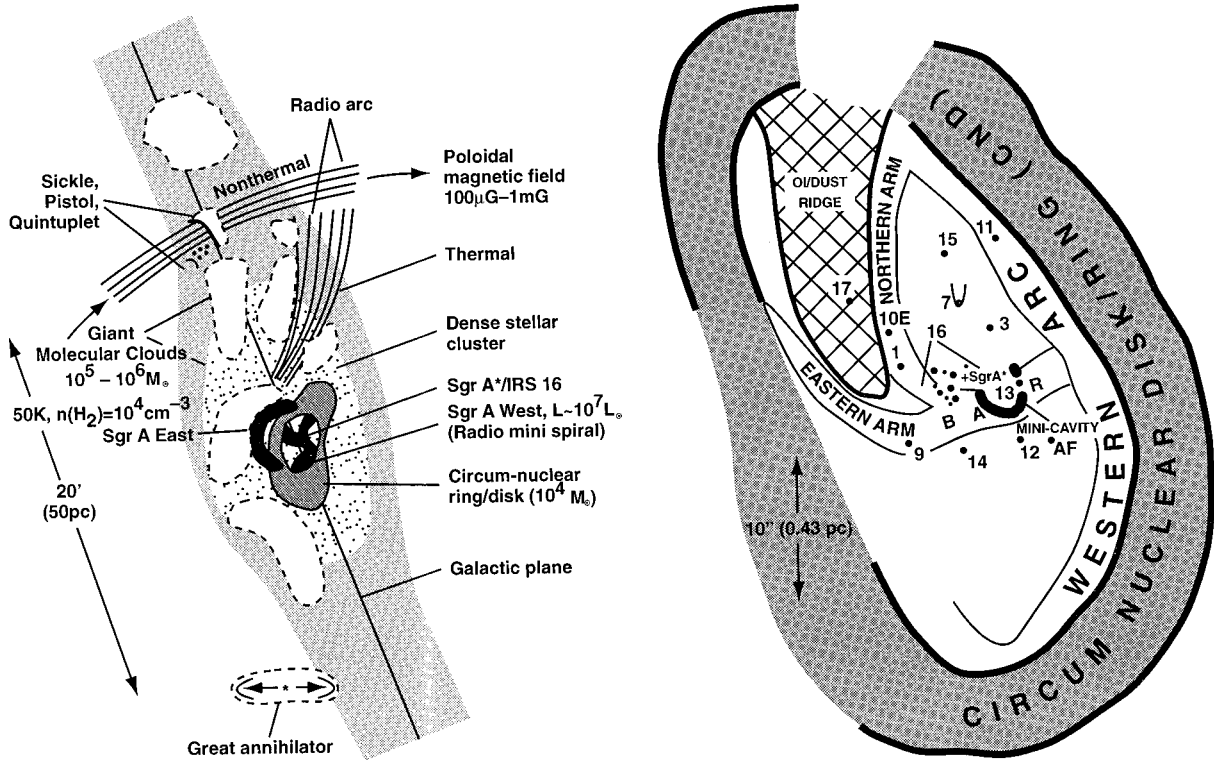


FIG. 34. A schematic of the center of our Milky Way Galaxy. A significant fraction of our knowledge of the galactic center comes from infrared and millimeter observations of the extensive PDRs irradiated by the intense far-ultraviolet fluxes of this active region. From Genzel *et al.* (1994).

158- μm luminosity to far-infrared luminosity in the central several hundred parsecs is due to considerable dust heating by photons below the threshold for carbon ionization or H_2 excitation.

PDR studies have also delineated the structure, dynamics, and excitation mechanisms in the central ~ 30 pc of the Galaxy. Lugten *et al.* (1986), Genzel *et al.* (1990), and Poglitsch *et al.* (1991) study this region primarily in [CII] 158- μm emission. They show that a large fraction of the neutral gas, up to 10%, lies in C^+ regions, which suggests that $\gtrsim 30\%$ of the neutral gas is in PDRs. The large [CII] intensities from some clouds indicate that they are relatively close (< 15 pc) to the Galactic Center, and connecting bridges suggest that the outlying clouds feed material into the center. Genzel *et al.* (1990), Erickson *et al.* (1991), and Timmermann, Genzel, *et al.* (1996) determine that the thermal radio filaments and the "Sickle" region, which lie 10–20 pc from the center, are cloud edges (HII/PDR interfaces) illuminated by as yet largely unseen hot stars.

A prominent structure in the central 10 pc is the circumnuclear disk (CND, see Fig. 34) or torus, first observed in the far-infrared continuum by Becklin *et al.* (1982). Subsequent studies¹⁶ indicate a mass of 10^4 – $10^5 M_\odot$, with an inner radius of about 1.5 pc and an outer radius $\gtrsim 8$ pc. The [CI] rotation of the circumnuclear disk suggests an isothermal stellar density distribution ($M \propto r$) with an enclosed mass of $\sim 2 \times 10^7 M_\odot$ at the periphery of the circumnuclear disk. However, the gas dynamics are consistent with a possible additional central point mass (black hole) of $\lesssim 2 \times 10^6 M_\odot$, for which there is other dynamical evidence (Genzel *et al.*, 1994; Eckart and Genzel, 1996). The atomic carbon is comparable to the CO abundance; this is ten times its value in local giant molecular clouds. The circumnuclear disk seems to consist of several streamers of material and is quite clumpy and turbulent (Jackson *et al.*, 1993). Wolfire *et al.* (1990) and Burton, Hollenbach, and Tielens (1990) compare PDR models to the observations, to derive an incident far-ultraviolet flux $G_0 \sim 10^5$ from the central cavity. This flux is incident on a clumpy structure with densities ranging from 10^5 to 10^7 cm^{-3} (Table II). The Roche critical density for tidal disruption in this region is 10^7 cm^{-3} , so the lower-density clumps are transitory phenomena. Simple PDR models do not produce enough [CI] or CO $J=7-6$; clumpy PDR models do better (Sec. IV.A; Harris *et al.*, 1985, Burton, Hollenbach, and Tielens, 1990). Overall, there is evidence for a mass infall rate into the central $r < 1.5$ pc cavity of $\sim 10^{-2} M_\odot \text{ yr}^{-1}$, which can feed a central black hole or a future starburst (Jackson *et al.*, 1993). The existence of hot massive stars in the central cavity suggests a recent episode of star formation. At least $200 M_\odot$ of neutral

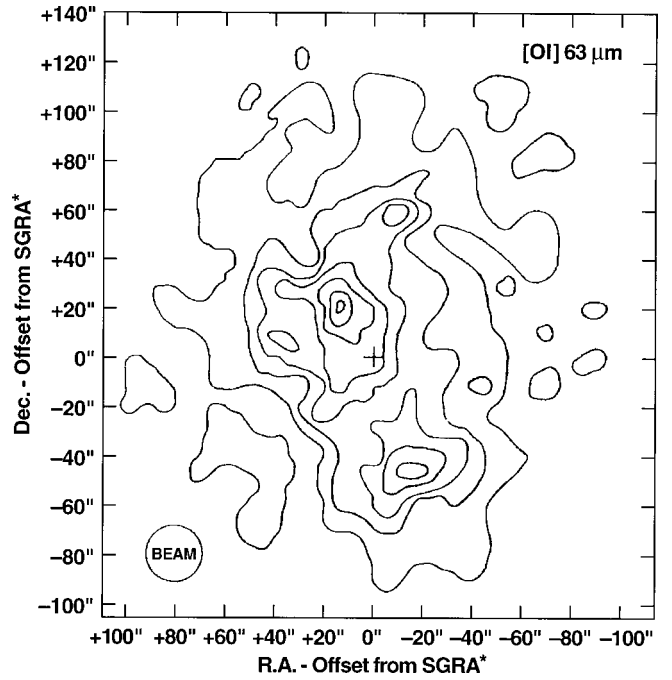


FIG. 35. The [OI] 63- μm map of the galactic center. The contour unit is $5.2 \times 10^{-3} \text{ erg s}^{-1} \text{ cm}^{-2} \text{ sr}^{-1}$. The peak is $3.8 \times 10^{-1} \text{ erg s}^{-1} \text{ cm}^{-2} \text{ sr}^{-1}$. The cross indicates the location of IRS 16*. For scale, $1' = 3$ pc. The double peaks indicate the edge-on torus of the circumnuclear disk. From Jackson *et al.* (1993).

PDR gas has been observed in [OI] in the central cavity (Jackson *et al.*, 1993); this gas provides evidence for a possible building reservoir of material available for star formation.

I. Starburst galactic nuclei

The center of the Galaxy is interesting in part because it is the closest example of a galactic nucleus and may provide clues to the interesting phenomena unique to this environment. However, one needs to keep in mind that most extragalactic PDR observations have been made of very infrared-bright galactic nuclei, which may present more extreme conditions of star-forming activity. Wolfire *et al.* (1990) show how theoretical PDR models can be compared with infrared and ^{12}CO observations to derive numerous interesting average physical parameters that describe the ISM in the central ~ 1 kpc of relatively nearby, IR-bright galaxies (see Table II). The infrared continuum spectra of these galaxies are generally attributed to emission from dust heated by OB stars formed in recent bursts of star formation (e.g., Devoreux and Young, 1990; Xu, 1990; Mouri and Taniguchi, 1992; Walterbos and Greenawalt, 1996). Carral *et al.* (1994) and Lord *et al.* (1996) present energetic and spectroscopic arguments that the [CII] and [OI] generally originate in PDRs in starburst nuclei, and not in shocks driven by stellar winds and supernovae or x rays from supernovae blast waves. Typically, the beam size for

¹⁶In [OI] these include Genzel *et al.*, 1984, 1985; Jackson *et al.*, 1993; see Fig. 35; in [CII] Genzel *et al.*, 1985; Lugten *et al.*, 1986; Poglitsch *et al.*, 1991; in [CI] Serabyn *et al.*, 1994; in [SiII] Herter *et al.*, 1986, 1989; Graf *et al.*, 1988; and in mid J CO Genzel *et al.*, 1985, and Harris *et al.*, 1985.

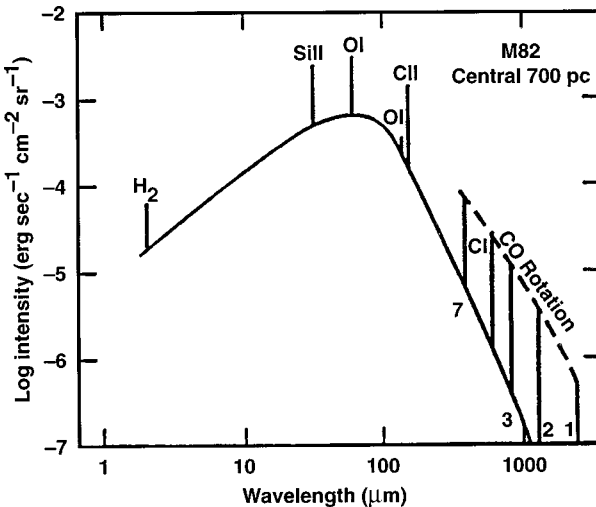


FIG. 36. The infrared spectrum from the central 700 pc of the starburst galaxy M82. The spectrum of M82 is taken from Genzel (1992) with the [CI] emission from Schilke *et al.* (1993) added. The line emission from HII regions has been excluded.

these observations is of order $1'$, which corresponds to 1.4 kpc at a distance of 5 Mpc.¹⁷

Figure 36 shows the infrared spectrum from the central 700 pc of M82, with the emission lines from HII regions removed. The derived average gas densities in the PDR clouds for these bright starburst regions (Table II for M82) are $\sim 10^4 \text{ cm}^{-3}$, and the incident far-ultraviolet flux $G_0 \sim 10^3 - 10^4$. Büttgenbach *et al.* (1992) observed [CI] 609- μm emission in IC342 and Stutzki *et al.* (1997) observed both [CI] lines in M82 and found similar cloud densities and far-ultraviolet fluxes in these starburst galaxies. The atomic (C^+) temperatures are $\sim 200 - 300 \text{ K}$, and the mass in the C^+ component is very significant, ranging from 2 to 10% of the total gas mass. The gas-phase silicon abundances are high, $x_{\text{Si}} \sim 2 \times 10^{-5}$ (~ 0.5 solar), in M82 and NGC 253. This may result from starburst activity that produces shock waves, which partially vaporize interstellar grains and raise the gas-phase abundances of refractories like silicon. A significant amount of [SiII] emission, and to a lesser extent [CII], may originate from relatively diffuse ($n_e \sim 100 \text{ cm}^{-3}$) HII regions in these nuclei (Carra *et al.*, 1994; Lord *et al.*, 1996). Figure 37 shows the relative contribution of HII regions and PDRs to the [CII] as a function of the electron density in the HII region; pressure equilibrium between the HII region and the surrounding PDR is assumed. The Wolfire *et al.* (1990) models compared to the IR observations derive a surprising number of clouds and cloud sizes; there are nu-

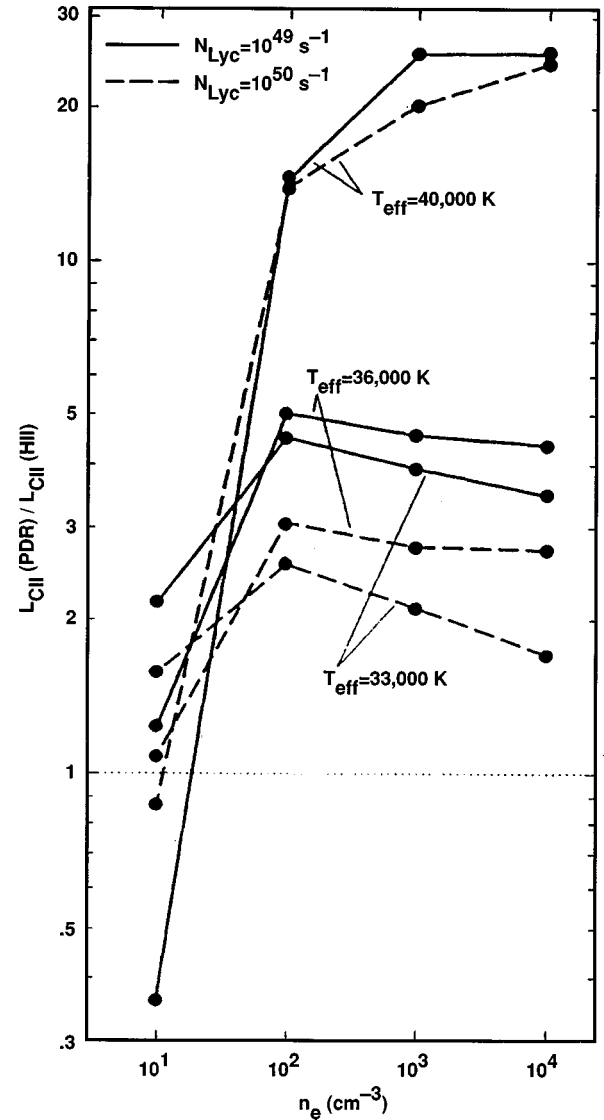


FIG. 37. Ratio of [CII] 158 μm PDR luminosity to [CII] 158 μm HII region luminosity as a function of the electron density in the HII region (Carra *et al.*, 1994). Thermal pressure equilibrium between the PDR and HII region is assumed, and the HII region is ionization bounded. The effective temperature of the central star T_{eff} and its Lyman continuum photon luminosity N_{LyC} are indicated. The values at 10 cm^{-3} are upper limits. The horizontal dotted line indicates where $L_{\text{CII}}(\text{PDR}) = L_{\text{CII}}(\text{HII})$; PDRs dominate [CII] emission except in very diffuse regions.

merous ($N \sim 10^5$) small ($R \leq 1 \text{ pc}$) clouds present. These “clouds” are individual entities in the sense that they cannot shadow each other from the far-ultraviolet flux. Nevertheless, they may be clustered together in sheets or filaments. Aalto *et al.* (1991a, 1991b, 1995, 1997) also derive small, dense, warm clouds from observations of CO isotopes and HCN in the nuclei of merging and infrared-bright galaxies. Figure 38 schematically illustrates the derived interstellar medium conditions in the central 500 pc (diameter) of the representative starburst galaxy NGC 253. The average conditions in the central regions of these starburst galaxies are far different from

¹⁷Results have been obtained for M82 by Watson *et al.* (1984), Crawford *et al.* (1985), Lugten *et al.* (1986), Wolfire *et al.* (1990), Harris *et al.* (1991), Schilke *et al.* (1993), White *et al.* (1994), Lord *et al.* (1996), and Stutzki *et al.* (1997) and for NGC 253 and NGC 3256 by Aalto *et al.* (1991a), Stacey *et al.* (1991), Carra *et al.* (1994), Harrison *et al.* (1995), and Israel *et al.* (1995).

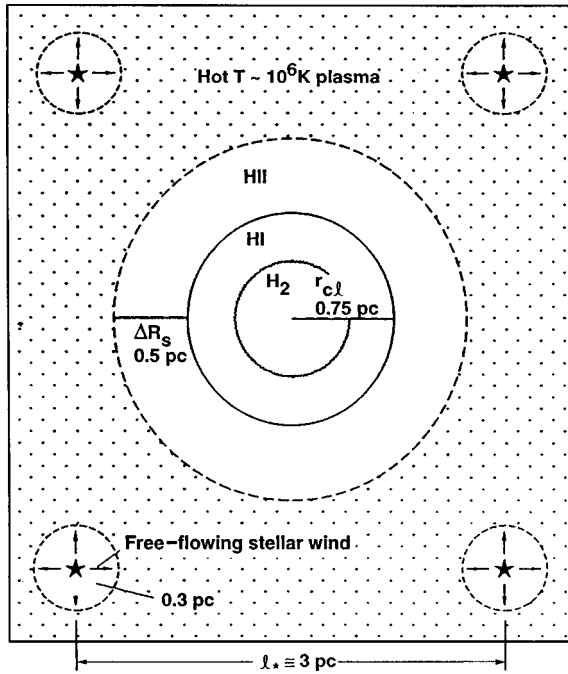


FIG. 38. A schematic of the ISM of the central 250 pc of the starburst galaxy NGC 253 (Carral *et al.*, 1994). Most of the volume is filled with $T \sim 1-3 \times 10^6$ K plasma with density $\sim 1-3 \text{ cm}^{-3}$ (dotted regions). Neutral clouds of radius $r_{cl} \sim 0.75$ pc (or sheets or filaments of thickness ~ 0.75 pc) are embedded in this gas. They have dense ($\sim 10^5 \text{ cm}^{-3}$) molecular cores labeled “H₂” and thick atomic PDR surfaces labeled “HI” with densities $\sim 10^4 \text{ cm}^{-3}$ and $T \sim 200-300$ K. The HII gas may form shells of thickness $\Delta R_s \sim 0.5$ pc around the neutral clouds. The O stars are ~ 3 pc apart, and their freeflowing winds penetrate ~ 0.3 pc into the hot plasma.

the average ISM conditions in the solar vicinity: the pressures, densities, and far-ultraviolet fields are higher by factors of order 10^3 , 10^2 , and 10^4 , respectively. They resemble the conditions found in PDRs associated with Galactic reflection nebulae such as NGC 2023.

Two problems have emerged in comparing starburst nuclei with PDR models. Recent observations of [CI] 609 μm emission from M82 (Schilke *et al.*, 1993; White *et al.*, 1994; Stutzki *et al.*, 1997) and NGC 253 (Harrison *et al.*, 1995; Israel *et al.*, 1995) indicate that the C/CO column density ratio and the [CI]/[CII] intensity ratio are higher by a factor of 2–20 than in Galactic PDRs or standard PDR models. Greatly enhanced cosmic-ray ionization rates (300 times the local value) or enhanced C/O abundance ratios have been invoked by some of these authors to explain the strong [CI]. However, Israel *et al.* (1995) invoke a simpler model of a clumpy medium to produce enhanced [CI]. In addition, Harris *et al.* (1991) have observed CO $J=6-5$ emission in NGC 253, M82, and IC342 to be stronger than standard PDR models would predict, similar to the discrepancy observed in classic Galactic PDRs like Orion (see Sec. IV.A). This may reflect an underestimate of the gas temperature in the models.

Starburst and Seyfert galactic nuclei have recently been studied with the Infrared Space Observatory

(ISO). Many of the studies focused on the ionized gas, but a number also measured pure rotational lines of H₂ from a warm, $T \sim 100-200$ K, presumably PDR component of the molecular gas (Kunze *et al.*, 1996; Rigopoulou *et al.*, 1996; Sturm *et al.*, 1996; Valentijn *et al.*, 1996). A common result was that the warm molecular component comprised a surprisingly large percentage of the total molecular mass, of order 3–10%.

Starburst and Seyfert galactic nuclei have also been studied with higher spatial resolution ($\lesssim 1''$) in the vibrational H₂ lines and in [FeII] 1.64- μm emission. The origin of these lines is still controversial for a number of sources. For the pure starburst galaxies, the [FeII] seems likely to originate from supernova shock waves with a small contribution from PDRs (Kawara *et al.*, 1988; Mouri *et al.*, 1990b, 1993; Burton, Hollenbach, and Tielens, 1990). For active-galactic-nucleus galaxies, not only may the winds and jets from the central source generate shocks, but the x rays from this source may excite the [FeII] in partially ionized clouds (Mouri *et al.*, 1990b, 1993; Blietz *et al.*, 1994; Moorwood and Oliva, 1994; Genzel *et al.*, 1995; Maloney *et al.*, 1996; Alonso-Herrero *et al.*, 1997; Greenhouse *et al.*, 1997; Veilleux *et al.*, 1997). Because starburst nuclei are violent environments with high rates of supernovae, because the observed H₂ 2–1 S(1)/1–0 S(1) ratios are often thermal, and because the H₂ seems to correlate with the [FeII], it was long assumed that the H₂ emission from galaxies was also shock dominated (see Moorwood and Oliva, 1990; Mouri *et al.*, 1990a). However, Lord *et al.* (1996) have discussed how the energetics of a stellar distribution may favor far-ultraviolet excitation. Likewise, Luhman *et al.* (1994) show that far-ultraviolet-excited H₂ dominates the global H₂ emission in Orion, even though strong shocks are present, and Luhman and Jaffe (1996) show that H₂ emission scales with other PDR tracers in several Galactic molecular clouds. Goldader *et al.* (1995) show a correlation between the H₂ luminosity and the far-infrared luminosity for ultraluminous infrared bright galaxies. Pak *et al.* (1996) show that large-scale emission from the Galactic Center, NGC 253, and M82 follows this same relation, implying that all are far-ultraviolet excited. In addition, far-ultraviolet-pumped H₂ can produce a thermal vibrational spectrum at high densities (see Sec. IV.B). Therefore there has been a recent shift towards the idea that H₂ emission in galaxies may in some cases be mostly far-ultraviolet excited (Puxley *et al.*, 1990; Israel and Koornneef, 1991; Tanaka *et al.*, 1991; Pak *et al.*, 1996). Mouri (1994) discusses spectroscopic methods of separating PDR, shock, and x-ray components of the H₂ emission. Goldader *et al.* (1997), Sugai *et al.* (1997), and Vanzi and Rieke (1997) present recent observations and discussion of the shock versus PDR origin of H₂ and [FeII] emission. One place where the H₂ emission may not arise in PDRs is within a few hundred parsecs of an active galactic nucleus, where x-ray heating may dominate (Mouri *et al.*, 1990a; Rotacuic *et al.*, 1991; Blietz *et al.*, 1994; Moorwood and Oliva, 1994; Maloney *et al.*, 1996; Maloney, 1997a, 1997b; Veilleux *et al.*, 1997; see Sec. V.B below).

V. PDRS IN DIFFERENT RADIATION FIELDS

A. Planetary nebulae

Observations of HI, Na I, [CII], [OI], H₂, CO, and other trace molecules such as OH, HCO⁺, and CO⁺ demonstrate that a significant mass of neutral PDR material, of order $1 M_{\odot}$ compared to $\sim 0.1 M_{\odot}$ of ionized gas, is associated with planetary nebulae (for references, see recent reviews by Huggins, 1992, 1993; Dinerstein, 1991, 1995; Tielens 1993a; Natta and Hollenbach, 1998). Clearly, studies of these PDRs are crucial for a proper understanding of the dynamical and morphological evolution of the ejected material.

The evolution of a planetary nebula begins with a dusty molecular wind from an asymptotic branch star ($\dot{M} \sim 10^{-6} - 10^{-4} M_{\odot} \text{ yr}^{-1}$, $v_{RG} \sim 10 \text{ km s}^{-1}$). During the protoplanetary nebula phase, the star rapidly (time scale $\leq 10^3 \text{ yr}$) evolves to the blue and creates a fast, $v \sim 1000 \text{ km s}^{-1}$, wind. The fast wind drives a shell into the slow molecular wind at a speed of $\sim 20 - 25 \text{ km s}^{-1}$ (Kwok *et al.*, 1978). The increasingly high-energy UV photons from the evolving star illuminate the circumsellar shell and carve out an ionized and atomic zone in the molecular gas (Pottasch, 1980). Spherical shells tend to completely ionize in a relatively short time, $t \leq 10^3 \text{ yr}$ (e.g., Bobrowsky and Zipoy, 1989; Tielens, 1993a; Gussie *et al.*, 1995; Natta and Hollenbach, 1998). However, observations of the ionized and neutral gas (e.g., Huggins *et al.*, 1992; Graham *et al.*, 1993; Latter *et al.*, 1995; Kastner *et al.*, 1996; Young *et al.*, 1997) clearly show that the ejecta are clumped or nonspherical (e.g., disk or toruslike). The very evolved Helix nebula shows particularly clear examples of molecular clumps surviving until late stages of the planetary nebula's evolution (Huggins *et al.*, 1992; O'Dell and Handron, 1996). Theoretical models confirm that in evolved ($t \geq 10^3 \text{ yr}$) planetary nebulae molecules will survive in dense ($n \geq 10^5 \text{ cm}^{-3}$) clumps or tori even though the far-ultraviolet fluxes are large, $G_0 \sim 10^4 - 10^6$ (Tielens, 1993a; Natta and Hollenbach, 1998).

Tielens (1993a) and Natta and Hollenbach (1998) discuss PDR modeling of planetary nebulae. Proper models require a time-dependent calculation of the partial shells or clumps, including the effects of rapid changes in the stellar effective temperature G_0 and n , as well as the advance or retreat of the ionization front with respect to the PDR gas. The H₂ emission is generally thermal emission of H₂ warmed in the PDR to $T \sim 1000 - 2000 \text{ K}$ by grain photoelectric heating, H₂ far-ultraviolet pump heating, and soft x-ray heating. Goldshmidt and Sternberg (1995) suggest that strong H₂ emission from young planetaries is produced in young, nonequilibrium PDRs, in which the H₂ has not been fully dissociated.

Shock heating, often invoked in the past, may be less important than previously believed. For protoplanetary nebulae powered by cool stars, such as GL 2688, and for very evolved, low-luminosity planetary nebulae, such as the Helix, shocks may still play a role in determining the observed spectral characteristics (Justtanont *et al.*, 1997; Cox *et al.*, 1998).

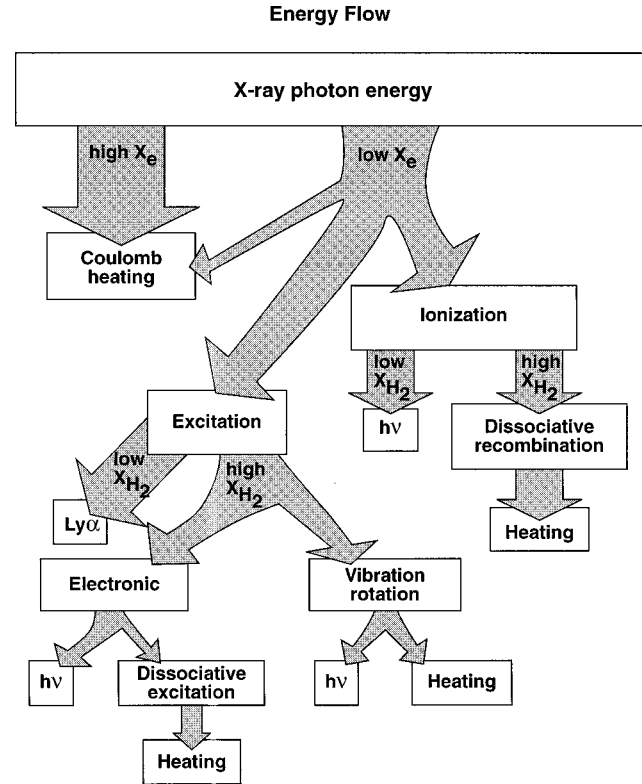


FIG. 39. Flow chart illustrating the loss routes for energetic electrons in dense atomic and molecular gas (Maloney *et al.*, 1996). The widths of the arrows indicate the approximate fractions of the primary photoelectron energy that are deposited in the indicated processes, with branching depending on the value of the electron fraction x_e and the molecular hydrogen fraction x_{H_2} . The energy that goes into exciting the vibration-rotation lines of H₂ is thermalized if the gas density is above the relevant critical densities; otherwise it emerges in emission lines.

Bachiller *et al.* (1997) recently studied a large sample of planetary nebulae in a number of molecular transitions and concluded that PDR chemistry must be invoked to explain the molecular chemistry, for example, the large enhancements of CN, HNC, and HCO⁺. Considerable work is underway to predict HI, [CII], [OI], H₂, and other molecular emission and to compare existing observations with PDR models to determine physical conditions such as the ejected mass (Natta and Hollenbach, 1998; Latter *et al.*, 1998).

B. X-ray dissociation regions

Completely analogous to photodissociation regions, x-ray dissociation regions (XDRs) can be defined as predominantly neutral gas in which x rays dominate the chemistry and/or the heating (Maloney *et al.*, 1996; Sternberg *et al.*, 1998). X rays can dominate the gas heating by photoionizing atoms and molecules and depositing a significant fraction of the primary and secondary electron energy in heat. Figure 39 shows the complicated energy flow that is initiated by the absorption of an x ray photon. X rays can also dominate much of the

chemistry through the collisional dissociation and ionization of species by secondary electrons and through photodissociation and photoionization by far-ultraviolet photons produced via excitation of H and H₂ in collisions with secondaries. Molecular gas can be exposed to x rays in a wide range of astrophysical environments: in active galactic nuclei, near supernova remnants or fast shocks, around planetary nebulae with very hot central stars, and in molecular clouds with embedded x-ray sources such as massive stars, young stellar objects with x-ray-active chromospheres, x-ray binaries, or accreting compact objects. In some cases, like the planetary nebula cases discussed in Sec. V.A, the x rays are soft ($h\nu \lesssim 1$ keV) and are absorbed in the PDR, so that the PDR and XDR coincide. However, in many cases, hard x rays penetrate to columns $N \gtrsim 10^{22}$ cm⁻² and have profound effects on the chemical and thermal structure of far-ultraviolet-opaque molecular gas.

The earliest investigations of the effects of x-ray irradiation on molecular gas were those of Langer (1978), Krolik and Kallman (1983), and Lepp and McCray (1983). Langer focused especially on x-ray-initiated sequences of reactions which could produce CH and CH⁺ in diffuse clouds. Krolik and Kallman investigated the effects of relatively weak x-ray ionization from embedded stellar sources on the chemistry and ionization balance of the Orion molecular cloud, assuming a fixed gas temperature. Lepp and McCray calculated the thermal, chemical, and ionization equilibrium of an x-ray-irradiated cloud, for the specific model of a compact source of x rays embedded in an isobaric molecular cloud. In addition, they showed that x-ray heating could be a potentially important mechanism for producing vibrationally excited H₂ emission. Krolik and Lepp (1989) examined the physical and chemical state of extremely dense molecular gas exposed to intense x-ray fluxes in the specific context of a ~1-pc molecular torus around the nucleus of a Seyfert galaxy. Draine and Woods (1990, 1991) performed time-dependent calculations of the evolution of an initially cold parcel of gas exposed to strong x-ray emission from a supernova shock. Applications were made to the very bright H₂ emission in the interacting galaxy NGC 6240. Other aspects of the chemistry, thermal balance, and H₂ excitation in XDRs have been treated by Voit (1991), Wolfire and Königl (1993), Gredel and Dalgarno (1995), Lepp and Dalgarno (1996), Tiné *et al.* (1997), and Yan and Dalgarno (1997).

Recently, Maloney *et al.* (1996) have done a comprehensive parameter study of equilibrium XDRs, studying the density range $n = 10^3 - 10^5$ cm⁻³ and x-ray ionization rates that range from cosmic-ray ionization rates to rates that nearly completely ionize the gas. The chemical abundances and temperatures in the gas primarily depend on the x-ray energy absorption rate per particle, H_x , divided by n , equivalent to an ionization parameter. For relatively high values of H_x/n , the gas is atomic, warm ($T \sim 10^4$ K), and moderately ionized (electron abundance $x_e \sim 0.01 - 0.1$). Considerable [OI] 6300 Å and [FeII] 1.26, 1.64 μm emission is produced. For somewhat lower values of H_x/n , the gas tempera-

ture drops to $T \sim 10^3$ K, the H₂ abundance rises to $10^{-3} - 10^{-2}$, and considerable H₂ 2 μm emission is generated. At lower values of H_x/n , the emission is dominated by the pure rotational transitions of abundant molecules like CO and by a number of atomic fine-structure lines like [OI] 63 μm, [SiII] 35 μm, and [CII] 158 μm, which are very bright over a major fraction of the parameter space. Maloney *et al.* discuss the spectroscopic differences between XDRs and PDRs, in particular, the large line-to-continuum ratios for bright lines in XDRs, and show that [FeII] and H₂ emission observed in Seyfert nuclei may often originate in XDRs, and not in shocks as had been previously speculated (see Sec. IV.I, above).

Figure 40 presents images of H₂ 1–0 S(1), CO $J = 2-1$, and optical [OIII] emission in the central 300 pc of the Seyfert galaxy NGC 1068. The [OIII] marks the narrow-line region associated with this active galactic nucleus. The ionized narrow-line region has only a few percent of the mass contained in the large torus seen in CO and appears to emerge from the poles of the torus. The H₂ emission is coincident with the molecular torus seen in CO and is likely excited by the x rays from the central active galactic nucleus, some ~100 pc away (Moorwood and Oliva, 1988; Kawara *et al.*, 1990; Rotaciuc *et al.*, 1991; Maloney, 1997a). The [FeII] emission (not shown in the figure) has also been attributed to XDR sources by Mouri *et al.* (1990a, 1990b, 1993), Blietz *et al.* (1994), Greenhouse *et al.* (1997), and Maloney (1997a).

Models of x-ray dissociation regions have been used to interpret and predict the spectrum from the molecular cloud which may surround the x-ray source 1E1740.7-2942, a positron annihilation source (sometimes called the “Great Annihilator”) near the Galactic Center. It has been suggested that this source is powered by Bondi-Hoyle accretion from the cloud onto a compact object, such as a stellar mass black hole (Bally and Leventhal, 1991; Sunyaev *et al.*, 1991). Phillips, Lazio, and Joseph (1995) found a 15'' offset between HCO⁺ emission and the radio continuum hotspots which are used to locate the compact object (Rodriguez *et al.*, 1992; Mirabel *et al.*, 1992). They suggested that the offset occurs because of enhanced destruction or reduced formation of HCO⁺ in the x-ray field near the compact object, a suggestion confirmed by XDR models (Lepp and Dalgarno, 1996; Yan and Dalgarno, 1997). Maloney *et al.* (1997a, 1997b) use XDR models to predict ISO-observable line fluxes in, for example, [OI] 63 μm, [CII] 158 μm, and [SiII] 35 μm emission produced if the compact objects does indeed reside inside a high-column-density molecular cloud. If ISO observes these lines, comparisons with the models will provide estimates of the gas density, column density, volume filling factor in the vicinity of the x-ray source, and x-ray luminosity of the source averaged over the last ~100 years, and these comparisons will constrain models for accretion from the interstellar medium.

Neufeld *et al.* (1994) and Neufeld and Maloney (1995) applied XDR models to the higher densities, n

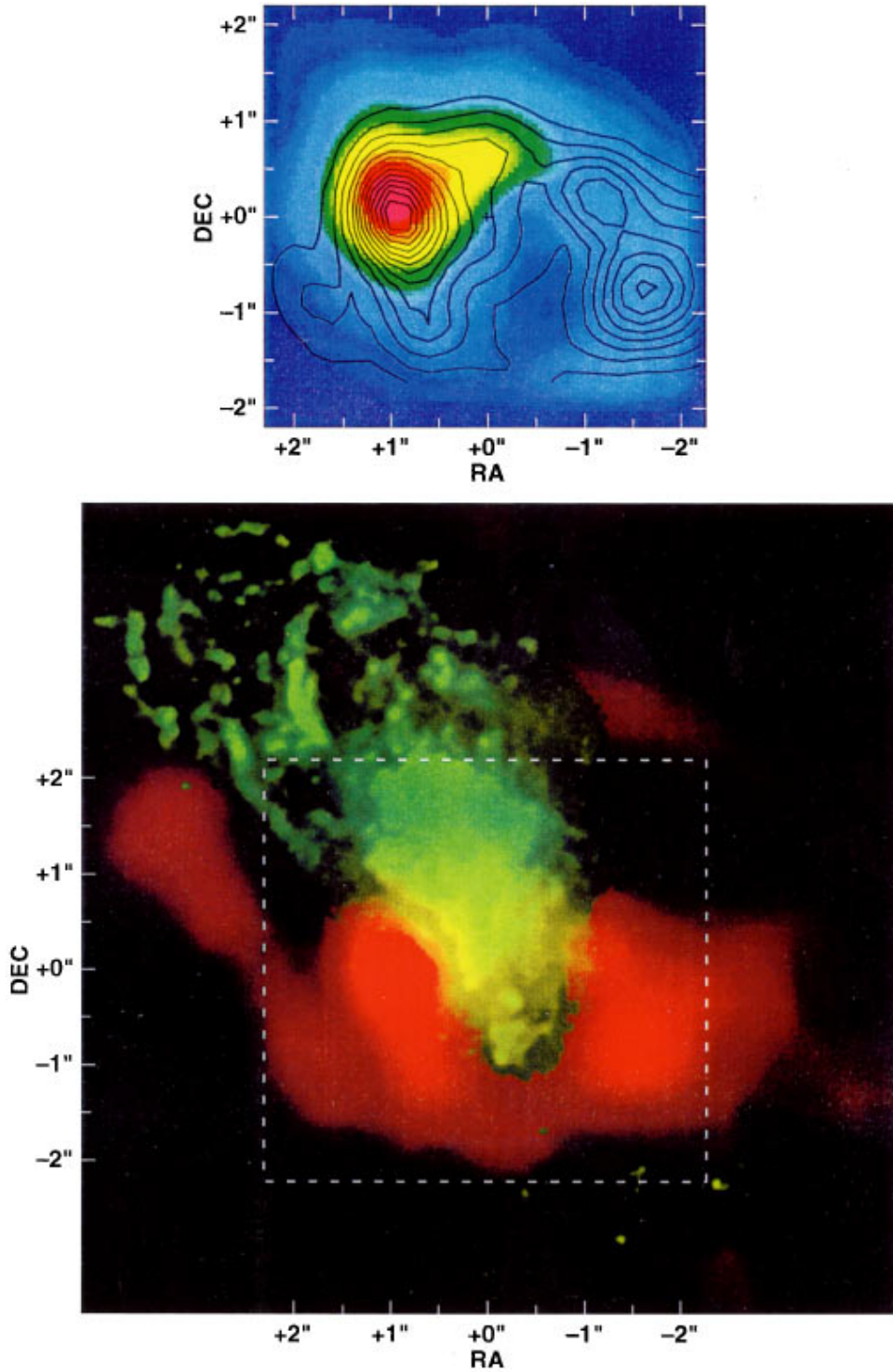


FIG. 40. (Color) Images of the central 300 pc ($1'' \sim 70$ pc) of the Seyfert galaxy NGC 1068. The lower panel shows a $0.7''$ resolution IRAM (Institut de Radio Astronomie Millimetrique) interferometric image of CO $J=2-1$ emission (in red, courtesy of L. Tacconi) superimposed on an HST optical [OIII] emission (green, from Evans *et al.*, 1991) from the narrow-line region (NLR). The upper panel shows the same CO emission (contours) superimposed on an image of the H₂ 1-0S(1) emission (colors, courtesy of N. Thatte). The H₂ is likely excited by x rays from the active galactic nucleus at the center (see text).

$\sim 10^9$ cm $^{-3}$, and x-ray fluxes incident upon the much smaller $\sim 0.1-1$ pc disks or tori which orbit the central engines of active galactic nuclei. They showed that luminous water maser emission is characteristically produced under these conditions (see also Wallin and Watson,

1997). The maser emission will be beamed in the plane of the orbiting disks or tori, explaining the origin of the observed extragalactic H₂O “megamaser” sources. Sixteen megamasers are now known, all associated with active galactic nuclei (see Maloney, 1997b, and references

therein). Because the megamasers are so powerful, they can be observed with extremely high precision, and their dynamical (Keplerian) motions can be mapped very accurately. In the megamaser nucleus of the spiral galaxy NGC4258, such measurements provide some of the best evidence for the existence of a massive black hole ($2 \times 10^7 M_\odot$ in NGC4258) in the center of a galaxy (Greenhill *et al.*, 1995; Maoz, 1998).

VI. DIFFUSE, TRANSLUCENT, AND MOLECULAR CLOUDS IN THE INTERSTELLAR RADIATION FIELD

A. Diffuse and translucent clouds

Because diffuse and translucent clouds are relatively simple, they are considered prime “laboratories” for interstellar chemistry and they have been modeled for decades. A number of detailed models for diffuse and translucent clouds have appeared in the literature, often focusing on H₂ excitation and the abundances of trace molecules (Glassgold and Langer 1974, 1976; Black and Dalgarno, 1976; van Dishoeck and Black, 1986, 1989; Viala, 1986; Viala *et al.*, 1988; Federman and Huntress, 1989). These models have been reviewed by van Dishoeck and Black (1988) and van Dishoeck (1991, 1998). Observations of other simple molecules such as CH, CH⁺, C₂, CO, CN, and OH similarly provide constraints on the chemical models (van Dishoeck and Black, 1988, 1989; Federman *et al.*, 1980, 1984, 1994; Danks *et al.*, 1984). Likewise, Turner (see Turner, 1996, and references therein) has developed translucent cloud models in order to understand the basic ion-molecule chemistry of a number of observed molecular species including HCO⁺, H₂CO, NH₃, N₂H⁺, SO, SO₂, CS, H₂S, SO⁺, and HCS⁺.

Some of the premier outstanding problems in the study of diffuse PDR clouds are therefore also of interest for studies of dense PDRs. The formation of CH⁺ is a prime example; its high abundance has been a mystery for many decades. The “natural” way to CH⁺ through the reaction of C⁺ with H₂ is endothermic by 0.4 eV. It is now generally thought that shocks, which at one point looked so promising (Elitzur and Watson, 1978), cannot be responsible for interstellar CH⁺ because the expected velocity shifts are not observed (Lambert *et al.*, 1990; Gredel *et al.*, 1993). Moreover, the observed absence of other molecules (e.g., OH) that are easily formed in the warm post-shock gas leads to contradictions with the models. A variety of other processes have been proposed that might conceivably lead to high CH⁺ column densities but most cannot explain simultaneously all of the observations, perhaps because more than one process is operative (Duley *et al.*, 1992). For example, reactions with far-ultraviolet pumped vibrationally excited H₂ could in some sources be important (Snow, 1993), but are unlikely to explain the more general CH⁺ problem. Currently, the most promising solution is chemistry driven by turbulence (see Sec. II.B.2; Falgarone *et al.*, 1995; Spaans, 1995). Turbulent chemistry may also be of importance in dense PDRs.

Another problem is the role of grain surface chemistry in the composition of diffuse clouds. While grain surface chemistry is generally accepted for H₂ formation, it is otherwise ignored in studies of diffuse clouds or PDRs. Observations of NH in diffuse clouds, in combination with CH and OH observations, may be an important probe of the role of grain surface chemistry (Wagenblast *et al.*, 1993). NH has now been observed towards ζ Oph, ζ Per, and HD 27778 with a column density of $\approx 10^{12} \text{ cm}^{-2}$ or about 10^{-4} of the gas-phase atomic N column density (Meyer and Roth, 1991; Crawford and Williams, 1997). NH is notoriously difficult to form through gas-phase routes because the initiating reaction of N with H₂ is highly endothermic (see Sec. II.B.3.b). Gas phase models for diffuse clouds based upon this reaction fail to reproduce the observed column density by a factor of 30 because of the low gas temperatures. In contrast, models that include formation of NH on grain surfaces readily reproduce the observations for typical conversion factors of 0.3 of the accreted N (Wagenblast *et al.*, 1993). Possibly, vibrationally excited H₂^{*} plays a role in initiating nitrogen chemistry in diffuse clouds as well (Sec. II.B.3.b). This reaction produces a fraction f_{NH} of the gas-phase N in the form of NH given by $f_{\text{NH}} \approx n(\text{H}_2^*)/1 \text{ cm}^{-3}$, which is $\approx 10^{-9}n^2$ (n in cm^{-3}) in the regime where a considerable fraction of the hydrogen is atomic. Clearly, this fraction is very density sensitive and in the moderately dense diffuse clouds towards ζ Oph and ζ Per this reaction may be of importance, albeit, perhaps, not as important as in dense PDRs. In any case, the low NH/CH and NH/OH argue against an important contribution of grains to the chemistry of OH and CH. Wagenblast *et al.* (1993) calculate modest ($\approx 10\%$) enhancements to the OH column density and none to CH from grain surface reactions. Grain chemistry in dense PDRs, such as the formation and release of methanol to create methanol and OH masers (Sec. IV.G), warrants serious consideration (Hartquist *et al.*, 1995).

It is now becoming increasingly clear that diffuse clouds are highly inhomogeneous at the smallest scales. First, VLBI studies of galactic HI absorption towards extragalactic background sources shows structure at the 100-AU scale (Dieter *et al.*, 1976; Diamond *et al.*, 1989; Davis *et al.*, 1996). Second, time variability in the 21-cm absorption towards high-velocity pulsars give similar results (Frail *et al.*, 1994). Third, variations in the strength of the optical absorption lines of NaI and CaII between binary stars show variations on 1000's of AU scale (Meyer and Blades, 1996; Watson and Meyer, 1996; Blades *et al.*, 1997; see Fig. 41). As summarized by Heiles (1997), dense, tiny-scale structures are ubiquitous in diffuse clouds. Likely these reflect the presence of draped sheets and filaments with thicknesses of ≈ 30 AU and radii of curvature of hundreds of AU in diffuse clouds (Heiles, 1997). These sheets and/or filaments, with densities $\sim 1000 \text{ cm}^{-3}$, may contribute $\approx 20\%$ of the cloud column density, yet occupy only a few percent of the volume. The remainder is filled with lower-density ($\sim 100 \text{ cm}^{-3}$), but still cold, neutral gas. Clearly, such an

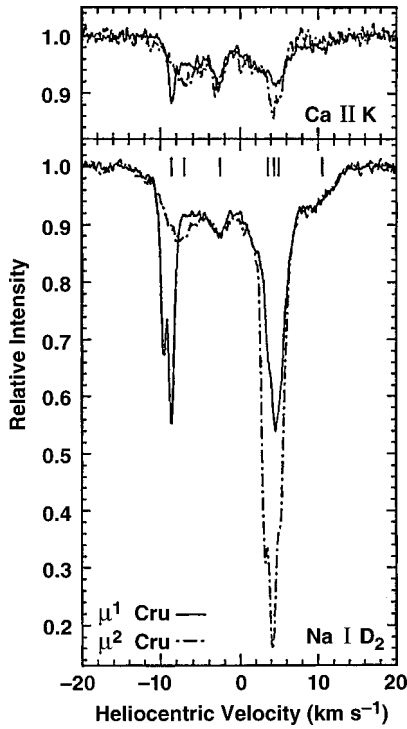


FIG. 41. The interstellar CaII and NaI absorption lines towards both members of the double star μ Cru. These show line-strength variations that are indicative of the presence of structure in the ISM on scales smaller than the double star separation (≈ 7000 AU; Meyer and Blades, 1996).

open structure will have a profound influence on the penetration of the far-ultraviolet radiation (see Sec. II.A) and hence on the ionic and molecular abundances; the NaI to CaII variations seem to imply as much (Meyer and Blades, 1996; Blades *et al.* 1997). The implications of this tiny-scale structure for our understanding of interstellar chemistry and the structure of the interstellar medium in general have not yet been fully grasped.

B. Molecular clouds

Models of molecular clouds in the interstellar radiation field follow the attenuation of the far ultraviolet into the opaque regions where carbon is mostly incorporated into CO (Glassgold and Langer, 1975; Langer, 1976; Clavel *et al.*, 1978; de Jong *et al.*, 1980; Viala, 1986; Andersson and Wannier, 1993). The photodissociation of CO and its self-shielding received detailed treatment by Glassgold *et al.* (1985), van Dishoeck and Black (1988), and Viala *et al.* (1988). We shall discuss in Sec. VII more global aspects of the effect of the interstellar radiation field on molecular clouds, such as the formation and destruction of molecular clouds and the regulation of star formation in galaxies. We discuss here three applications of the effect of the interstellar radiation field and higher far-ultraviolet fluxes on individual molecular clouds.

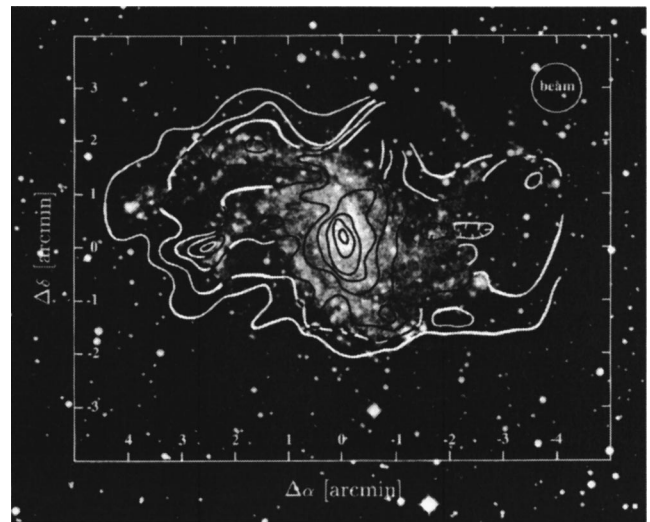


FIG. 42. Integrated [CII] line intensity contours with contour interval of 1×10^{-5} erg s $^{-1}$ cm $^{-2}$ sr $^{-1}$ and a peak value of 7×10^{-5} erg s $^{-1}$ cm $^{-2}$ sr $^{-1}$ superimposed on an optical image of NGC 6946 (Madden *et al.*, 1993). For scale, $1' \approx 2.9$ kpc.

1. HI halos of molecular clouds

Stacey *et al.* (1991) observed [CII] 158 μ m emission and found that a considerable fraction of the interstellar material in the central regions of spiral galaxies lies in dense C $^+$ zones presumably on the surfaces of molecular clouds. Much of the HI 21 cm emission from the inner disks of galaxies may therefore be the result of the photodissociation of molecular clouds by the UV starlight of nearby O and B stars, a conclusion in accord with those of Allen *et al.* (1986, 1997) and Tilanus and Allen (1989) based on high-spatial-resolution maps of HI in M83, M81, and M51. Madden *et al.* (1993) have mapped NGC 6946 in [CII] 158 μ m (Fig. 42) and concluded that as much as 70–80 % of the observed HI, especially in the inner regions, may be photodissociated H $_2$. Allen (1996) reviews this point of view. In a similar vein, Shaya and Federman (1986) proposed a galactic model in which the HI originates on the surfaces of molecular clouds to explain the radial distribution of HI and the correlation of HI surface density with morphological class.

These extragalactic observations are related to the observations of HI halos around molecular clouds in the galaxy (see Wannier *et al.*, 1983, for an early discussion). Elmegreen and Elmegreen (1987) found huge HI “superclouds” associated with molecular cloud complexes in the first Galactic quadrant, with masses $\sim 10^6$ – $4 \times 10^7 M_\odot$ and average densities $n \sim 9$ cm $^{-3}$. Chromey *et al.* (1989) and Green and Padman (1993) studied a $\sim 2 \times 10^5 M_\odot$ halo of low-density (2–30 cm $^{-3}$) HI surrounding the Orion molecular clouds, sufficient to shield the molecular material from photodissociative radiation and provide a pressure link to the low-density intercloud medium. Figure 43 shows the HI cloud surrounding the B3-B4-B5 molecular cloud complex. On a smaller scale, Spaans and Neufeld (1997) model the relative amounts of HI and H $_2$ in the diffuse cloud G236+39 and show how the 3D geometry of the cloud affects the relative

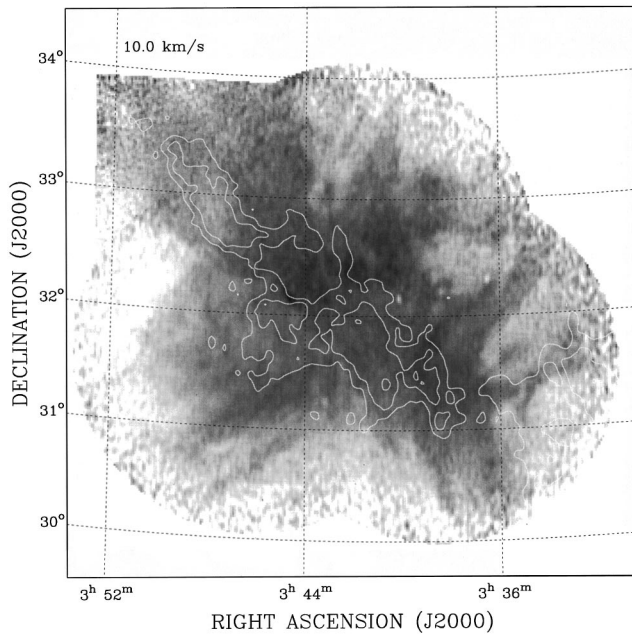


FIG. 43. The HI cloud (gray scale) surrounding the molecular cloud complex B3-B4-B5. White contours, CO $J=1-0$. Both maps at 10 km s^{-1} . For scale, $1^\circ \approx 2.3 \text{ pc}$. Figure courtesy of G. Moriarty-Schieven.

columns of the two species. Andersson *et al.* (1991, 1992), Wannier *et al.* (1991, 1993), Andersson and Wannier (1993), and Moriarty-Schieven *et al.* (1997) made extensive studies of these halos and found them to be warm, extended, and probably expanding into the diffuse medium. These halos may therefore be the observational signature of the far-ultraviolet photoevaporation of molecular clouds. In stronger far-ultraviolet fields associated with HII regions, the photodissociation of H₂ and the photoevaporation process is observed even more readily in HI 21-cm emission (Roger and Pedlar, 1981; Roger, 1982; Roger and Irwin, 1982; Joncas *et al.*, 1992; Roger and Leahy, 1993; Heyer *et al.*, 1996; Moriarty-Schieven *et al.*, 1996).

2. C⁺ halos around molecular cores in the Magellanic Clouds and irregulars

A number of observations have been made of the Magellanic Clouds in CO, [CII] 158 μm , and other PDR lines (e.g., Boreiko and Betz, 1991; Rubio *et al.*, 1993a, 1993b; Mochizuki *et al.*, 1994; Poglitsch *et al.*, 1995; Israel *et al.*, 1996; Stark *et al.*, 1997). One of the major conclusions of this work is that the low metallicity in the Magellanic Clouds leads to a greater penetration of the far ultraviolet and a greater CO dissociation in molecular clumps. The result is that the ratio of [CII]/CO is on average 20 times the typical value in the Galactic plane (Mochizuki *et al.* 1994), although there is considerable variation from point to point (Israel *et al.*, 1996). Pak *et al.* (1998) present [CII], H₂, and CO observations of the Magellanic Clouds and model the giant molecular clouds in these galaxies as having larger column densities than Milky Way giant molecular clouds, with rela-

tively small CO cores and extended [CII] halos. Similarly, the CI/CO ratio is also (modestly) enhanced (by a factor of 2) compared to the galactic value (Stark *et al.*, 1997). Since H₂ may exist in the C⁺ zones because of self-shielding, the ratio X of H₂ mass to CO $J=1-0$ luminosity may be significantly higher in the Magellanic Clouds than in the Galaxy (Israel, 1997). Madden *et al.* (1997) arrive at a similar conclusion from [CII] observations of IC10, an irregular galaxy with low metallicity.

3. CO line profiles and the H₂ mass to CO $J=1-0$ luminosity ratio

Because the optically thick ^{12}CO $J=1-0$ emission originates largely from the far-ultraviolet-heated PDRs on the “surfaces” of opaque molecular clouds, PDR modeling should be able to reproduce the line intensities and profiles. Tauber and Goldsmith (1990) and Wolfire *et al.* (1993) construct models that self-consistently calculate the chemistry, thermal balance, and radiative transfer appropriate for a PDR model. They conclude that clumpy models can reproduce the observed centrally peaked profiles; Falgarone *et al.* (1994) point out that turbulent velocity fields with some coherence reproduce the observed smoothness of the profiles better than randomly moving clumps.

There has been considerable discussion over the last decade concerning the correlation of the luminosity of ^{12}CO $J=1-0$ with the molecular mass of a cloud (e.g., Solomon *et al.*, 1987). Wolfire *et al.* (1993) applied PDR models to study this correlation. The observations indicate that there is roughly a constant column density, or A_V , through molecular clouds ($A_V \sim 7.5$; see Solomon *et al.*, 1987; McKee, 1989; Sec. VII.E). In this case, the cloud's mass is proportional to its area and, if the CO line integrated intensity is relatively constant from cloud to cloud, the CO luminosity will trace area and therefore mass. (For a dissenting view, that cloud densities are constant and that the mass is proportional to their volume, see Leisawitz, 1990). Wolfire *et al.* (1993) have subjected model molecular clouds to an external far-ultraviolet flux G_0 and have self-consistently calculated the temperature and CO abundance as a function of position in clouds of various mass in order to predict the ^{12}CO $J=1-0$ luminosity. The PDR models match the observed correlation well, largely independent of G_0 in the range $0.1 \leq G_0 \leq 10^3$. Sodroski *et al.* (1995) present empirical evidence that the correlation factor changes by a factor of 20 when one compares the Galactic center with Galactic molecular clouds at 13 kpc. This change is hard to reconcile with the model of Wolfire *et al.*, although the metallicity gradient may enhance the factor gradient in this case.

VII. THE GLOBAL INTERSTELLAR MEDIUM OF GALAXIES

A. The neutral phases of the interstellar medium

As discussed in the Introduction, diffuse gas in the ISM is known to exist in three dominant phases: (i) cold,

diffuse neutral atomic clouds ($T \approx 100$ K; $n \approx 30 \text{ cm}^{-3}$), (ii) warm neutral and ionized intercloud gas ($T \approx 8000$ K; $n \approx 0.3 \text{ cm}^{-3}$), and (iii) a hot ionized medium ($T \approx 10^6$ K; $n \approx 3 \times 10^{-3} \text{ cm}^{-3}$; McKee and Ostriker, 1977; Kulkarni and Heiles, 1987). Much of the mass is in the cloud phase, but the volume is largely filled by the low-density phases. The origin and interrelationship of these phases and their heating and ionization sources are amongst the most fundamental questions in this field.

While the diffuse cold and warm neutral regions are not traditionally thought of as PDRs, there is no reason not to identify them as PDRs since many of the physical and chemical processes that regulate them are identical to those in dense PDRs. (As a corollary, we point out that, because of their high surface brightness and compactness, dense PDRs are more amenable to observations and can therefore shed considerable light on the structure and evolution of the general diffuse ISM.) The earliest models for the phases of the diffuse ISM identified cosmic rays as the dominant energy and ionization source (Field *et al.*, 1969). After it was shown that the cosmic-ray flux was much less than was required to explain observations of the ISM (Spitzer and Jenkins, 1975; Barsuhn and Walmsley, 1977; van Dishoeck and Black, 1986), far-ultraviolet photons took over the heating role. In particular, the heating of the interstellar gas was attributed to the far-ultraviolet photoelectric ejections of energetic electrons from small ($\approx 100 \text{ \AA}$) dust grains (de Jong, 1977, 1980; Draine, 1978). However, our incomplete understanding of the interstellar photoelectric effect precluded firm identification of this process as the dominant heating source of the cloud and of warm intercloud media, and various other mechanisms were explored (e.g., hydrodynamic wave dissipation; Ferrière *et al.*, 1988).

The studies of dense PDRs can clarify these issues. The high surface brightness of PDRs and the good correlation of the cooling line and dust continuum luminosity unambiguously identify the far-ultraviolet flux as the heating source. Observational studies of PDRs therefore provide strong constraints on the photoelectric heating of interstellar gas. Moreover, studies of the “dust” near-IR emission from PDRs highlight the importance of PAH molecules in the overall radiative balance. This has led to an overall improved understanding of the photoelectric process in the interstellar medium. Current models for the photoelectric effect working on PAHs and small dust grains are in good agreement with the observed cooling rate of the interstellar diffuse clouds (Verstraete *et al.*, 1990; Bakes and Tielens, 1994). Wolfire *et al.* (1995) have used these new photoelectric heating rates to calculate the thermal balance and stability of interstellar gas. These models also include a detailed treatment of the ionization and heating rate due to soft x rays and cosmic rays. The results show that a stable two-phase medium (cold or warm neutral medium) can exist with pressures in the range $P_{\min}/k \approx 10^3 \text{ cm}^{-3} \text{ K} < P/k < P_{\max}/k \approx 10^4 \text{ cm}^{-3} \text{ K}$ (see also Verstraete *et al.*, 1990). Below P_{\min} , only the warm neutral

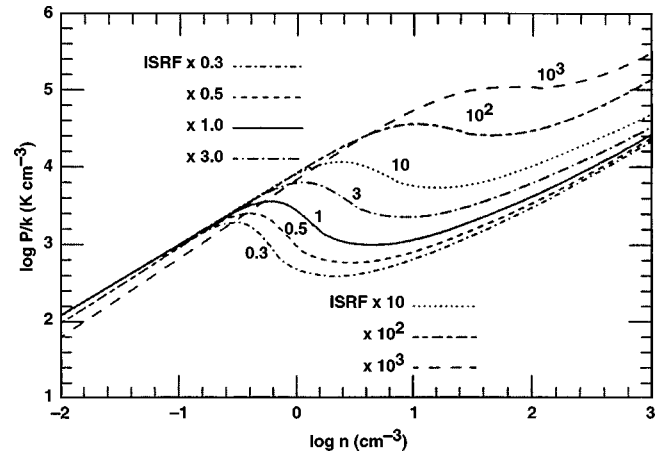


FIG. 44. A phase diagram for the warm-neutral-medium and cold-neutral-medium phases of the ISM (Wolfire *et al.*, 1995). The lines plotted denote thermal balance, where the heating is mainly by grain photoelectric heating and the cooling mainly by [CII] for $n \geq 1 \text{ cm}^{-3}$ (the cold neutral medium) and by [CII], [OI], Ly α , and recombination cooling for lower density (the warm neutral medium). For a given pressure, an equilibrium solution exists on the line if the slope is positive. The plot shows the effect of a varying interstellar radiation field (ISRF) where the standard local ISRF is taken from Draine (1978).

medium can exist; above P_{\max} , only the cold neutral medium can exist. The cloud and intercloud media are both heated primarily by grain photoelectric heating. The intercloud phase is mainly cooled by Lyman α , [CII], and [OI] fine-structure lines and electron recombination onto charged grains. The cloud phase is mainly cooled by the [CII] $158 \mu\text{m}$ line (Wolfire *et al.*, 1995). Figure 44 shows a phase diagram from Wolfire *et al.* of the ISM, demonstrating that two phases are possible over a wide range of far-ultraviolet radiation field, with higher pressures required for two phases when the radiation field increases. For the local interstellar radiation field, a thermal pressure of $P/k \sim 1-3 \times 10^3$ (consistent with that observed) is needed for a two-phase medium.

Norman and Spaans (1997), Spaans and Carollo (1997), and Spaans and Norman (1997) have constructed global, multiphase models of the ISM of protogalaxies partly in order to understand the origin and evolution of primordial starbursts and their dependence on the age, mass, and shape of the protogalaxy. They find that the starbursts occur at the onset of a multiphase ISM, with the presence of a cold neutral medium and dust which leads to opaque, star-forming clouds. There is a threshold metallicity of about $0.01 Z_{\odot}$ above which a multiphase ISM forms, cold neutral medium clouds are born, and star formation dramatically increases. More massive and/or spherical protogalaxies reach this threshold sooner (redshifts $z \geq 2$) than flattened and/or less massive protogalaxies (redshifts $z \sim 1.5$), and Spaans and Norman explain the early evolution of dwarf galaxies in this context. Stark (1997) points out that starbursts associated with protogalaxies at $z \sim 2-6$ will be extremely luminous in [CII] $158 \mu\text{m}$ and the fluxes may be detectable by ground-based (Antarctica) submillimeter telescopes.

B. The HI/H₂ transition in galaxies and the formation of molecular clouds

Elmegreen (1991, 1993) has constructed simple analytic models of the self-shielding of H₂ in order to study the galactic conditions necessary to produce molecular clouds in the presence of an external far-ultraviolet flux. He distinguishes between diffuse clouds (non-self-gravitating) and self-gravitating clouds and shows that diffuse clouds can be molecular, whereas self-gravitating clouds can be atomic, depending on the external pressure P_e on the cloud, the far-ultraviolet flux G_0 , the metallicity Z , and the cloud mass M . A shielding function $S \propto P_e^{13/12} M^{-1/2} Z G_0^{-1}$ determines whether a given cloud is molecular or atomic: large S implies a shielded molecular cloud. The functional form of the shielding function shows why the most massive clouds in a galaxy might be atomic, why outer galaxy clouds with low P_e might be atomic, why large regions of galaxies can spontaneously convert to molecular form following either an interaction that triggers mass accretion or the passage of a spiral density wave (both increase P_e), and why the H₂ can convert back to H once O or B stars form and G_0 rises. Elmegreen and Parravano (1994) show that the pressure may drop below P_{\min} (see Sec. VII.A) in the outer part of a galaxy, leading to the conversion of all cold atomic clouds to a warm phase and to a much lower star formation rate per unit mass, consistent with observations (Walterbos and Braun, 1996). Honma *et al.* (1995) apply the Elmegreen model to explain the observed rapid transition from H₂ to HI as a function of galactocentric radius in some face-on galaxies. They find that a gradient in metallicity is crucial for the development of a sharp transition, because both the H₂ shielding by dust and H₂ formation on dust depend on Z .

C. The destruction of molecular clouds

Once O and early B-type stars are formed in molecular clouds, extreme-ultraviolet-induced photoevaporation begins to ionize and evaporate the clouds, limiting the lifetimes of giant molecular clouds ($M \gtrsim 10^5 M_\odot$) to ~ 30 –40 Myr (Williams and McKee, 1997). However, far-ultraviolet photons also destroy the molecular clouds by dissociating the molecules and heating the atomic gas. We have already discussed (Sec. VI.B.1) the observations of spiral arms in galaxies, where HI often appears downstream of the molecular gas, indicating that the more massive stars formed in the arms have photodissociated the clouds. Without considering the dynamics of the photoevaporating gas, Diaz-Miller *et al.* (1998) treat the photodissociation of clouds of different density and mass by a distribution of newly formed stars. They find that lower-mass stars, which do not produce substantial HII regions, may nevertheless photodissociate a considerable fraction of the cloud and may even limit the formation of higher-mass stars in relatively low-mass clouds. Arthur and Lizano (1997) treat the relative importance of photoevaporation and hydrodynamic effects in the ablation of self-gravitating globules in compact

HII regions. Further study of the photodissociation and photoevaporation of molecular clouds is warranted, coupling a realistic clump distribution of a molecular cloud with a dynamical model of the photoionization, photodissociation, and photoevaporation produced by both the extreme-ultraviolet and far-ultraviolet fluxes from the young stars born in the cloud.

D. The [CII] emission from the galaxy

The FIRAS instrument on COBE has surveyed the galaxy in the far-infrared dust continuum and various interesting lines, including the [CII] 158 μm and [NII] 205 μm lines (Wright *et al.* 1991; Bennett *et al.*, 1994; see Fig. 4). Figure 45 shows the [CII] 158 μm map of the Milky Way (Bennett *et al.*, 1994). The large beam ($\approx 7^\circ$) makes COBE sensitive to extended low-surface-brightness emission associated with interstellar dust and gas. Still, some structure is apparent, including the Orion molecular cloud and the molecular ring. The [CII] line is the dominant cooling line of the interstellar gas, with an observed luminosity of $5 \times 10^7 L_\odot$ or $L(\text{CII})/L(\text{far-infrared}) \approx 3 \times 10^{-3}$ averaged over the galaxy. Figure 45 also presents the BICE observation with a 15' beam of the galactic plane in the direction toward the galactic center (Nakagawa *et al.*, 1998). On this scale, as well, there is a good correlation between the [CII] and the far-infrared dust continuum emission, but the diffuse components are more pronounced in the [CII] line: For the diffuse components, [CII]/far infrared $\approx 0.6\%$, while active star-forming regions have [CII]/far infrared $\approx 0.2\%$. In the galactic center, on the other hand, the [CII]/far-infrared ratio is considerably lower, perhaps due to a cooler illuminating radiation field (compare Sec. III.D) dominated by bulge stars (Nakagawa *et al.*, 1995).

The origin of this galactic [CII] emission has recently been reviewed by Tielens (1994, 1997). Three interstellar components have been proposed as possible “carriers”: the diffuse galactic HI clouds, PDRs on molecular cloud surfaces, and the diffuse HII plasma. This plasma may be extended low-density HII regions or the lower-pressure and larger-scale warm ionized medium. We shall discuss each of these in turn; their estimated contributions are summarized in Table III.

1. Diffuse HI clouds (cold neutral medium)

Because of their temperatures and densities, diffuse HI clouds will radiate most of their cooling through the [CII] 158 μm line (Dalgarno and McCray, 1972; Black, 1993). For a few lines of sight the expected [CII] line emission has been measured in an indirect way; i.e., through far-ultraviolet measurements of the population of the upper level of this fine-structure transition (Pottasch *et al.*, 1979). These observations yielded an emissivity per H atom of about 10^{-25} erg/s. A subsequent study measured a somewhat lower cooling rate of 3×10^{-26} erg/s/H-atom (Gry *et al.*, 1992). The earlier study concentrated on lines of sight characterized by relatively high far-ultraviolet radiation fields and hence high cool-

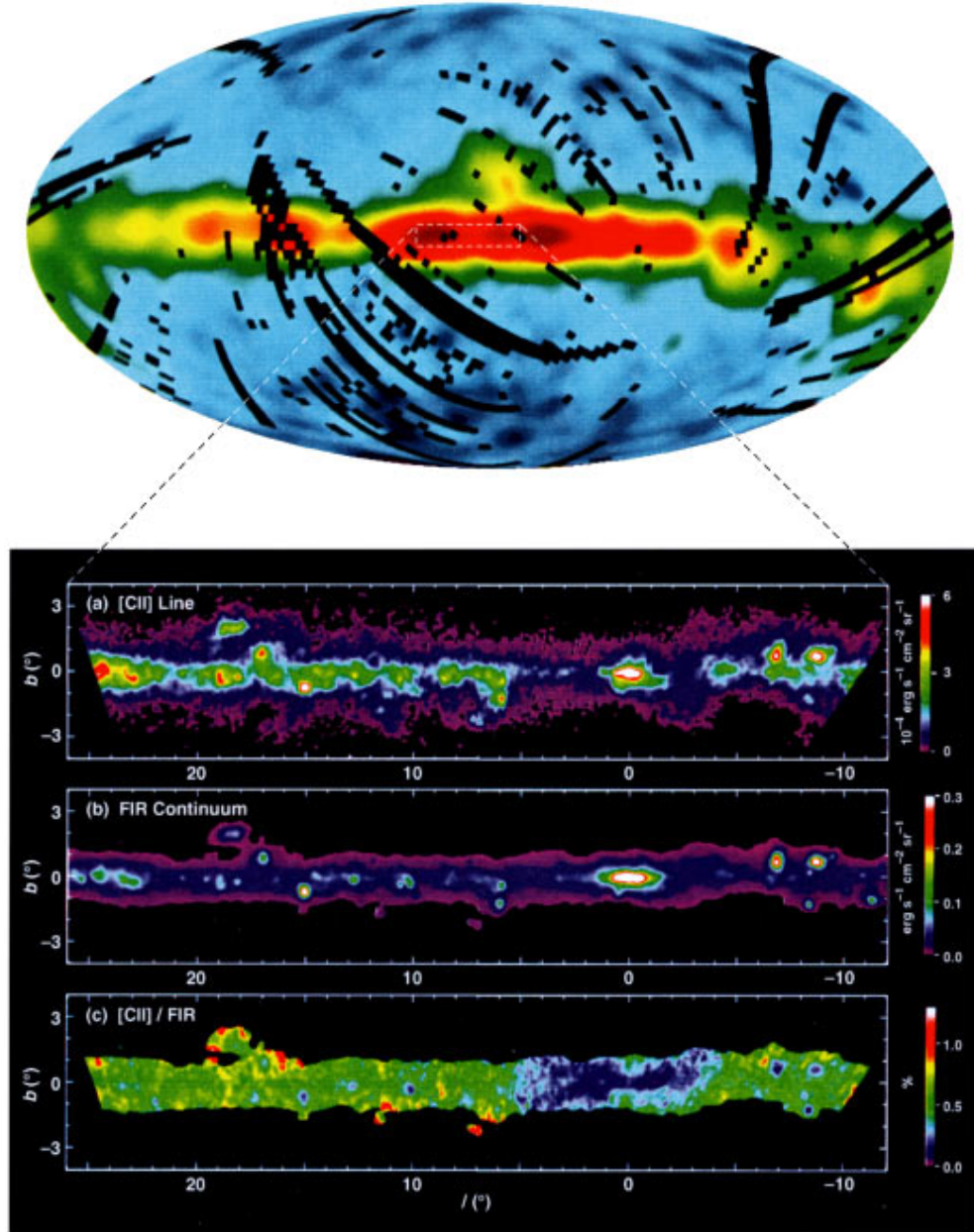


FIG. 45. (Color) The [CII] emission of the galaxy observed by the FIRAS instrument on COBE (top panel, Bennett *et al.*, 1994). The galactic plane is horizontal with the galactic center at the center. The spatial resolution is of order 7° . The bottom panels show the far-infrared [CII] line intensity map ($I_{\text{[CII]}}$) obtained by BICE, the far infrared continuum map (I_{FIR}) obtained from IRAS 60- and 100- μm maps, and the ratio of the far-infrared [CII] line emission to the far-infrared continuum emission ($I_{\text{[CII]}}/I_{\text{FIR}}$). The spatial resolution is about $15'$. From Nakagawa *et al.* (1998). Note that the bottom panels are much-higher-spatial-resolution maps of a small portion of the COBE map on top.

TABLE III. Diffuse galactic [CII] emission.

Component	Cooling rate $\text{erg s}^{-1} \text{H-atom}^{-1}$	Galactic luminosity L_\odot	$I_{\text{CII}} \sin b $ (halo) $\text{erg cm}^{-2} \text{s}^{-1} \text{sr}^{-1}$
Diffuse HI clouds	5. (-26)	3. (7)	7. (-7)
Warm neutral medium	5. (-27)	3. (6)	7. (-8)
Warm ionized medium	5. (-26)	7. (7)	4. (-7)
HI halos ^a	5. (-26)	1. (7)	-
Observed	3.-10. (-26)	5. (7)	14. (-7)

^aPDRs associated with HI surfaces of molecular clouds.

ing rates (see Sec. II.C.4). The latter study was predominantly of stars with relatively low average densities and, consequently, a large admixture of warm neutral medium. The warm neutral medium cools largely through Lyman α and [OI] 6300 Å emission and is an inefficient [CII] 158 μm emitter. Direct measurements of the [CII] 158 μm emission from high-galactic-latitude clouds, which also yield $3 \times 10^{-26} \text{ erg/s/H atom}$ (Bock *et al.*, 1993; Caux and Gry, 1997), likely also have a relatively large contribution of warm neutral medium to the HI. Allowing for these systematic effects, an average cooling rate of $5 \times 10^{-26} \text{ erg/s/H atom}$ is derived for diffuse HI clouds (Bakes and Tielens, 1994; Wolfire *et al.*, 1995). For a total galactic HI mass of $3.5 \times 10^9 M_\odot$, with about half in diffuse HI clouds, a total galactic [CII] luminosity of $\approx 3 \times 10^7 L_\odot$ is estimated from diffuse HI gas, which is somewhat less than has been observed by COBE (Table III).

2. PDRs on molecular cloud surfaces

Airborne studies directed towards the molecular ring show a good correlation between the [CII] emission and the CO emission but not the HI emission (Stacey *et al.*, 1985; Shibai *et al.*, 1991). While part of this might just reflect a large contribution of warm neutral medium to the HI in the inner galaxy, which does not contribute substantially to the [CII] emission, this suggests that the galactic [CII] emission is associated with PDRs on molecular cloud surfaces created by nearby OB associations and/or the ambient interstellar radiation field (i.e., HI halos). Indeed, the Taurus, Orion-Monoceros, and Scorpius-Ophiuchus molecular cloud complexes are readily apparent in the COBE [CII] map (see Fig. 44). The physical conditions in these HI halos are very similar to those in the diffuse HI gas (Elmegreen and Elmegreen, 1987; Andersson and Wannier, 1993) and hence they are expected to have similar photoelectric heating efficiencies (see Sec. II). Thus, in this interpretation, the observed CII/CO correlation would imply that molecular clouds and their halos intercept much of the total available far-ultraviolet radiation field. This conclusion is based mainly upon analysis of the [CII] emission along a few scans across the galaxy associated with molecular clouds exhibiting massive star formation (i.e., W43, NGC 6334; Shibai *et al.*, 1991). Studies of individual OB association/molecular cloud regions in the solar neighborhood have shown that a considerable fraction of the stellar luminosity is reradiated by the dust in the molecular cloud during the early phases of evolution (the embedded and blister phases of HII regions, $\sim 30\%$ of an O star's lifetime; Leisawitz and Hauser, 1988; Cox *et al.*, 1990). However, this is not true for the galaxy as a whole. IRAS and COBE studies concluded that only about 20% of the galactic IR emission is starlight reprocessed by molecular clouds. Much of the remainder (70%) originates in HI gas (Sodroski *et al.*, 1989; 1997; Bloemen *et al.*, 1990). Whether this HI gas could be the diffuse halos of molecular clouds is controversial. In the later phases, a significant fraction of the OB associa-

tion's light escapes from the local environment. Moreover, in the solar neighborhood, half the O stars are field stars, whose light similarly escapes. Hence, on the whole, PDRs on molecular cloud surfaces are not expected to be the dominant source of the galactic CII emission and may only contribute $\sim 2/7$ ths as much as the diffuse (non-halo) cold neutral medium (Table III).

3. Diffuse HII regions and warm ionized medium

COBE also measured the emission in the [NII] 205 μm line (Wright *et al.*, 1991; Bennett *et al.*, 1994). The ionization potential of neutral N is slightly above that of H and hence this emission has to originate in largely ionized H $^+$ zones: warm ionized medium or extended low-density regions. Such low-density HII regions can also be important sources of [CII] emission (Shibai *et al.*, 1991; Heiles, 1994) and, indeed, the observed [NII] emission correlates well—but not linearly—with the [CII] emission ($I_{\text{NII}} \propto I_{\text{CII}}^{1.5}$; Bennett *et al.*, 1994). At the low densities of such regions, N $^+$ and C $^+$ are the dominant ionization stages of these elements and, assuming C and N gas-phase abundances of 1.4×10^{-4} and 6.5×10^{-5} (Cardelli *et al.*, 1996), the expected [CII]/[NII] intensity ratio is 10 (Heiles, 1994). The observed galactic [NII] luminosity ($6.8 \times 10^6 L_\odot$; Bennett *et al.*, 1994) translates then into a [CII] luminosity of $6.8 \times 10^7 L_\odot$, quite comparable to the observed galactic [CII] emission (Table II). If N is a secondary nucleosynthesis product, the N/C abundance ratio in the inner galaxy might be up by a factor of 1.4 (similar to the observed N/O galactic gradient; Simpson *et al.* 1994) and the [CII] luminosity from the warm ionized medium down by the same factor. If the warm-ionized-medium phase dominates the production of [CII], the correlation of CO and [CII] suggests that [CII] and [NII] come from the extended low-density regions associated with the molecular clouds and O stars of the inner Galaxy.

The observed nonlinear correlation between [CII] and [NII] suggests that the warm ionized medium is an important contributor to the [CII] emission at the higher observed intensities—i.e., for $I_{\text{CII}} \approx 10^{-4} \text{ erg cm}^{-2} \text{ s}^{-1} \text{ sr}^{-1}$ corresponding to the inner galaxy—but not at lower intensities. There is room, then, for a significant contribution from diffuse HI regions.

4. Discussion

There are three plausible origins for the observed galactic [CII] 158 μm emission observed with COBE: diffuse HI clouds, PDR surfaces of molecular clouds, and the warm ionized medium. The contribution of each of these components depends on the location in the galaxy as well as the scale size of the observations. Their contribution to the total galactic [CII] emission is summarized in Table III. Each of these estimates is uncertain by 50% and hence, except for the warm neutral medium, each of them could be the dominant one.

In the local ISM, diffuse HI clouds dominate the [CII] emission with typical intensities of $1-10 \times 10^{-7} \text{ erg cm}^{-2} \text{ s}^{-1} \text{ sr}^{-1}$. For the halo, we adopt a total

HI column of $3-4 \times 10^{20}$ cosec $|b|$ cm $^{-2}$ (Lockman *et al.*, 1986) of which on average 50% is in diffuse clouds. Per H nucleus, the [CII] emission from the warm ionized medium is as important (Wolfire *et al.*, 1995), but locally the mass of HII is only one-third that of HI (Reynolds, 1993). Indeed, for a typical H α intensity from the local warm ionized medium of 3×10^{-7} cosec $|b|$ erg cm $^{-2}$ s $^{-1}$ sr $^{-1}$ (Reynolds, 1993), the expected [CII] emission is 2×10^{-7} erg cm $^{-2}$ s $^{-1}$ sr $^{-1}$. If, instead, we scale from the COBE [NII] observations ($I_{\text{NII}} = 4 \times 10^{-8}$ cosec $|b|$ erg cm $^{-2}$ s $^{-1}$ sr $^{-1}$; Bennett *et al.*, 1994), the contribution of the warm-ionized medium is a factor of 2 larger. Locally, molecular clouds contribute little to the total [CII] emission. Taken together, these different components can account for much of the observed local [CII] emission. It should be emphasized that the HI and HII distributions are very irregular and these estimates should only be considered as averages.

Towards the inner galaxy, the ISM pressure increases and hence the density in the warm ionized medium increases as well. In addition, the extended low-density regions may become more abundant. The [CII] contribution from both these sources then becomes comparatively more important. Indeed, judging from the [NII] observations, the warm ionized medium may contribute substantially to the [CII] emission from the inner galaxy (and hence the total CII luminosity). As discussed above, the contribution to the galactic CII emission from PDRs on molecular cloud surfaces is likely less significant, unless HI halos make up a large fraction of the cold neutral medium.

At high latitudes, a substantial proportion of the far-ultraviolet stellar flux is absorbed in the warm neutral medium, which is an inefficient [CII] emitter. At least 15% of the ionizing stellar flux from OB stars has to escape into the halo to explain the warm ionized medium (Reynolds, 1993) and, likely, the escaping far-ultraviolet flux is even larger. Because of the larger scale height, this far-ultraviolet flux will heat the warm neutral medium rather than diffuse clouds. Since the warm neutral medium is an inefficient [CII] emitter, the [CII] scale height is expected to be substantially smaller than the HI emission scale height. Similarly, far-infrared emission by dust in the warm-neutral-medium phase is also likely the cause of the rapid drop in the efficiency [$I(\text{CII})/I(\text{far infrared})$] with galactic latitude observed by COBE (Bennett *et al.*, 1994).

5. Energy balance of the interstellar gas

The observed CII emission is a lower limit to the total heating rate of the ISM of the Galaxy. Table IV compares the observations to the various energy sources of the interstellar gas. The mechanical energy input by supernovae is calculated assuming a supernova rate of 2×10^{-2} yr $^{-1}$ and an energy per supernova of 10^{51} erg. The mechanical energy input by Wolf-Rayet and OB stars is taken from van der Hucht *et al.* (1987). Since a large fraction of the mechanical energy will be dissipated by strong shocks, and such shocks are inefficient

TABLE IV. Energy sources.

Source	Luminosity [L $_{\odot}$]
Observations	
[CII] 158 μ m	5 (7)
FIR	1.7 (10)
Stellar luminosities	
All stars	4 (10)
OBA	8 (9)
Mechanical energy	
SN	2 (8)
WR	6 (6)
OBA	2 (6)

[CII] emitters, it is clear that the heating of the interstellar gas has to result from tapping into the stellar extreme-ultraviolet and far-ultraviolet energy reservoir (see Sec. II.C.4). The efficiency of grain photoelectric heating [$L(\text{CII})/L(\text{far infrared})$] inferred from the COBE observations is only ≈ 0.003 . The CII observations of local diffuse clouds in the UV imply much higher efficiencies (0.05). The low efficiency derived from the IR observations may reflect the heating of interstellar dust by visible (and far-red) rather than far-ultraviolet photons. Long-wavelength photons are not very efficient in heating the gas through the photoelectric effect (Spaans *et al.*, 1994). Alternatively, toward the galactic center where most of the luminosity originates, a significant proportion of the far-ultraviolet stellar flux may be absorbed in the warm neutral medium, which is an inefficient [CII] emitter.

An interesting sidenote to the [CII] observations of the Galaxy are found in Malhotra *et al.* (1997), who present ISO observations of $L(\text{CII})/L(\text{far infrared})$ for a sample of 30 “normal” galaxies. They find that in two-thirds of the cases the observed ratio is $\sim 2-7 \times 10^{-3}$, similar to the Galaxy. In the other one-third of the galaxies, the ratio decreases with increasing dust temperature (G_0), suggesting that the positive charging of the grains reduces the efficiency.

At this point in time, it seems fair to conclude that the origin of the galactic [CII] emission as well as the heating of the diffuse interstellar gas is not (yet) completely understood. Further studies, in particular, of the atomic fine-structure line emission along a few well-defined lines of sight (e.g., ζ Oph, ζ Per, α Per, α Vir) are within reach with ISO and could lead to a direct determination of the heating efficiency of the interstellar gas as a function of the physical conditions. Analysis of the BICE data will also provide an important testbed for the various theories for the origin of the galactic [CII] emission.

E. Far-ultraviolet regulation of star formation in galaxies

Perhaps the most important process in a spiral galaxy is the ongoing cycle of stellar birth and death, the cycle of interstellar gas and dust forming stars and of stars

blowing off material to replenish the gas and dust in the ISM. What sets the stellar birth rate in a galaxy? It has long been suspected that a feedback process exists whereby stars themselves regulate their own formation rate. This feedback exists because the winds, ultraviolet fluxes, and supernova explosions of stars have an overall destructive effect on the opaque molecular clouds that form stars. In short, if too many stars form, they destroy their spawning grounds and the formation rate is quenched. Several of the feedback mechanisms proposed involve far-ultraviolet processes in the PDR neutral gas.

McKee (1989) and Bertoldi and McKee (1996) explain the regulation of low-mass star formation and the observed constancy of A_V (~ 7.5) or column density in molecular clouds with a PDR model. They assume that the rate of low-mass star formation is governed by ambipolar diffusion (cf. Shu *et al.*, 1987) and that newly formed stars inject mechanical energy (via winds) into the cloud. These winds interact with the ambient cloud and generate turbulence, which supports the cloud against gravitational collapse. In the ambipolar diffusion process, the trace ions remain coupled to the magnetic field, whose pressure prevents collapse of the ions, while the neutrals gravitationally collapse through the fixed ions, retarded by collisions with them. The ambipolar diffusion rate is therefore set by the ionization fraction, which depends on the dust shielding of the external far-ultraviolet flux. In the model, as the cloud collapses, A_V increases and the cloud shields out more far-ultraviolet radiation, the far-ultraviolet-produced ionization level decreases, the ambipolar diffusion rate increases, and therefore the star formation rate increases. However, cloud collapse is halted as the increased star formation injects turbulent energy. Equilibrium is achieved when $A_V \sim 7.5$ throughout the cloud. The external far-ultraviolet flux, in controlling the ionization fraction in most of the cloud, regulates the low-mass star formation rate and the cloud column density (or A_V). One of the predictions of this model is that in regions of low metallicities (or grain opacity per H nucleus), the clouds will still achieve equilibrium when $A_V \sim 7.5$. This implies that the typical hydrogen column through a cloud will increase with Z^{-1} , where Z is the metallicity. Pak *et al.* (1998) present observations and models of clouds in the low-metallicity Magellanic Clouds which support this prediction.

Parravano (1987, 1988, 1989) proposes that a global feedback mechanism exists in galaxies whereby the galaxy-wide rate of high-mass star formation is also regulated by the interaction of the far ultraviolet with the neutral gas. Non-gravitationally-bound neutral gas may exist in two phases (cold, ~ 100 K, and warm, $\sim 10^4$ K) in a galaxy, if the ISM pressure lies in a critical range $P_{\min} < P < P_{\max}$ (Field *et al.*, 1969; see Sec. VII.A and Fig. 43). For pressures $P < P_{\min}$ only the warm diffuse phase exists. Parravano makes two assumptions in his modeling: (i) grain photoelectric heating dominates both phases so that P_{\min} monotonically increases with G_0 (see Fig. 43), and (ii) molecular, star-forming clouds

grow out of the cold phase (e.g., out of the coalescence of cold-phase clouds). If the pressure P of the ISM is greater than P_{\min} , the cold phase exists, molecular clouds grow, OB stars form, G_0 increases, and P_{\min} rises. If P_{\min} exceeds P , however, the cold phase no longer exists, star formation drops, which causes G_0 to decrease, which, in turn, lowers P_{\min} . Thus the global OB star formation rate is regulated so that $P_{\min} \sim P$ in galaxies. Parravano (1988, 1989) offers some observational support of this prediction in external galaxies. Rapid self-regulation can lead to steady star formation rates (Parravano *et al.*, 1990), but delayed self-regulation, such as occurs when there is a significant delay between the formation of the cold phase and the appearance of non-obsured OB stars, can lead to overstability and strong oscillations of the star formation rate around the self-regulated value (Parravano, 1996). Parravano and Mantilla (1991) discuss the radial dependence of the state of the ISM in the Galaxy when both the McKee (1989) mechanism and the above self-regulation mechanism are operative.

VIII. CONCLUSIONS, SUMMARY, AND FUTURE DIRECTIONS

Research on photodissociation regions has shown us the importance of far-ultraviolet photons in the physics and chemistry of the interstellar medium. These regions emit much of the infrared radiation (line and continuum) in galaxies. Most of the mass of the gas and dust in the Galaxy resides in PDRs and is significantly affected, via either chemistry or heating, by the far-ultraviolet flux. PDR models are relevant to regions as diverse as the warm neutral medium, cold neutral medium, molecular components of the ISM, reflection nebulae, planetary nebulae, and protoplanetary disks, as well as to neutral gas associated with HII regions, red giant winds, and galactic nuclei. Much of the gas is heated by the grain photoelectric heating mechanism and cooled by [CII] 158 μm and [OI] 63 μm emission. The spectra from PDRs are characterized by luminosity ratios $(L_{\text{CII}} + L_{\text{OI}})/L_{\text{IR}} \sim 10^{-3} - 10^{-2}$. Photodissociation regions are the origin of an important fraction of the observed [CII] 158 μm , [OI] 63, and 145 μm , [SiII] 35 μm , [CI] 370 and 609 μm , low J CO, and CI recombination radiation. They also emit significant H_2 rovibrational emission. In regions such as Orion, NGC 2023, NGC 7027, the Galactic center, and starburst galaxy nuclei, the spectra diagnose physical conditions such as the gas density, the clumpiness of the clouds, the far-ultraviolet radiation field, and the elemental abundances. New models of x-ray-illuminated molecular clouds may explain near-IR (e.g., H_2 2 μm and [FeII] 1.64 μm) observations of Seyfert nuclei and supernova remnants without invoking shocks or star formation. Grain photoelectric heating explains the existence of two neutral phases of the ISM. Photodissociation models are required to understand the formation and destruction of molecular clouds in the ISM and the distribution of HI and H_2 in galaxies. These models predict

the observed correlations of [CII] 158 μm emission with $^{12}\text{CO } J=1-0$ emission, of $(L_{\text{CII}}+L_{\text{OI}})$ with L_{IR} , and of $^{12}\text{CO } J=1-0$ with H_2 mass. The far-ultraviolet flux in PDRs may regulate low- and high-mass star formation in galaxies and may regulate the column density of gravitationally bound, star-forming molecular clouds. Therefore, although the ISM may be “violent” and rent with supernova shocks, the relatively gentle photodissociation, photoionization, and heating of the bulk of the gas by UV photons from the more massive stars play an enormous role in determining the density, structure, chemistry, temperature, and evolution of the ISM.

Over the next decade, new instrumental developments are sure to provide a further deepening of our understanding of PDR-related science. High spectral resolution, near- and mid-IR spectrometers on 10-m class telescopes (Keck, VLT), large telescope arrays operational in the millimeter wavelength region, and the opening up of the far-infrared window to 2.5–4-meter telescopes—first on the Stratospheric Observatory For Infrared Astronomy (SOFIA) and then on the Far-Infrared and Submillimeter Telescope (FIRST)—will allow detailed studies of the distribution of various tracers of PDR structure. Of particular interest will be mapping the gas temperature distribution using pure rotational H_2 transitions and comparing those with distribution of the far-infrared dust radiation and the unidentified infrared features due to PAH molecules. This way, empirical gas-heating efficiencies can be derived and theoretical models of the photoelectric heating can be tested in detail. Recall that present gas temperatures derived from pure rotational H_2 lines measured with the SWS on ISO exceed predicted gas temperatures (see Sec. IV.B). High-level CO lines also indicate higher gas temperatures. Whether this indicates the importance of (warm) clumps or the presence of another heating source is at present unclear. Dissipation of magnetohydrodynamic turbulence may play a more prominent role in the heating of interstellar gas than hitherto thought. Also, radiation pressure on dust grains can under some circumstances (high far-ultraviolet field and low density, $G_0/n \gtrsim 10^2$) lead to viscous heating of the gas. In general, the effect of radiation pressure on PDR dust needs to be studied, as significant drifting of the grains with respect to the gas will lead to changes in the far-ultraviolet opacity of PDRs and in the H_2 formation rates in them. In addition, detailed studies of the abundances of various molecular species in a number of well-studied PDRs (the Orion Bar, NGC 2023, etc.) will provide insight into the role of far-ultraviolet photons in the chemical evolution of these regions and will provide detailed tests of models of interstellar chemistry.

Photodissociation regions seem to show structure on all scales. The importance of this structure for the global characteristics of these regions is, observationally, not entirely clear. On the largest scales, PDRs show open structures allowing far-ultraviolet radiation to penetrate deep into molecular clouds. On smaller scales, however, the influence of clumps on the far-ultraviolet intensity seems more limited, but they do dominate the observa-

tional characteristics of the region in some (high-density) tracers. The origin and evolution of these clumps are an obvious area of further study. The high thermal pressures associated with these warm regions far exceeds that of the surrounding interclump PDR gas and requires an attractive stabilizing force, presumably gravity. Likely, these clumps contain a central, low-mass protostar and they are the PDR counterparts of the protoplanetary disks observed in the ionized gas (see Sec. III.C). The photoevaporation of the disks/envelopes around such newly formed stars might then already have begun during the PDR phase. A region like the Orion molecular cloud core, OMC1, contains thousands of newly formed, mainly low-mass stars. The few massive stars formed in such a cluster are likely to profoundly affect the early life history of these newly formed stars—their total mass, survivability of their disks, planet formation—through their strong stellar winds, their ionizing photons, and their far-ultraviolet photons. The improved spatial resolution of future observing facilities can clarify the relative importance of these processes.

The origin and evolution of galaxies is closely tied to the cyclical interaction of stars and the interstellar medium. Stars shape the ISM through the injection of gas and dust and through their radiative and mechanical energy, while the ISM forms new stars and planetary systems through gravitational collapse. As emphasized throughout this review, far-ultraviolet photons play an important role in the structure, composition, and observational characteristics of the ISM. On a galactic scale, many questions still remain. The origin of the galactic [CII] 158 μm emission is one of these. More generally, what are the densities, pressures, filling factors, porosities, dynamics, ionization sources, and cooling processes of the different phases that make up the ISM throughout the Milky Way? On this global scale, the mass interchange between the different phases is of particular interest. For example, are molecular clouds largely dispersed through the mechanical energy input from massive stars or through the photoevaporation caused by their UV photons? Also, is there an intimate physical relationship between the warm-ionized-medium, warm-neutral-medium, and cold-neutral-medium phases of the ISM? High-resolution spectroscopy of nearby galaxies in the sub-mm and far infrared will be instrumental in addressing these issues. Ultimately, studies of this kind are of prime importance for our understanding of the origin and evolution of the ISM in the Milky Way, in nearby galaxies, and in distant galaxies extending to the earliest protogalaxies at high redshift.

ACKNOWLEDGMENTS

We wish to thank F. Bertoldi, B. Draine, D. Jaffe, T. Nakagawa, A. Sternberg, H. Störzer, J. Stutzki, and F. Wyrowski, for comments on earlier versions of the paper, for discussions, and for providing material in advance of publication. We particularly wish to thank A. Sternberg and E. van Dishoeck for their very careful reading of this paper, which resulted in numerous im-

gements of the manuscript. This research was supported in part by the NASA Astrophysical Theory Program which funds the Center for Star Formation Studies, a consortium of researchers from NASA Ames, UC Berkeley, and UC Santa Cruz.

REFERENCES

- Aalto, S., R. S. Booth, J. H. Black, and L. E. B. Johansson, 1995, *Astron. Astrophys.* **300**, 369.
- Aalto, S., R. S. Booth, L. E. B. Johansson, and J. H. Black, 1991a, *Astron. Astrophys.* **247**, 291.
- Aalto, S., L. E. B. Johansson, R. S. Booth, and J. H. Black, 1991b, *Astron. Astrophys.* **249**, 323.
- Aalto, S., S. J. E. Radford, N. Z. Scoville, and A. I. Sargent, 1997, *Astron. Astrophys.* **475**, L107.
- Abgrall, H., J. LeBourlot, G. Pineau des Forets, E. Roueff, D. R. Flower, and L. Heck, 1992, *Astron. Astrophys.* **253**, 525.
- Allamandola, L. J., A. G. G. M. Tielens, and J. R. Barker, 1985, *Astrophys. J.* **290**, L25.
- Allen, M. and G. W. Robinson, 1975, *Astrophys. J.* **195**, 81.
- Allen, R. J., 1996, in *Changing Perceptions of the Morphology, Dust Content, and Dust-Gas Ratios in Galaxies*, edited by D. Block and P. Grosbol (Kluwer, Dordrecht), p. 50.
- Allen, R. J., P. D. Atherton, and R. P. J. Tilanus, 1986, *Nature (London)* **319**, 296.
- Allen, R. J., J. H. Knapen, R. Bohlin, and T. P. Stecher, 1997, *Astrophys. J.* **487**, 171.
- Alonso-Herrero, A., M. J. Rieke, G. H. Rieke, and M. Ruiz, 1997, *Astrophys. J.* **482**, 747.
- Andersson, B.-G., R. S. Roger, and P. G. Wannier, 1992, *Astron. Astrophys.* **260**, 355.
- Andersson, B.-G., and P. G. Wannier, 1993, *Astrophys. J.* **402**, 585.
- Andersson, B.-G., P. G. Wannier, and M. Morris, 1991, *Astrophys. J.* **366**, 464.
- Arthur, S. J., and S. Lizano, 1997, *Astrophys. J.* **484**, 810.
- Bachiller, R., T. Forveille, P. J. Huggins, and P. Cox, 1997, *Astron. Astrophys.* **324**, 1123.
- Bakes, E. L. O., and A. G. G. M. Tielens, 1994, *Astrophys. J.* **427**, 822.
- Bakes, E. L. O., and A. G. G. M. Tielens, 1998, *Astrophys. J.* **499**, 258.
- Balick, B., R. H. Gammon, and L. H. Doherty, 1974, *Astrophys. J.* **188**, 45.
- Bally, J., and W. D. Langer, 1982, *Astrophys. J.* **255**, 143.
- Bally, J., W. D. Langer, A. S. Stars, and R. W. Wilson, 1987, *Astrophys. J. Lett.* **312**, L45.
- Bally, J., and M. Leventhal, 1991, *Nature (London)* **353**, 234.
- Bally, J., R. Sutherland, D. Johnstone, and D. Devine, 1998, *Astron. J.* **116**, 293.
- Barsuhn, J., and C. M. Walmsley, 1977, *Astron. Astrophys.* **54**, 345.
- Becklin, E. E., I. Gatley, and M. W. Werner, 1982, *Astrophys. J.* **258**, 135.
- Bennett, C. L., et al., 1994, *Astrophys. J.* **434**, 587.
- Bergin, E. A., P. F. Goldsmith, R. L. Snell, and W. D. Langer, 1997, *Astrophys. J.* **482**, 285.
- Bertoldi, F., 1998, in preparation.
- Bertoldi, F., and B. T. Draine, 1996, *Astrophys. J.* **458**, 222.
- Bertoldi, F., and C. McKee, 1996, in *Amazing Light*, edited by R. Y. Chiao (Springer, New York), p. 41.
- Black, J. H., 1993, in *The First Symposium on the Galactic Cirrus and Diffuse Interstellar Clouds*, edited by M. Cutri and W. B. Latter (ASP, San Francisco), p. 355.
- Black, J. H., and A. Dalgarno, 1976, *Astrophys. J.* **203**, 132.
- Black, J. H., and A. Dalgarno, 1977, *Astrophys. J., Suppl.* **34**, 405.
- Black, J. H., and E. F. van Dishoeck, 1987, *Astrophys. J.* **322**, 412.
- Blades, J. C., M. S. Sahu, L. He, I. A. Crawford, M. J. Barlo, and F. Diego, 1997, *Astrophys. J.* **478**, 648.
- Blietz, M., M. Cameron, S. Drapatz, R. Genzel, A. Krabbe, P. Van der Werf, A. Sternberg, and M. Ward, 1994, *Astrophys. J.* **421**, 92.
- Bloemen, J. B. G. M., E. R. Deul, and P. Thaddeus, 1990, *Astron. Astrophys.* **233**, 437.
- Bobrowsky, M., and D. M. Zipoy, 1989, *Astrophys. J.* **347**, 307.
- Bock, J. J., V. V. Hristov, M. Kawada, H. Matsuura, T. Matsumoto, S. Matsuura, P. D. Mauskopf, P. L. Richards, M. Tanaka, and A. E. Lange, 1993, *Astrophys. J. Lett.* **410**, L115.
- Boissé, P., 1990, *Astron. Astrophys.* **228**, 483.
- Boland, W., and T. de Jong, 1982, *Astrophys. J.* **261**, 110.
- Boreiko, R. T., and A. L. Betz, 1991, *Astrophys. J.* **369**, 382.
- Boreiko, R. T., and A. L. Betz, 1996a, *Astrophys. J.* **464**, L83.
- Boreiko, R. T., and A. L. Betz, 1996b, *Astrophys. J.* **467**, L113.
- Boreiko, R. T., and A. L. Betz, 1997, *Astrophys. J., Suppl. Ser.* **111**, 409.
- Bregman, J., 1989, in *Interstellar Dust*, edited by L. J. Allamandola and A. G. G. M. Tielens (Reidel, Dordrecht), p. 109.
- Bregman, J., L. J. Allamandola, A. G. G. M. Tielens, T. R. Geballe, and F. C. Witteborn, 1989, *Astrophys. J.* **344**, 791.
- Buch, V., and Q. Zhang, 1991, *Astrophys. J.* **379**, 647.
- Burke, J. R., and D. J. Hollenbach, 1983, *Astrophys. J.* **265**, 223.
- Burstein, P., R. J. Borken, W. L. Kraanhaar, and W. T. Sanders, 1977, *Astrophys. J.* **213**, 405.
- Burton, M., 1992, *Aust. J. Phys.* **45**, 463.
- Burton, M., M. Bulmer, A. Moorhouse, T. R. Geballe, and P. W. J. L. Brand, 1992, *Mon. Not. R. Astron. Soc.* **257**, 1P.
- Burton, M., T. R. Geballe, P. W. J. L. Brand, and A. Moorhouse, 1990, *Astrophys. J.* **352**, 625.
- Burton, M., D. J. Hollenbach, and A. G. G. M. Tielens, 1990, *Astrophys. J.* **365**, 620.
- Burton, M., D. J. Hollenbach, A. G. G. M. Tielens, 1992, *Astrophys. J.* **399**, 563.
- Burton, M., and P. Puxley, 1990, in *Interstellar Medium of External Galaxies*, edited by D. J. Hollenbach (NASA, Ames Research Center), p. 238.
- Büttgenbach, T. H., J. Keene, T. G. Phillips, and C. K. Walker, 1992, *Astrophys. J.* **397**, L15.
- Cardelli, J. A., G. C. Clayton, and J. S. Mathis, 1989, *Astrophys. J.* **345**, 245.
- Cardelli, J. A., D. M. Meyer, M. Jura, and B. D. Savage, 1996, *Astrophys. J.* **467**, 334.
- Carra, P., D. J. Hollenbach, S. D. Lord, S. W. J. Colgan, M. R. Haas, R. H. Rubin, and E. F. Erickson, 1994, *Astrophys. J.* **423**, 223.
- Caux, E., and C. Gry, 1997, in *First ISO Workshop on Analytical Spectroscopy*, ESA-SP 419, p. 253.
- Cesarsky, D. A., 1982, *Astron. Astrophys.* **113**, L7.
- Charnley, S. B., 1997, *Astrophys. J.* **481**, 396.
- Chièze, J. P., G. Pineau des Forets, and E. Herbst, 1991, *Astrophys. J.* **373**, 110.

- Chièze, J. P., and G. Pineau des Forets, 1990, in *Physical Processes in Fragmentation and Star Formation*, edited by R. Capuzzo-Dolcetta, C. Chiosi, and A. DiFazio (Kluwer, Dordrecht), p. 17.
- Chièze, J. P., and G. Pineau des Forets, 1989, *Astron. Astrophys.* **221**, 89.
- Chokshi, A., A. G. G. M. Tielens, M. W. Werner, and M. W. Castelaz, 1988, *Astrophys. J.* **334**, 803.
- Chromey, F. R., B. G. Elmegreen, and D. M. Elmegreen, 1989, *Astrophys. J.* **98**, 2203.
- Chrystostomou, A., P. W. J. L. Brand, M. G. Burton, and A. Moorhouse, 1992, *Mon. Not. R. Astron. Soc.* **256**, 528.
- Chrystostomou, A., P. W. J. L. Brand, M. G. Burton, and A. Moorhouse, 1993, *Mon. Not. R. Astron. Soc.* **265**, 329.
- Chu, Y.-H., and W. D. Watson, 1983, *Astrophys. J.* **267**, 151.
- Churchwell, E., M. Felli, D. O. S. Wood, and M. Massi, 1987, *Astrophys. J.* **321**, 516.
- Clavel, J., Y. P. Viala, and N. Bel, 1978, *Astron. Astrophys.* **65**, 435.
- Cohen, M., L. Allamandola, A. G. G. M. Tielens, J. Bregman, J. P. Simpson, F. C. Witteborn, D. Wooden, and D. Rank, 1986, *Astrophys. J.* **302**, 737.
- Cohen, M., A. G. G. M. Tielens, J. Bregman, F. C. Witteborn, D. M. Rank, L. J. Allemandola, D. H. Wooden, and M. de Muizon, 1989, *Astrophys. J.* **341**, 246.
- Cox, D. P., and B. W. Smith, 1974, *Astrophys. J. Lett.* **189**, L105.
- Cox, P., L. deHarveng, and A. Leene, 1990, *Astron. Astrophys.* **230**, 181.
- Cox, P., et al., 1998, *Astrophys. J. Lett.* **495**, L23.
- Crawford, I. A., and D. A. Williams, 1997, *Mon. Not. R. Astron. Soc.* **291L**, L53.
- Crawford, M. K., R. Genzel, C. H. Townes, and D. M. Watson, 1985, *Astrophys. J.* **291**, 755.
- Dalgarno, A., 1985, in *Molecular Astrophysics*, edited by G. H. F. Diercksen, W. F. Huebner, and P. W. Langhof (Reidel, Dordrecht), p. 281.
- Dalgarno, A., J. H. Black, and J. C. Weisheit, 1973, *Astrophys. Lett.* **14**, 77.
- Dalgarno, A., and R. A. McCray, 1972, *Annu. Rev. Astron. Astrophys.* **10**, 375.
- Danks, A. C., S. R. Federman, and D. L. Lambert, 1984, *Astron. Astrophys.* **130**, 62.
- Davis, R. J., P. J. Diamond, and W. M. Goss, 1996, *Mon. Not. R. Astron. Soc.* **283**, 1105.
- de Jong, T., 1977, *Astron. Astrophys.* **55**, 137.
- de Jong, T., 1980, *Highlights Astrophys.* **5**, 301.
- de Jong, T., A. Dalgarno, and W. Boland, 1980, *Astron. Astrophys.* **91**, 68.
- Devereux, N. A., and J. S. Young, 1990, *Astrophys. J.* **350**, L25.
- d'Hendecourt, L., and A. Léger, 1987, *Astron. Astrophys.* **180**, L9.
- Diamond, P. J., W. M. Goss, J. D. Romney, R. S. Booth, P. M. W. Kalberla, and U. Mebold, 1989, *Astrophys. J.* **347**, 302.
- Diaz-Miller, R. I., J. Franco, and S. N. Shore, 1998, *Astrophys. J.* **501**, 192.
- Dieter, N. D.H., W. J. Welch, and J. D. Romney, 1976, *Astrophys. J. Lett.* **206**, L113.
- Dinerstein, H. L., 1991, *Publ. Astron. Soc. Pac.* **103**, 861.
- Dinerstein, H. L., 1995, in *Asymmetrical Planetary Nebulae*, edited by N. Soker and A. Harpaz (AIP, New York), p. 35.
- Dlott, D. D., 1989, in *Laser Spectroscopy of Solids II*, edited by W. M. Yen (Springer, Berlin), p. 167.
- Draine, B. T., 1978, *Astrophys. J., Suppl.* **36**, 595.
- Draine, B. T., and N. Anderson, 1985, *Astrophys. J.* **292**, 494.
- Draine, B. T., and F. Bertoldi, 1996, *Astrophys. J.* **468**, 269.
- Draine, B. T., and H. M. Lee, 1984, *Astrophys. J.* **285**, 89.
- Draine, B. T., and W. G. Roberge, 1984, *Astrophys. J.* **282**, 491.
- Draine, B. T., and D. T. Woods, 1990, *Astrophys. J.* **363**, 464.
- Draine, B. T., and D. T. Woods, 1991, *Astrophys. J.* **383**, 621.
- Duley, W. W., T. W. Hartquist, A. Sternberg, R. Wagenblast, and D. A. Williams, 1992, *Mon. Not. R. Astron. Soc.* **255**, 463.
- Duley, W. W., and D. A. Williams, 1981, *Mon. Not. R. Astron. Soc.* **196**, 269.
- Duley, W. W., and D. A. Williams, 1988, *Mon. Not. R. Astron. Soc.* **231**, 969.
- Duley, W. W., and D. A. Williams, 1993, *Mon. Not. R. Astron. Soc.* **260**, 37.
- Eckart, A., and R. Genzel, 1996, *Nature (London)* **383**, 415.
- Eidelsberg, M., J. J. Benayoun, Y. Viala, F. Rostas, P. L. Smith, K. Yoshino, G. Stark, and C. A. Shettle, 1992, *Astron. Astrophys.* **265**, 839.
- Elitzur, M., and T. de Jong, 1980, *Astron. Astrophys.* **67**, 323.
- Elitzur, M., and W. D. Watson, 1978, *Astrophys. J.* **222**, L141.
- Elmegreen, B. G., 1991, in *Dynamics of Galaxies and Molecular Cloud Distribution*, edited by F. Combes and F. Casoli (Kluwer, Dordrecht), p. 45.
- Elmegreen, B. G., 1993, *Astrophys. J.* **411**, 170.
- Elmegreen, B. G., and D. M. Elmegreen, 1987, *Astrophys. J.* **320**, 182.
- Elmegreen, B. G., and A. Parravano, 1994, *Astrophys. J.* **425**, L121.
- Erickson, E. F., S. W. J. Colgan, J. P. Simpson, R. H. Rubin, M. Morris, and M. R. Haas, 1991, *Astrophys. J.* **370**, L69.
- Escalante, V., A. Sternberg, and A. Dalgarno, 1991, *Astrophys. J.* **375**, 630.
- Evans, I. N., H. C. Ford, A. L. Kinney, R. R. J. Antonucci, L. Armus, and S. Caganoff, 1991, *Astrophys. J. Lett.* **369**, L27.
- Falgarone, E., D. C. Lis, T. G. Phillips, A. Pouquet, D. H. Porter, and P. R. Woodward, 1994, *Astrophys. J.* **436**, 728.
- Falgarone, E., G. Pineau des Forets, and E. Roueff, 1995, *Astron. Astrophys.* **300**, 870.
- Falgarone, E., and T. Phillips, 1996, *Astrophys. J.* **472**, 191.
- Federman, S. R., A. E. Glassgold, and J. Kwan, 1979, *Astrophys. J.* **227**, 466.
- Federman, S. R., A. E. Glassgold, E. B. Jenkins, and E. J. Shaya, 1980, *Astrophys. J.* **242**, 545.
- Federman, S. R., A. C. Danks, and D. L. Lambert, 1984, *Astrophys. J.* **287**, 219.
- Federman, S. R., and W. T. Huntress, 1989, *Astrophys. J.* **338**, 140.
- Federman, S. R., C. J. Strom, D. L. Lambert, J. A. Cardelli, V. V. Smith, and C. L. Joseph, 1994, *Astrophys. J.* **424**, 772.
- Felli, M., E. Churchwell, T. Wilson, and G. B. Taylor, 1993, *Astron. Astrophys., Suppl. Ser.* **98**, 137.
- Ferrière, K., E. G. Zweibel, and J. M. Shull, 1988, *Astrophys. J.* **332**, 984.
- Field, G. B., D. W. Goldsmith, and H. J. Habing, 1969, *Astrophys. J. Lett.* **155**, L149.
- Field, G. B., W. B. Somerville, and K. Dressler, 1966, *Annu. Rev. Astron. Astrophys.* **4**, 207.
- Flannery, B. P., W. Roberge, and G. B. Rybicki, 1980, *Astrophys. J.* **236**, 598.
- Flower, D. R., J. LeBourlot, G. Pineau des Forets, and E. Roueff, 1994, *Astron. Astrophys.* **282**, 225.

- Frail, D. A., J. M. Weisberg, J. M. Cordes, and C. Mathers, 1994, *Astrophys. J.* **436**, 144.
- Fuente, A., J. Martín-Pintado, J. Cernicharo, and R. Bachiller, 1993, *Astron. Astrophys.* **276**, 473.
- Fuente, A., J. Martín-Pintado, and R. Gaume, 1995, *Astrophys. J. Lett.* **442**, L33.
- Fuente, A., and J. Martín-Pintado, 1997, *Astrophys. J.* **477**, L107.
- Fuente, A., A. Rodriguez-Franco, and J. Martín-Pintado, 1996, *Astron. Astrophys.* **312**, 599.
- Garay, G., J. M. Moran, and M. J. Reid, 1987, *Astrophys. J.* **314**, 535.
- Gardiner, W. C., 1977, *Acc. Chem. Res.* **10**, 326.
- Gatley, I., T. Hasegawa, H. Suzuki, R. Garden, P. Brand, J. Lightfeet, W. Glencross, H. Okuda, and T. Nagata, 1987, *Astrophys. J., Lett. Ed.* **318**, L73.
- Geballe, T. R., 1997, in *From Stardust to Planetesimals*, edited by Y. Pendleton and A. G. G. M. Tielens (ASP, San Francisco), p. 119.
- Geballe, T. R., A. G. G. M. Tielens, L. J. Allamandola, A. Moorhouse, and P. W. J. L. Brand, 1989, *Astrophys. J.* **341**, 278.
- Genzel, R., 1991, in *The Physics of Star Formation and Early Stellar Evolution*, edited by C. Lada and N. Kylafis (Kluwer, Dordrecht), p. 155.
- Genzel, R., 1992, in *The Galactic Interstellar Medium: Saas Fee Lectures 1991*, edited by W. Burton, R. Genzel, and B. G. Elmegreen (Springer, New York), p. 1.
- Genzel, R., A. I. Harris, D. T. Jaffe, and J. Stutzki, 1988, *Astrophys. J.* **332**, 1049.
- Genzel, R., A. I. Harris, and J. Stutzki, 1989, in *Infrared Spectroscopy in Astronomy, ESA SP-290*, edited by M. Kessler (ESA, Noordwijk), p. 115.
- Genzel, R., D. Hollenbach, and C. H. Townes, 1994, *Rep. Prog. Phys.* **57**, 417.
- Genzel, R., D. Lutz, E. Sturm, E. Egami, D. Kunze, A. Moorwood, D. Rigopoulou, H. Spoon, A. Sternberg, L. Tacconi-Garman, L. Tacconi, and N. Thatte, 1998, *Astrophys. J.* **498**, 579.
- Genzel, R., G. J. Stacey, A. I. Harris, C. H. Townes, N. Geis, U. U. Graf, A. Poglitsch, and J. Stutzki, 1990, *Astrophys. J.* **356**, 160.
- Genzel, R., D. M. Watson, M. K. Crawford, and C. H. Townes, 1985, *Astrophys. J.* **297**, 766.
- Genzel, R., D. M. Watson, C. H. Townes, H. L. Dinerstein, D. J. Hollenbach, D. F. Lester, M. Werner, and J. W. V. Storey, 1984, *Astrophys. J.* **276**, 551.
- Genzel, R., L. Weitzel, L. E. Tacconi-Garman, M. Blaetz, M. Cameron, A. Krabbe, D. Lutz, and A. Sternberg, 1995, *Astrophys. J.* **444**, 129.
- Gerola, H., and A. E. Glassgold, 1978, *Astrophys. J., Suppl.* **37**, 1.
- Gierens, K., J. Stutzki, and G. Winnewisser, 1992, *Astron. Astrophys.* **259**, 271.
- Glassgold, A., 1996, *Annu. Rev. Astron. Astrophys.* **34**, 241.
- Glassgold, A., P. J. Huggins, and W. D. Langer, 1985, *Astrophys. J.* **290**, 615.
- Glassgold, A. E., and W. D. Langer, 1974, *Astrophys. J.* **193**, 73.
- Glassgold, A. E., and W. D. Langer, 1975, *Astrophys. J.* **197**, 347.
- Glassgold, A. E., and W. D. Langer, 1976, *Astrophys. J.* **206**, 85.
- Goldader, J. D., R. D. Joseph, R. Doyon, and D. B. Sanders, 1995, *Astrophys. J.* **444**, 97.
- Goldader, J. D., R. D. Joseph, R. Doyon, and D. B. Sanders, 1997, *Astrophys. J.* **474**, 104.
- Goldshmidt, O., and A. Sternberg, 1995, *Astrophys. J.* **439**, 256.
- Graf, P., T. Herter, G. E. Gull, and J. R. Houck, 1988, *Astrophys. J.* **330**, 803.
- Graf, U. U., A. Eckart, R. Genzel, A. I. Harris, A. Poglitsch, A. P. G. Russell, and J. Stutzki, 1993, *Astrophys. J.* **405**, 249.
- Graham, J. R., E. Serabyn, T. M. Herbst, K. Matthews, G. Neugebauer, B. T. Soifer, T. D. Wilson, and S. Beckwith, 1993, *Astrophys. J.* **105**, 250.
- Gredel, R., and A. Dalgarno, 1995, *Astrophys. J.* **446**, 852.
- Gredel, R., E. F. van Dishoeck, and J. H. Black, 1993, *Astron. Astrophys.* **269**, 477.
- Gredel, R., E. F. van Dishoeck, and J. H. Black, 1994, *Astron. Astrophys.* **285**, 300.
- Green, D. A., and R. Padman, 1993, *Mon. Not. R. Astron. Soc.* **263**, 535.
- Greenhill, L. J., D. R. Jiang, J. M. Moran, M. J. Reid, K. Y. Lo, and M. J. Claussen, 1995, *Astrophys. J.* **440**, 619.
- Greenhouse, M. A., S. Satyapal, C. E. Woodward, J. Fischer, K. L. Thompson, W. J. Forrest, J. L. Pipher, N. Raines, H. A. Smith, D. M. Watson, and R. J. Rudy, 1997, *Astrophys. J.* **476**, 105.
- Gry, C., J. Lequeux, and F. Boulanger, 1992, *Astron. Astrophys.* **266**, 457.
- Guilloteau, S., M. T. Stier, and D. Downes, 1983, *Astron. Astrophys.* **126**, 10.
- Gussie, G. T., A. R. Taylor, P. E. Dewdney, and R. S. Roger, 1995, *Mon. Not. R. Astron. Soc.* **273**, 790.
- Güsten, R., and D. Fiebig, 1988, *Astron. Astrophys.* **204**, 253.
- Habing, H. J., 1968, *Bull. Astron. Inst. Netherlands* **19**, 421.
- Hansen, M. M., I. D. Howarth, and P. S. Conti, 1997, *Astrophys. J.* **489**, 698.
- Harris, A. I., D. T. Jaffe, M. Silber, and R. Genzel, 1985, *Astrophys. J., Lett. Ed.* **294**, L93.
- Harris, A. I., R. E. Hills, J. Stutzki, U. U. Graf, A. P. G. Russell, and R. Genzel, 1991, *Astrophys. J. Lett.* **382**, L75.
- Harrison, A., P. Puxley, A. Russell, and P. Brand, 1995, *Mon. Not. R. Astron. Soc.* **277**, 413.
- Hartquist, T. W., K. M. Menten, S. Lepp, and A. Dalgarno, 1995, *Mon. Not. R. Astron. Soc.* **272**, 184.
- Hartquist, T., and A. Sternberg, 1991, *Mon. Not. R. Astron. Soc.* **248**, 48.
- Hasegawa, T., I. Gatley, R. P. Garden, P. W. J. L. Brand, M. Ohishi, M. Hayashi, and N. Kaifu, 1987, *Astrophys. J., Lett. Ed.* **318**, L77.
- Hayashi, M., T. Hasegawa, I. Gatley, R. Garden, and N. Kaifu, 1985, *Mon. Not. R. Astron. Soc.* **215**, 31P.
- Heck, E. L., D. R. Flower, J. LeBourlot, G. Pineau des Forets, and E. Roueff, 1992, *Mon. Not. R. Astron. Soc.* **258**, 377.
- Heck, E. L., D. R. Flower, J. LeBourlot, G. Pineau des Forets, E. Roueff, 1993, *Mon. Not. R. Astron. Soc.* **262**, 795.
- Hegmann, M., and W. H. Kegel, 1996, *Mon. Not. R. Astron. Soc.* **283**, 167.
- Heiles, C., 1994, *Astrophys. J.* **436**, 720.
- Heiles, C., 1997, *Astrophys. J.* **481**, 193.
- Helou, G., et al., 1996, *Astron. Astrophys.* **315**, L157.
- Herbst, E., 1987, in *Interstellar Processes*, edited by D. J. Hollenbach and H. Thronson (Reidel, Dordrecht), p. 611.
- Herbst, E., and S. Knudson, 1981, *Astrophys. J.* **245**, 529.

- Herbst, E., and C. M. Leung, 1989, *Astrophys. J.*, Suppl. Ser. **69**, 271.
- Herrmann, F., S. C. Madden, T. Nikola, A. Poglitsch, R. Timmermann, N. Geis, C. H. Townes, and G. J. Stacey, 1997, *Astrophys. J.* **481**, 343.
- Herter, T., G. E. Gull, S. T. Megeath, N. Rowlands, and J. R. Houck, 1989, *Astrophys. J.* **342**, 696.
- Herter, T., J. R. Houck, P. Graf, and G. E. Gull, 1986, *Astrophys. J. Lett.* **309**, L13.
- Heyer, M. H., et al., 1996, *Astrophys. J. Lett.* **464**, L175.
- Hill, J. K., and D. J. Hollenbach, 1978, *Astrophys. J.* **225**, 390.
- Hillenbrand, L., 1997, *Astrophys. J.* **113**, 1733.
- Hippelein, H., and G. Münch, 1978, *Astron. Astrophys.* **68**, L7.
- Hippelein, H. H., and G. Münch, 1989, *Astron. Astrophys.* **213**, 323.
- Hobson, M. P., T. Jenness, R. Padman, and P. F. Scott, 1994, *Mon. Not. R. Astron. Soc.* **266**, 972.
- Hobson, M. P., and P. A. G. Scheuer, 1993, *Mon. Not. R. Astron. Soc.* **264**, 145.
- Hogerheijde, M. R., D. J. Jansen, and E. F. van Dishoeck, 1995, *Astron. Astrophys.* **294**, 792.
- Hollenbach, D. J., 1988, *Astrophys. Lett. Commun.* **26**, 191.
- Hollenbach, D. J., 1990, in *The Evolution of the Interstellar Medium*, edited by L. Blitz (ASP, San Francisco), p. 167.
- Hollenbach, D. J., and C. F. McKee, 1979, *Astrophys. J.*, Suppl. **41**, 555.
- Hollenbach, D. J., and C. F. McKee, 1989, *Astrophys. J.* **342**, 306.
- Hollenbach, D. J., and A. Natta, 1995, *Astrophys. J.* **455**, 133.
- Hollenbach, D. J., and E. E. Salpeter, 1970, *J. Chem. Phys.* **53**, 79.
- Hollenbach, D. J., and E. E. Salpeter, 1971, *Astrophys. J.* **163**, 155.
- Hollenbach, D. J., T. Takahashi, and A. G. G. M. Tielens, 1991, *Astrophys. J.* **377**, 192.
- Hollenbach, D. J., and A. G. G. M. Tielens, 1996, in *The Physics and Chemistry of Interstellar Clouds*, edited by G. Winnewisser and G. C. Pelz (Springer, Berlin), p. 164.
- Hollenbach, D. J., and A. G. G. M. Tielens, 1997, *Annu. Rev. Astron. Astrophys.* **35**, 179.
- Hollenbach, D. J., M. Werner, and E. E. Salpeter, 1971, *Astrophys. J.* **163**, 165.
- Honma, M., Y. Sofue, and N. Arimoto, 1995, *Astron. Astrophys.* **304**, 1.
- Howe, J. E., D. T. Jaffe, R. Genzel, and G. Stacey, 1991, *Astrophys. J.* **373**, 158.
- Howe, J. E., D. T. Jaffe, E. N. Grossman, W. F. Wall, J. G. Mangum, and G. J. Stacey, 1993, *Astrophys. J.* **410**, 179.
- Huggins, P. J., 1992, in *Mass Loss on the AGB and Beyond*, edited by H. Schwarz (ESO, Noordwijk), p. 35.
- Huggins, P. J., 1993, in *Planetary Nebulae, IAU 155*, edited by R. Weinberger and A. Acker (Kluwer, Dordrecht), p. 147.
- Huggins, P. J., R. Bachiller, P. Cox, and T. Forveille, 1992, *Astrophys. J. Lett.* **401**, L43.
- Hunter, D. A., and W. D. Watson, 1978, *Astrophys. J.* **226**, 477.
- Ingalls, J. G., R. A. Chamberlin, T. M. Bania, J. M. Jackson, A. P. Lane, and A. A. Stark, 1997, *Astrophys. J.* **479**, 296.
- Israel, F. P., 1997, *Astron. Astrophys.* **328**, 471.
- Israel, F. P., P. R. Maloney, N. Geis, F. Herrmann, S. C. Madden, A. Poglitsch, and G. J. Stacey, 1996, *Astrophys. J.* **465**, 738.
- Israel, F. P., and J. Koornneef, 1991, *Astron. Astrophys.* **250**, 475.
- Israel, F. P., G. J. White, and F. Baas, 1995, *Astron. Astrophys.* **302**, 343.
- Jackson, J. M., N. Geis, R. Genzel, A. I. Harris, S. Madden, A. Poglitsch, G. J. Stacey, and C. H. Townes, 1993, *Astrophys. J.* **402**, 173.
- Jaffe, D. T., R. Genzel, A. I. Harris, J. Howe, G. J. Stacey, and J. Stutzki, 1990, *Astrophys. J.* **353**, 193.
- Jaffe, D. T., and J. E. Howe, 1989, *Rev. Mex. Astron. Astrofis.* **18**, 55.
- Jaffe, D. T., and V. Pankonin, 1978, *Astrophys. J.* **226**, 869.
- Jaffe, D. T., S. Zhou, J. E. Howe, F. Herrmann, S. C. Madden, A. Poglitsch, P. P. Van der Werf, and G. J. Stacey, 1994, *Astrophys. J.* **436**, 203.
- Jansen, D. J., M. Spaans, M. R. Hogerheijde, and E. F. van Dishoeck, 1995a, *Astron. Astrophys.* **303**, 541.
- Jansen, D. J., E. F. van Dishoeck, J. H. Black, M. Spaans, and C. Sosin, 1995b, *Astron. Astrophys.* **302**, 223.
- Jansen, D. J., E. F. van Dishoeck, J. Keene, R. T. Boreiko, and A. Betz, 1996, *Astron. Astrophys.* **309**, 899.
- Jenkins, E. B., M. Jura, and M. Loewenstein, 1983, *Astrophys. J.* **270**, 88.
- Jenkins, E. B., and D. A. Meloy, 1974, *Astrophys. J. Lett. Ed.* **193**, L121.
- Joblin, C., A. G. G. M. Tielens, L. J. Allamandola, and T. R. Geballe, 1996, *Astrophys. J.* **458**, 610.
- Johnstone, D., D. Hollenbach, and J. Bally, 1998, *Astrophys. J.* **499**, 758.
- Joncas, G., D. Durand, and R. S. Roger, 1992, *Astrophys. J.* **387**, 591.
- Jones, M. E., S. E. Barlow, G. B. Ellison, and E. E. Ferguson, 1986, *Chem. Phys. Lett.* **130**, 218.
- Jourdain de Muizon, M., L. B. d'Hendecourt, and T. R. Geballe, 1990, *Astron. Astrophys.* **235**, 367.
- Jura, M., 1974, *Astrophys. J.* **191**, 375.
- Jura, M., 1975, *Astrophys. J.* **197**, 575.
- Jura, M., 1976, *Astrophys. J.* **204**, 12.
- Justtanont, K., A. G. G. M. Tielens, C. J. Skinner, and M. Haas, 1997, *Astrophys. J.* **476**, 319.
- Kastner, J. H., D. A. Weintraub, I. Gatley, K. M. Merrill, and R. G. Probst, 1996, *Astrophys. J.* **462**, 777.
- Kawara, K., M. Nishida, and B. Gregory, 1990, *Astrophys. J.* **352**, 433.
- Kawara, K., M. Nishida, and Y. Taniguchi, 1988, *Astrophys. J. Lett.* **328**, L41.
- Keene, J., G. A. Blake, T. G. Phillips, P. J. Huggins, and C. A. Beichman, 1985, *Astrophys. J.* **299**, 967.
- Keene, J., D. C. Lis, T. G. Phillips, and P. Schilke, 1997, in *Molecules in Astrophysics: Probes and Processes*, edited by E. van Dishoeck (Kluwer, Dordrecht), p. 129.
- Keene, J., P. Schilke, J. Kooi, D. C. Lis, D. M. Mehringer, and T. G. Phillips, 1998, *Astrophys. J. Lett.* **494**, L107.
- Knapp, G. R., R. L. Brown, T. B. H. Kuiper, and R. K. Kakar, 1976a, *Astrophys. J.* **204**, 781.
- Knapp, G. R., T. B. H. Kuiper, and R. L. Brown, 1976b, *Astrophys. J.* **206**, 109.
- Köster, B., H. Störzer, J. Stutzki, and A. Sternberg, 1994, *Astron. Astrophys.* **284**, 545.
- Kramer, C., J. Stutzki, and G. Winnewisser, 1996, *Astron. Astrophys.* **307**, 915.
- Krolik, J. H., and T. R. Kallman, 1983, *Astrophys. J.* **267**, 610.
- Krolik, J. H., and S. Lepp, 1989, *Astrophys. J.* **347**, 179.

- Kulkarni, S. R., and C. Heiles, 1987, in *Interstellar Processes*, edited by D. J. Hollenbach and H. A. Thronson (Reidel, Dordrecht), p. 87.
- Kunze, D., et al., 1996, *Astron. Astrophys.* **315**, L101.
- Kwok, S., R. Purton, and P. M. Fitzgerald, 1978, *Astrophys. J. Lett. Ed.* **219**, L125.
- Lada, C., 1976, *Astrophys. J., Suppl.* **32**, 603.
- Lambert, D. L., Y. Sheffer, R. L. Gilliland, and S. R. Federman, 1990, *Astrophys. J.* **420**, 756.
- Langer, W. D., 1976, *Astrophys. J.* **206**, 699.
- Langer, W. D., 1978, *Astrophys. J.* **225**, 860.
- Laques, P., and J. L. Vidal, 1979, *Astron. Astrophys.* **73**, 97.
- Latter, W. B., D. M. Kelly, J. L. Hora, and L. K. Deutsch, 1995, *Astrophys. J., Suppl. Ser.* **100**, 159.
- Latter, W. B., C. K. Walker, and P. R. Maloney, 1993, *Astrophys. J. Lett.* **419**, L97.
- Latter, W. B., A. G. G. M. Tielens, and D. J. Hollenbach, 1998, in preparation.
- Leach, S., 1987, in *Polycyclic Aromatic Hydrocarbons and Astrophysics*, edited by A. Léger, L. d'Hendecourt, and N. Bocca (Reidel, Dordrecht), p. 99.
- Le Bourlot, J., G. Pineau des Forêts, E. Roueff, A. Dalgarno, and R. Gredel, 1995, *Astrophys. J.* **449**, 178.
- Le Bourlot, J., G. Pineau des Forêts, E. Roueff, and D. R. Flower, 1993, *Astron. Astrophys.* **267**, 233.
- Lee, H-H., E. Herbst, G. Pineau des Forêts, E. Roueff, and J. Le Bourlot, 1996, *Astron. Astrophys.* **311**, 690.
- Lee, K. T., J. M. Bowman, A. F. Wagner, and G. C. Schatz, 1982, *J. Chem. Phys.* **76**, 3583.
- Leen, T. M., and M. M. Graff, 1988, *Astrophys. J.* **325**, 411.
- Léger, A., and J. L. Puget, 1984, *Astron. Astrophys.* **137**, L5.
- Leisawitz, D., 1990, *Astrophys. J.* **359**, 319.
- Leisawitz, D., and M. G. Hauser, 1988, *Astrophys. J.* **332**, 954.
- Lemaire, J. L., D. Field, M. Gerin, S. Leach, G. Pineau des Forêts, F. Rostas, and D. Rouan, 1996, *Astron. Astrophys.* **308**, 895.
- Lepp, S., and A. Dalgarno, 1988, *Astrophys. J.* **335**, 769.
- Lepp, S., and A. Dalgarno, 1996, *Astron. Astrophys.* **306**, L21.
- Lepp, S., A. Dalgarno, E. F. van Dishoeck, and J. H. Black, 1988, *Astrophys. J.* **329**, 418.
- Lepp, S., and R. McCray, 1983, *Astrophys. J.* **269**, 560.
- Light, G. C., 1978, *J. Chem. Phys.* **68**, 2831.
- Lin, J., and G. Vidali, 1996, in *The Cosmic Dust Connection*, edited by J. M. Greenberg (Kluwer, Dordrecht), p. 323.
- Lis, D. C., P. Schilke, and J. Keene, 1997, in *CO: 25 Years of Millimeter Wave Spectroscopy*, edited by W. B. Latter, S. J. E. Radford, P. R. Jewell, J. G. Mangum, and J. Bally (Kluwer, Dordrecht), p. 128.
- Lockman, F. J., L. M. Hobbs, and J. M. Shull, 1986, *Astrophys. J.* **301**, 380.
- London, R., 1978, *Astrophys. J.* **225**, 405.
- Lord, S. D., D. J. Hollenbach, M. R. Haas, R. H. Rubin, S. W. J. Colgan, and E. F. Erickson, 1996, *Astrophys. J.* **465**, 703.
- Lugten, J. B., R. Genzel, M. K. Crawford, and C. H. Townes, 1986, *Astrophys. J.* **306**, 691.
- Luhman, M. L., and D. T. Jaffe, 1996, *Astrophys. J.* **463**, 191.
- Luhman, M. L., D. T. Jaffe, L. D. Keller, and S. Pak, 1994, *Astrophys. J. Lett.* **436**, L185.
- Luhman, M. L., D. T. Jaffe, A. Sternberg, F. Herrmann, and A. Poglitsch, 1997, *Astrophys. J. Lett.* **482**, 298.
- Luhman, M. L., K. L. Luhman, T. Benedict, D. T. Jaffe, and J. Fischer, 1997, *Astrophys. J. Lett.* **480**, L133.
- Madden, S. C., N. Geis, R. Genzel, F. Herrmann, J. Jackson, A. Poglitsch, G. J. Stacey, and C. H. Townes, 1993, *Astrophys. J.* **407**, 579.
- Madden, S. C., A. Poglitsch, N. Geis, G. J. Stacey, and C. H. Townes, 1997, *Astrophys. J.* **483**, 200.
- Malhotra, S., et al., 1997, *Astrophys. J.* **491**, L27.
- Maloney, P., 1997a, in *Proceedings of the Ringberg Workshop on NGC 1068*, edited by L. Tacconi and J. Gallimore, *Astrophys. Space Sci.* **248**, 105.
- Maloney, P., 1997b, in *Accretion Phenomena and Related Outflows*, edited by D. Wickramasinghe, L. Ferrario, and G. Bicknell (ASP, San Francisco), p. 113.
- Maloney, P., D. J. Hollenbach, and A. G. G. M. Tielens, 1996, *Astrophys. J.* **466**, 561.
- Maoz, E., 1998, *Astrophys. J. Lett.* **494**, L181.
- Marconi, A., L. Testi, A. Natta, and C. M. Walmsley, 1998, *Astron. Astrophys.* **330**, 696.
- Martin, P. G., and M. E. Mandy, 1995, *Astrophys. J.* **455**, L89.
- Martin, P. G., D. H. Schwarz, and M. E. Mandy, 1996, *Astrophys. J.* **461**, 265.
- Martini, P., K. Sellgren, and J. L. Hora, 1997, *Astrophys. J.* **484**, 296.
- Massi, M., E. Churchwell, and M. Felli, 1988, *Astron. Astrophys.* **194**, 116.
- Matilla, K., D. Lemke, L. K. Haikala, R. J. Laureijs, A. Léger, K. Lehtinen, Ch. Leinert, and P. G. Mezger, 1996, *Astron. Astrophys.* **315**, L353.
- Mathis, J. S., 1990, *Annu. Rev. Astron. Astrophys.* **28**, 37.
- Mathis, J. S., 1997, in *From Stardust to Planetesimals*, edited by Y. Pendleton and A. G. G. M. Tielens. (ASP, San Francisco), p. 87.
- Mathis, J. S., W. Rumpl, and K. H. Nordsieck, 1977, *Astrophys. J.* **217**, 425.
- Matsuura, H., T. Nakagawa, H. Shibai, H. Okuda, K. Mizutani, T. Maihara, Y. Kobayashi, N. Hiromoto, T. Nishimura, and F. J. Low, 1989, *Astrophys. J.* **339**, L69.
- McCaughrean, M. J., and J. R. Stauffer, 1994, *Astrophys. J.* **111**, 1977.
- McCray, R., and T. P. Snow, 1979, *Annu. Rev. Astron. Astrophys.* **17**, 213.
- McCullough, P. R., R. Q. Fugate, J. C. Christou, B. L. Ellerbroek, C. H. Higgins, J. M. Spinharne, R. A. Cleis, and J. F. Moroney, 1995, *Astrophys. J.* **438**, 394.
- McKee, C. F., 1989, *Astrophys. J.* **345**, 782.
- McKee, C. F., and J. P. Ostriker, 1977, *Astrophys. J.* **218**, 148.
- McKee, C. F., J. W. V. Storey, D. M. Watson, and S. Green, 1982, *Astrophys. J.* **259**, 647.
- Meixner, M., M. R. Haas, A. G. G. M. Tielens, E. F. Erickson, and M. Werner, 1992, *Astrophys. J.* **390**, 499.
- Meixner, M., and A. G. G. M. Tielens, 1993, *Astrophys. J.* **405**, 216.
- Meixner, M., and A. G. G. M. Tielens, 1995, *Astrophys. J.* **446**, 907.
- Melnick, G., G. E. Gull, and M. Harwit, 1979, *Astrophys. J.* **227**, L29.
- Menten, K. M., K. J. Johnston, E. J. Wadiak, C. M. Walmsley, and T. L. Wilson, 1988, *Astrophys. J. Lett.* **331**, L41.
- Menten, K. M., M. J. Reid, P. Pratap, J. M. Moran, and T. L. Wilson, 1992, *Astrophys. J.* **401**, L39.
- Meyer, D. M., and J. C. Blades, 1996, *Astrophys. J.* **464**, L179.
- Meyer, D. M., and K. C. Roth, 1991, *Astrophys. J.* **376**, L49.
- Millar, T. J., and E. Herbst, 1990, *Astron. Astrophys.* **231**, 466.

- Minchin, N. R., and G. J. White, 1995, *Astron. Astrophys.* **302**, L25.
- Minchin, N. R., G. J. White, and D. Ward-Thompson, 1995, *Astron. Astrophys.* **301**, 894.
- Minchin, N. R., G. J. White, and R. Padman, 1993, *Astron. Astrophys.* **277**, 595.
- Mirabel, I. F., L. F. Rodriguez, B. Cordier, J. Paul, and F. Lebrun, 1992, *Nature (London)* **358**, 215.
- Mochizuki, K., T. Nakagawa, Y. Doi, Y. Y. Yui, H. Okuda, H. Shibai, M. Yui, T. Nishimura, and F. J. Low, 1994, *Astrophys. J.* **430**, L37.
- Monteiro, T., 1991, *Astron. Astrophys.* **241**, L5.
- Moorwood, A. F. M., and E. Oliva, 1988, *Astron. Astrophys.* **203**, 278.
- Moorwood, A. F. M., and E. Oliva, 1990, *Astron. Astrophys.* **239**, 78.
- Moorwood, A. F. M., and E. Oliva, 1994, *Astrophys. J.* **429**, 602.
- Moran, J. M., B. F. Burke, A. H. Barrett, A. E. Rogers, J. C. Carter, and D. D. Cubaback, 1968, *Astrophys. J. Lett.* **152**, L97.
- Moriarty-Schieven, G. H., T. Xie, and N. A. Patel, 1996, *Astrophys. J. Lett.* **463**, L105.
- Moriarty-Schieven, G. H., B-G. Anderson, and P. G. Wannier, 1997, *Astrophys. J.* **475**, 642.
- Morris, M., and E. Serabyn, 1996, *Annu. Rev. Astron. Astrophys.* **34**, 645.
- Mouri, H., 1994, *Astrophys. J.* **427**, 777.
- Mouri, H., K. Kawara, and Y. Taniguchi, 1993, *Astrophys. J.* **406**, 52.
- Mouri, H., K. Kawara, Y. Taniguchi, and M. Nishida, 1990a, *Astrophys. J. Lett.* **356**, L39.
- Mouri, H., M. Nishida, Y. Taniguchi, and K. Kawara, 1990b, *Astrophys. J.* **360**, 55.
- Mouri, H., and Y. Taniguchi, 1992, *Astrophys. J.* **386**, 68.
- Münch, G., and H. Hippelein, 1982, *Ann. (N.Y.) Acad. Sci.* **395**, 170.
- Murthy, J., A. Dring, R. C. Henry, J. W. Kruk, W. P. Blair, R. A. Kimble, and S. T. Durrance, 1993, *Astrophys. J.* **408**, L97.
- Nakagawa, T., Y. Doi, Y. Y. Yui, H. Okuda, K. Mochizuki, H. Shibai, T. Nishimura, and F. J. Low, 1995, *Astrophys. J.* **455**, L35.
- Nakagawa, T., Y. Y. Yui, Y. Doi, H. Okuda, H. Shibai, K. Mochizuki, T. Nishimura, and F. Low, 1998, *Astrophys. J., Suppl. Ser.* **115**, 259.
- Natta, A., C. M. Walmsley, and A. G. G. M. Tielens, 1994, *Astrophys. J.* **428**, 209.
- Natta, A., and D. J. Hollenbach, 1998, *Astron. Astrophys.* **337**, 517.
- Nelson, R. P., and W. D. Langer, 1997, *Astrophys. J.* **482**, 796.
- Neufeld, D., and P. R. Maloney, 1995, *Astrophys. J.* **447**, L17.
- Neufeld, D. A., P. R. Maloney, and S. Conger, 1994, *Astrophys. J.* **436**, L127.
- Neufeld, D., and M. Spaans, 1996, *Astrophys. J.* **473**, 894.
- Norman, C. A., and M. Spaans, 1997, *Astrophys. J.* **480**, 145.
- O'Dell, C. R., and K. D. Handron, 1996, *Astrophys. J.* **111**, 1630.
- O'Dell, C. R., and Z. Wen, 1994, *Astrophys. J.* **436**, 194.
- O'Dell, C. R., Z. Wen, and X. Hu, 1993, *Astrophys. J.* **410**, 696.
- O'Dell, C. R., and K. Wong, 1996, *Astrophys. J.* **111**, 846.
- Okuda, H., 1991, *Infrared Phys.* **32**, 365.
- Onaka, T., et al., 1996, *Publ. Astron. Soc. Jpn.* **48**, L59.
- Pak, S., D. T. Jaffe, and L. D. Keller, 1996, *Astrophys. J. Lett.* **457**, L43.
- Pak, S., D. T. Jaffe, E. F. van Dishoeck, L. E. B. Johansson, and R. S. Booth, 1998, *Astrophys. J.* **498**, 735.
- Palumbo, M. E., T. R. Geballe, and A. G. G. M. Tielens, 1997, *Astrophys. J.* **479**, 839.
- Pankonin, V., P. Thomasson, and J. Barsuhn, 1977, *Astron. Astrophys.* **54**, 335.
- Pankonin, V., and C. M. Walmsley, 1978, *Astron. Astrophys.* **67**, 129.
- Parmar, P. S., J. H. Lacy, and J. M. Achtermann, 1991, *Astrophys. J.* **372**, L25.
- Parravano, A., 1987, in *Supernova Remnants and the ISM, IAU 101*, edited by R. S. Roger and T. L. Landecker (Cambridge University Press, Cambridge, England), p. 513.
- Parravano, A., 1988, *Astron. Astrophys.* **205**, 71.
- Parravano, A., 1989, *Astrophys. J.* **347**, 812.
- Parravano, A., 1996, *Astrophys. J.* **462**, 594.
- Parravano, A., P. Rosenzweig, and M. Teran, 1990, *Astrophys. J.* **356**, 100.
- Parravano, A., and Ch. J. Mantilla, 1991, *Astron. Astrophys.* **250**, 70.
- Phillips, J. A., T. Lazio, and W. Joseph, 1995, *Astrophys. J. Lett.* **442**, L37.
- Phillips, T. G., and P. J. Huggins, 1981, *Astrophys. J.* **251**, 533.
- Pineau des Forets, G., E. Roueff, and D. R. Flower, 1990, *Mon. Not. R. Astron. Soc.* **244**, 668.
- Pirronello, V., O. Biham, C. Liu, L. Shen, and G. Vidali, 1997a, *Astrophys. J. Lett.* **483**, L131.
- Pirronello, V., C. Liu, L. Shen, and G. Vidali, 1997b, *Astrophys. J.* **475**, L69.
- Plume, R., D. T. Jaffe, and J. Keene, 1994, *Astrophys. J.* **425**, L49.
- Poglitsch, A., G. J. Stacey, N. Geis, M. Haggerty, J. Jackson, M. Rumitz, A. Genzel, and C. H. Townes, 1991, *Astrophys. J. Lett.* **374**, L33.
- Poglitsch, A., A. Krabbe, S. C. Madden, T. Nikola, N. Geis, L. E. B. Johansson, G. J. Stacey, and A. Sternberg, 1995, *Astrophys. J.* **454**, 293.
- Pottasch, S. R., 1980, *Astron. Astrophys.* **89**, 336.
- Pottasch, S. R., P. R. Wesselius, and R. J. van Duinen, 1979, *Astron. Astrophys.* **74**, L15.
- Prasad, S. S., K. R. Heere, and S. P. Tarafdar, 1991, *Astrophys. J.* **373**, 123.
- Prasad, S. S., and W. T. Huntress, 1980, *Astrophys. J., Suppl. Ser.* **43**, 1.
- Prasad, S. S., and W. T. Huntress, 1982, *Astrophys. J.* **260**, 590.
- Puxley, P. J., T. G. Hawarden, and C. M. Mountain, 1990, *Astrophys. J.* **364**, 77.
- Reid, M. J., A. D. Haschik, B. F. Burke, J. M. Moran, K. J. Johnston, and G. W. Swenson, 1980, *Astrophys. J.* **239**, 89.
- Reynolds, R. J., 1993, *Astrophys. J.* **392**, L35.
- Rigopoulou, D., et al., 1996, *Astron. Astrophys.* **315**, L125.
- Roberge, W. G., A. Dalgarno, and B. P. Flannery, 1981, *Astrophys. J.* **243**, 817.
- Roberge, W. G., D. Jones, S. Lepp, and A. Dalgarno, 1991, *Astrophys. J., Suppl. Ser.* **77**, 287.
- Roche, P. F., D. K. Aitken, and C. H. Smith, 1991, *Mon. Not. R. Astron. Soc.* **252**, 282.
- Rodriguez, L. F., I. F. Mirabel, and J. Marti, 1992, *Astrophys. J. Lett.* **401**, L15.
- Roelfsema, P. R., et al., 1996, *Astron. Astrophys.* **315**, L289.

- Roger, R. S., 1982, in *Regions of Recent Star Formation*, edited by R. S. Roger and P. E. Dewdney (Reidel, Dordrecht), p. 167.
- Roger, R. S., and P. E. Dewdney, 1992, *Astrophys. J.* **385**, 536.
- Roger, R. S., and J. A. Irwin, 1982, *Astrophys. J.* **256**, 127.
- Roger, R. S., and D. A. Leahy, 1993, *Astrophys. J.* **106**, 31.
- Roger, R. S., and A. Pedlar, 1981, *Astron. Astrophys.* **94**, 238.
- Rotaciuc, V., A. Krabbe, M. Cameron, S. Drapatz, R. Genzel, A. Sternberg, and J. W. V. Storey, 1991, *Astrophys. J.* **370**, L23.
- Rubio, M., J. Lequeux, and F. Boulanger, 1993a, *Astron. Astrophys.* **271**, 9.
- Rubio, M., J. Lequeux, F. Boulanger, R. S. Booth, G. Garay, T. de Graauw, F. P. Israel, L. E. B. Johansson, M. L. Kufner, and L. A. Numan, 1993b, *Astron. Astrophys.* **271**, 1.
- Russell, R. W., G. Melnick, G. E. Gull, and M. Harwit, 1980, *Astrophys. J., Lett. Ed.* **240**, L99.
- Russell, R. W., G. Melnick, S. D. Smeyers, N. T. Kurtz, T. R. Gosnell, M. Harwit, and M. W. Werner, 1981, *Astrophys. J., Lett. Ed.* **250**, L35.
- Savage, B. D., and J. S. Mathis, 1979, *Annu. Rev. Astron. Astrophys.* **17**, 73.
- Schatz, G. C., 1981, *J. Chem. Phys.* **74**, 1133.
- Schatz, G. C., A. F. Wagner, S. P. Walch, and J. M. Bowman, 1981, *J. Chem. Phys.* **74**, 4984.
- Schatz, G. C., and H. Elgersma, 1980, *Chem. Phys. Lett.* **73**, 21.
- Schilke, P., J. E. Carlstrom, J. Keene, and T. G. Phillips, 1993, *Astrophys. J.* **417**, L67.
- Schinke, R., V. Engel, U. Buck, H. Meyer, and G. H. F. Diercksen, 1985, *Astrophys. J.* **299**, 939.
- Schinke, R., and W. A. Lester, 1979, *J. Chem. Phys.* **72**, 3754.
- Sellgren, K., 1984, *Astrophys. J.* **277**, 623.
- Sellgren, K., L. J. Allamandola, J. D. Bregman, M. W. Werner, and D. H. Wooden, 1985, *Astrophys. J.* **299**, 416.
- Serabyn, E., J. Keene, D. C. Lis, and T. G. Phillips, 1994, *Astrophys. J., Lett.* **424**, L95.
- Shaya, E. J., and S. R. Federman, 1986, *Astrophys. J.* **319**, 76.
- Shematovich, V. I., B. M. Shustov, and D. S. Wiebe, 1997, *Mon. Not. R. Astron. Soc.* **292**, 601.
- Shibai, H., H. Okuda, T. Nakagawa, T. Maihara, K. Mizutani, H. Matsuhara, Y. Kobayashi, N. Hiromoto, F. J. Low, and T. Nishimura, 1993, *Adv. Space Res.* **13**, 201.
- Shibai, H., H. Okuda, T. Nakagawa, H. Matsuhara, T. Maihara, K. Mizutani, Y. Kobayashi, N. Hiromoto, T. Nishimura, and F. J. Low, 1991, *Astrophys. J.* **374**, 522.
- Shu, F. H., F. C. Adams, and S. Lizano, 1987, *Annu. Rev. Astron. Astrophys.* **25**, 23.
- Shull, J. M., 1978, *Astrophys. J.* **219**, 877.
- Simon, R., J. Stutzki, A. Sternberg, and G. Winnewisser, 1997, *Astron. Astrophys.* **327**, L9.
- Simpson, J. P., S. W. J. Colgan, R. H. Rubin, E. F. Erickson, and M. R. Haas, 1994, in *Proceedings of the Airborne Astronomy Symposium*, edited by M. R. Haas, J. A. Davidson, and E. F. Erickson (ASP, San Francisco), p. 53.
- Snow, T. P., 1993, *Astrophys. J., Lett.* **402**, L73.
- Sodroski, T. J., E. Dwek, M. G. Hauser, and F. J. Kerr, 1989, *Astrophys. J.* **336**, 762.
- Sodroski, T. J., *et al.*, 1995, *Astrophys. J.* **452**, 262.
- Sodroski, T. J., N. Odegard, R. G. Arendt, E. Dwek, J. L. Weiland, M. G. Hauser, and T. Kelsall, 1997, *Astrophys. J.* **480**, 173.
- Solomon, P. M., A. R. Rivolo, J. W. Barrett, and A. Yahil, 1987, *Astrophys. J.* **319**, 730.
- Spaans, M., 1995, Ph.D. thesis (University of Leiden).
- Spaans, M., 1996, *Astron. Astrophys.* **307**, 271.
- Spaans, M., J. H. Black, and E. F. van Dishoeck, 1999, *Astrophys. J., in press.*
- Spaans, M., and C. M. Carollo, 1997, *Astrophys. J. Lett.* **482**, L93.
- Spaans, M., and D. A. Neufeld, 1997, *Astrophys. J.* **484**, 785.
- Spaans, M., and C. A. Norman, 1997, *Astrophys. J.* **483**, 87.
- Spaans, M., A. G. G. M. Tielens, E. F. van Dishoeck, and E. L. O. Bakes, 1994, *Astrophys. J.* **437**, 270.
- Spaans, M., and E. F. van Dishoeck, 1997, *Astron. Astrophys.* **323**, 953.
- Spitzer, L., and E. Jenkins, 1975, *Annu. Rev. Astron. Astrophys.* **13**, 133.
- Stacey, G. J., P. J. Viscuso, C. E. Fuller, and N. T. Kurtz, 1985, *Astrophys. J.* **289**, 803.
- Stacey, G. J., N. Geis, R. Genzel, J. B. Lugten, A. Poglitsch, A. Sternberg, and C. H. Townes, 1991, *Astrophys. J.* **373**, 423.
- Stacey, G. J., D. T. Jaffe, N. Geis, R. Genzel, A. I. Harris, A. Poglitsch, J. Stutzki, and C. H. Townes, 1993, *Astrophys. J.* **404**, 219.
- Stark, A. A., 1997, *Astrophys. J.* **481**, 587.
- Stark, A. A., A. D. Bolatto, R. A. Chamberlin, A. P. Lane, T. M. Bania, J. M. Jackson, and K.-Y. Lo, 1997, *Astrophys. J.* **480**, L59.
- Stark, R., and E. F. van Dishoeck, 1994, *Astron. Astrophys.* **286**, L43.
- Stark, R., P. R. Wesselius, E. F. van Dishoeck, and R. J. Laureij, 1996, *Astron. Astrophys.* **311**, 282.
- Stauffer, J. R., C. F. Prosser, L. Hartmann, and M. J. McCaughrean, 1994, *Astrophys. J.* **108**, 1375.
- Stecher, T. P., and D. A. Williams, 1967, *Astrophys. J., Lett.* **149**, L29.
- Steiman-Cameron, T. Y., M. R. Haas, A. G. G. M. Tielens, and M. G. Burton, 1997, *Astrophys. J.* **478**, 261.
- Sternberg, A., 1986, Ph.D. thesis (Columbia University).
- Sternberg, A., 1988, *Astrophys. J.* **322**, 400.
- Sternberg, A., 1989, *Astrophys. J.* **347**, 863.
- Sternberg, A., 1990, *Astrophys. J.* **361**, 121.
- Sternberg, A., 1992, in *Astrochemistry of Cosmic Phenomena*, edited by P. D. Singh (Kluwer, Dordrecht), p. 329.
- Sternberg, A., 1998, in *The Molecular Astrophysics of Stars and Galaxies*, edited by T. Hartquist and D. Williams (Kluwer, Dordrecht), in press.
- Sternberg, A., and A. Dalgarno, 1989, *Astrophys. J.* **338**, 199.
- Sternberg, A., and A. Dalgarno, 1995, *Astrophys. J., Suppl. Ser.* **99**, 565.
- Sternberg, A., M. Yan, and A. Dalgarno, 1998, in *Molecules in Astrophysics: Probes and Processes*, edited by E. F. van Dishoeck (Kluwer, Dordrecht), p. 141.
- Storey, J. W. V., D. M. Watson, and C. H. Townes, 1979, *Astrophys. J.* **233**, 109.
- Störzer, H., and D. J. Hollenbach, 1998, *Astrophys. J.* **495**, 853.
- Störzer, H., J. Stutzki, and A. Sternberg, 1995, *Astron. Astrophys.* **296**, L9.
- Störzer, H., J. Stutzki, and A. Sternberg, 1996, *Astron. Astrophys.* **310**, 592.
- Störzer, H., J. Stutzki, and A. Sternberg, 1997, *Astron. Astrophys.* **323**, L13.
- Sturm, E., *et al.*, 1996, *Astron. Astrophys.* **315**, L133.
- Stutzki, J., *et al.*, 1997, *Astrophys. J., Lett.* **477**, L33.
- Stutzki, J., and R. Güsten, 1990, *Astrophys. J.* **356**, 513.

- Stutzki, J., G. J. Stacey, R. Genzel, U. U. Graf, A. I. Harris, D. T. Jaffe, J. B. Lugten, and A. Poglitsch, 1990, in *Submillimetre Astronomy*, edited by G. D. Watt and A. S. Webster (Kluwer, Dordrecht), p. 269.
- Stutzki, J., G. Stacey, R. Genzel, A. Harris, D. Jaffe, and J. Lugten, 1988, *Astrophys. J.* **332**, 379.
- Sugai, H., M. A. Malkan, M. J. Ward, R. I. Davies, and I. S. McLean, 1997, *Astrophys. J.* **481**, 186.
- Sunyaev, R., et al., 1991, *Astrophys. J.* **383**, L49.
- Tanaka, M., T. Hasegawa, S. S. Hayashi, P. W. J. L. Brand, and I. Gatley, 1989, *Astrophys. J.* **336**, 207.
- Tanaka, M., T. Hasegawa, and I. Gatley, 1991, *Astrophys. J.* **374**, 516.
- Tarafdar, S. P., S. S. Prasad, W. T. Huntress, K. R. Villere, and D. C. Black, 1985, *Astrophys. J.* **289**, 220.
- Tauber, J., and P. Goldsmith, 1990, *Astrophys. J. Lett.* **356**, L63.
- Tauber, J., D. C. Lis, J. Keene, P. Schilke, and T. H. Büttgenbach, 1995, *Astron. Astrophys.* **297**, 567.
- Tauber, J. A., A. G. G. M. Tielens, M. Meixner, and P. F. Goldsmith, 1994, *Astrophys. J.* **422**, 136.
- Tielens, A. G. G. M., 1989, in *Interstellar Dust*, edited by L. J. Allamandola and A. G. G. M. Tielens (Kluwer, Dordrecht), p. 239.
- Tielens, A. G. G. M., 1990a, in *Submillimetre Astronomy*, edited by G. D. Watt and A. S. Webster (Kluwer, Dordrecht), p. 13.
- Tielens, A. G. G. M., 1990b, in *Carbon in the Galaxy*, edited by J. Tarter, S. Chang, and D. DeFrees, NASA-CP 3061, p. 59.
- Tielens, A. G. G. M., 1993a, in *Planetary Nebulae*, edited by R. Weinberger and A. Acker (Kluwer, Dordrecht), p. 155.
- Tielens, A. G. G. M., 1993b, in *Dust and Chemistry in Astronomy*, edited by T. J. Millar and D. A. Williams (IOP, Bristol), p. 103.
- Tielens, A. G. G. M., 1994, in *Airborne Astronomy Symposium on the Galactic Ecosystem*, edited by M. R. Haas, J. A. Davidson, and E. F. Erickson (ASP, San Francisco), p. 3.
- Tielens, A. G. G. M., 1997, in *Diffuse Infrared Radiation and the IRTS*, edited by H. Okuda, T. Matsumoto, and T. L. Roellig (Kluwer, Dordrecht), p. 255.
- Tielens, A. G. G. M., 1998, in *Dust and Molecules in Evolved Stars*, edited by I. Cherchneff and T. J. Millar (Kluwer, Dordrecht), p. 1.
- Tielens, A. G. G. M., and L. Allamandola, 1987, in *Interstellar Processes*, edited by D. J. Hollenbach and H. J. Thronson (Kluwer, Dordrecht), p. 397.
- Tielens, A. G. G. M., and D. J. Hollenbach, 1985a, *Astrophys. J.* **291**, 722.
- Tielens, A. G. G. M., and D. J. Hollenbach, 1985b, *Astrophys. J.* **291**, 747.
- Tielens, A. G. G. M., and D. J. Hollenbach, 1985c, *Icarus* **61**, 40.
- Tielens, A. G. G. M., M. M. Meixner, P. P. van der Werf, J. Bregman, J. A. Tauber, J. Stutzki, and D. Rank, 1993, *Science* **262**, 86.
- Tielens, A. G. G. M., and D. C. B. Whittet, 1997, in *Molecules in Astrophysics: Probes and Processes* edited by E. F. van Dishoeck (Kluwer, Dordrecht), p. 45.
- Tilanus, R. P. J., and R. J. Allen, 1989, *Astrophys. J. Lett.* **339**, L57.
- Timmermann, R., F. Bertoldi, C. M. Wright, S. Drapatz, B. T. Draine, L. Haser, and A. Sternberg, 1996, *Astron. Astrophys.* **315**, L301.
- Timmermann, R., R. Genzel, A. Poglitsch, D. Lutz, S. C. Madden, T. Nicola, N. Geis, and C. H. Townes, 1996, *Astrophys. J.* **466**, 242.
- Tiné, S., S. Lepp, R. Gredel, and A. Dalgarno, 1997, *Astrophys. J.* **481**, 282.
- Turner, B. E., 1996, *Astrophys. J.* **461**, 246.
- Usuda, T., H. Sugai, H. Kawabata, Y. Inoue, H. Kataza, and M. Tanaka, 1996, *Astrophys. J.* **464**, 818.
- Valentijn, E. A., P. P. van der Werf, Th. de Graauw, and T. de Jong, 1996, *Astron. Astrophys.* **315**, L145.
- van der Hucht, K. A., P. M. Williams, and P. S. The, 1987, *Q. J. R. Astron. Soc.* **28**, 254.
- van der Werf, P. P., J. Stutzki, A. Sternberg, and A. Krabbe, 1996, *Astron. Astrophys.* **313**, 633.
- van Dishoeck, E. F., 1987, in *Astrochemistry*, edited by M. S. Vardya and S. P. Tarafdar (Kluwer, Dordrecht), p. 51.
- van Dishoeck, E. F., 1988, in *Rate Coefficients in Astrochemistry*, edited by T. J. Millar and D. A. Williams (Kluwer, Dordrecht), p. 49.
- van Dishoeck, E. F., 1991, in *Astrochemistry of Cosmic Phenomena*, edited by P. D. Singh (Kluwer, Dordrecht), p. 143.
- van Dishoeck, E. F., 1992, in *Infrared Astronomy with ISO*, edited by Th. Encrenaz and M. Kessler (Nova, New York), p. 283.
- van Dishoeck, E. F., 1998, in *The Molecular Astrophysics of Stars and Galaxies*, edited by T. W. Hartquist, D. A. Williams (Oxford University Press, Oxford), in press.
- van Dishoeck, E. F., and J. H. Black, 1986, *Astrophys. J., Suppl. Ser.* **62**, 109.
- van Dishoeck, E. F., and J. H. Black, 1988, *Astrophys. J.* **334**, 711.
- van Dishoeck, E. F., and J. H. Black, 1989, *Astrophys. J.* **340**, 273.
- Vanzi, L., and G. H. Rieke, 1997, *Astrophys. J.* **479**, 694.
- Veilleux, S., R. W. Goodrich, and G. J. Hill, 1997, *Astrophys. J.* **477**, 631.
- Verstraete, L., A. Léger, L. d'Hendecourt, O. Dutuit, and D. Deforneau, 1990, *Astron. Astrophys.* **237**, 436.
- Verstraete, L., J. L. Puget, E. Falgarone, S. Drapatz, C. M. Wright, and R. Timmermann, 1996, *Astron. Astrophys.* **315**, L337.
- Viala, Y. P., 1986, *Astrophys. J., Suppl. Ser.* **64**, 391.
- Viala, Y. P., C. Letzelter, M. Eidelberg, and F. Rostas, 1988, *Astron. Astrophys.* **193**, 265.
- Voit, G. M., 1991, *Astrophys. J.* **377**, 158.
- Wagenblast, R., 1992, *Mon. Not. R. Astron. Soc.* **259**, 155.
- Wagenblast, R., D. A. Williams, T. J. Millar, and L. A. M. Nejad, 1993, *Mon. Not. R. Astron. Soc.* **260**, 420.
- Wagner, A. F., and M. M. Graff, 1987, *Astrophys. J.* **317**, 423.
- Wallin, B. K., and W. D. Watson, 1997, *Astrophys. J.* **476**, 685.
- Walmsley, M., 1998, *Astrophys. Lett. Comm.*, Vol. 37-1.
- Walterbos, R. A., and R. Braun, 1996, in *Extragalactic Neutral Hydrogen*, edited by E. Skillman (ASP, San Francisco), p. 123.
- Walterbos, R. A., and B. Greenawalt, 1996, *Astrophys. J.* **460**, 696.
- Wannier, P. G., and S. M. Lichten, and M. Morris, 1983, *Astrophys. J.* **268**, 727.
- Wannier, P. G., B-G. Andersson, S. R. Federman, B. M. Lewis, Y. P. Viala, and E. Shaya, 1993, *Astrophys. J.* **407**, 163.
- Wannier, P. G., B-G. Andersson, M. Morris, and S. M. Lichten, 1991, *Astrophys. J. Lett.* **75**, 987.

- Warin, S., J. J. Benayoun, and Y. P. Viala, 1996, *Astron. Astrophys.* **308**, 535.
- Watson, J. K., and D. M. Meyer, 1996, *Astrophys. J.* **473**, L127.
- Watson, W. D., 1972, *Astrophys. J.* **176**, 103.
- Watson, D., R. Genzel, C. H. Townes, M. W. Werner, and J. W. V. Storey, 1984, *Astrophys. J. Lett.* **279**, L1.
- Werner, M. W., I. Gatley, E. E. Becklin, D. A. Harper, R. F. Loewenstein, C. M. Telesco, and H. A. Thronson, 1976, *Astrophys. J.* **204**, 420.
- White, G. J., B. Ellison, S. Claude, W. R. F. Dent, and P. N. Matheson, 1994, *Astron. Astrophys.* **284**, L23.
- White, G. J., and R. Padman, 1991, *Nature (London)* **354**, 511.
- White, G. J., and G. Sandell, 1995, *Astron. Astrophys.* **299**, 179.
- Williams, D. A., and T. W. Hartquist, 1984, *Mon. Not. R. Astron. Soc.* **210**, 141.
- Williams, D. A., and T. W. Hartquist, 1991, *Mon. Not. R. Astron. Soc.* **251**, 351.
- Williams, J., and C. F. McKee, 1997, *Astrophys. J.* **476**, 166.
- Willner, S. P., B. T. Soifer, R. W. Russell, R. R. Joyce, and F. C. Gillett, 1977, *Astrophys. J. Lett. Ed.* **217**, L121.
- Witt, A. N., J. K. Petersohn, R. C. Bohlin, R. W. O'Connell, M. S. Robert, A. M. Smith, and T. P. Stecher, 1992, *Astrophys. J.* **395**, L5.
- Witt, A. N., J. K. Petersohn, J. B. Holberg, J. Murthy, A. Dring, and R. C. Henry, 1993, *Astrophys. J.* **410**, 714.
- Wolfire, M. G., D. Hollenbach, C. F. McKee, A. G. G. M. Tielens, and E. L. O. Bakes, 1995, *Astrophys. J.* **443**, 152.
- Wolfire, M. G., D. J. Hollenbach, and A. G. G. M. Tielens, 1989, *Astrophys. J.* **344**, 770.
- Wolfire, M. G., D. J. Hollenbach, and A. G. G. M. Tielens, 1993, *Astrophys. J.* **402**, 195.
- Wolfire, M. G., and A. Königl, 1993, *Astrophys. J.* **415**, 204.
- Wolfire, M. G., A. G. G. M. Tielens, and D. J. Hollenbach, 1990, *Astrophys. J.* **358**, 116.
- Wright, E. L., *et al.*, 1991, *Astrophys. J.* **381**, 200.
- Wyrowski, F., P. Schilke, P. Hofner, and C. M. Walmsley, 1997, *Astrophys. J.* **487**, L171.
- Wyrowski, F., C. M. Walmsley, A. Natta, and A. G. G. M. Tielens, 1997, *Astron. Astrophys.* **324**, 1135.
- Xie, T., M. Allen, and W. D. Langer, 1996, *Astrophys. J.* **440**, 674.
- Xu, C., 1990, *Astrophys. J.* **365**, L47.
- Yan, M., and A. Dalgarno, 1997, *Astrophys. J.* **481**, 296.
- York, D. G., 1974, *Astrophys. J. Lett. Ed.* **192**, L127.
- Young, K., P. Cox, P. J. Huggins, T. Forveille, and R. Bachiller, 1997, *Astrophys. J.* **482**, L101.
- Young Owl, R., M. Meixner, M. Wolfire, and A. G. G. M. Tielens, 1999, *Astrophys. J.* in press.